MASTER THESIS IN GEOGRAPHY

Landform Interpretation and Landscape Evolution in Fosdalen, Western Norway

Norwegian University of Science and Technology

Department of Geography

Alexander Gjendem Gjørven

18.11.2014

Abstract

This thesis challenge the hitherto suggested deglaciation chronology in Fosdalen, western Norway. Through observations, lichenometry, and reinterpretation of previously mapped Younger Dryas moraines, the development of several landforms within the complex landscape is investigated.

Volume calculations and headwall retreat rates indicate a minimum compound cirque age of 510.000 yr. The Little Ice Age maximum for the respective cirque glaciers is estimated to 1769 and 1854 ± 4 yr.

Based on observations, it is suggested that former landform interpretations may be wrong due to equifinality. Hence during the Nor stadial, it is proposed that the Strynedalen valley glacier flowed westward through Fosdalen. Furthermore, a previously mapped Younger Dryas moraine has been reinterpreted as part of a hitherto unmapped debris -landform system, presumably consisting of minimum two rock slope failures deposited onto a cirque glacier during the Vinsrygg stadial.

Two identified relict rock glaciers below an active talus system, and ice/debris creep systems on the western cirque glacier foreland, indicate a former permafrost lower limit at 860 m a.s.l. during the Vinsrygg stadial. A lateral moraine at 840 m a.s.l. and a gently sloping subglacial till terrace indicate that the Lodalen valley glacier synchronously flowed into Fosdalen.

Finally, a flood plain and change of river course indicate a glacial lake outburst flooding. Combined with the reinterpreted landforms, the probability for the existence of a reconstructed Erdalen Event cirque glacier as suggested by Nesje and Dahl (1992) is impaired.

Preface

This master thesis is written in accordance with the master degree in Geography with Teacher Education program at the department of geography at Norwegian University of Science and Technology (NTNU). The thesis was supposed to be completed during June 2013. However, the writer was given an opportunity to be employed at a secondary school after the final trainee period spring 2012. This engagement increased for the year 2012/2013 to approximately 50 %. During this period, the writer also passed 22.5 credits (autumn), and 30 credits (spring). The workplace provided the writer a reference excellent enough to result in a temporary position as lead teacher at another school with 198 other applicants. This 100 % engagement was due mid-February 2014. The writer passed 22.5 credits during spring 2014, and resumed working on the master thesis, hence explaining the delayed completion date.

The project was chosen in cooperation with, and supervised by Ivar Berthling. Thank you ever so much for highly useful advice, and for bearing with me in the field. I would also like to thank Eirik Sørdal Brendsdal for his company during the first hike to the study area, and my father Arvid Gjørven for good questions, hypothesis and photographs in the field.

To my brother and siv.ing Andre Gjørven, and chief engineer Vegar Bøe, thank you so much for helping me with calculations on volumes, k-curves and lichenomtric data.

To my fellow students, I want to thank you for all the good times we have had these years. Charlotte Spikkerud, thank you for being the friend I needed through most of those years, you are a true inspiration. Fredrik Rønningen, thank you for being supportive both on and off the soccer field.

To my family, thank you for believing in me all this time, and for encouraging me to always perform the best I can. A very special thank you grandfather Ivar Gjørven, who refused to pass away until all the grandchildren were at least halfway through a higher education,
I love you.

Finally, Isabell Eide. Thank you for putting up with my endless chat about rock glaciers, and all the support you gave in and outside the study area. You are the true light in my world.
I love you.

Trondheim, November 18th, 2014
Alexander Gjendem Gjørven

Content

Diagrams

Attribute Data

1. Introduction

1.1 Background

Contemporary geomorphology has evolved from traditionally describing landforms, to describing the processes which creates the landforms. This new way is generally referred to as the *process-form paradigm* (Rhoads, 2005, André, 2003). In essence, arguments have been made that landforms are evolutionary processes. Only processes, i.e. the physical laws are claimed to be the real components which creates the landscape, while landforms are artificial abstracts developed by humans as a consequence of the time they live in, hence what they observe in nature (Berthling, 2011).

Landscape evolution is thus a concept which requires information from both processes and landform descriptions. Imbedded in this is *Classification*, which is a heavily discussed subject as to how scientists and remote sensing software divide these artificial abstracts (Rhoads and Thorn, 1996, Mayr and Bock, 2002, Minár and Evans, 2008, Giles and Franklin, 1998, Drăguţ and Blaschke, 2006).

Various agents, such as earth quakes, gully erosion, rock fall activity, debris flows, local glaciations, snow avalanches, weathering, permafrost conditions and climate may be processes which intertwine and influence systems both temporary and spatially. Descriptions of landforms and evidence of several of the agents mentioned above may to some extent accord for the spatial content in a landscape. In addition, dating and climate information may account for some of the temporary questions that follow such observations. Finally, morphostratigraphy may place landforms in time relative to each other, thus contribute to the understanding of landscape evolution.

Interestingly, different processes may cause landforms of similar geomorphometry, at least somewhere in the time-space continuum. This is known as *Equifinality*, and is one of the major discussions with regards to the origin of rock glaciers (Berthling, 2011, Millar and Westfall, 2008, Whalley and Azizi, 2003).

A well-known expression is "there is a time and a place for everything", and this thesis aims to investigate both of them in a geomorphological context.

Fosdalen, a contributory valley to the Lodalen valley in western Norway, consists of several topographic features, some of which are easy to explain. Other features however, seem much more complex.

First, a compound cirque and respective moraine systems are examined. Second a talus system and associated landforms are investigated. Third, a hitherto unmapped debris - landform system consisting of several ridges and furrows of unknown origin, along with associated features are attempted explained.

Moreover, former research in Fosdalen claim that a compound cirque glacier crossed the valley during the Erdalen event 9,100 ± 200 years ago (Nesje and Dahl, 1992), and additionally, a huge meandering ridge has been classified as a Younger Dryas lateral moraine (Nesje and Dahl, 1992, Thoresen, 1990, Lien, 1985).

These latter claims however, are made solely on the basis of theoretical depressions of fluctuating modifications of ELA, such as TP-ELA and TPW-ELA, and geomorphometric classifications that may be wrong due to equifinality and other influential conditions both during time of origin, and later.

It is for these reasons of outmost importance to comprise all aspects of the landscape i.e. all landform features, in order to interpret a landscape thoroughly. Next, studying both the ongoing, and former processes may be a step towards a more accurate history than is hitherto suggested. Based on present visual geomorphometric expressions in the study area, and reinterpretation of former research, several landforms and processes within the study area are investigated in order to support or contradict the previous claims. Finally, dating of the alpine growing lichen *Rhizocarpon geographicum* is applied in an attempt to date several landforms, or place them in time relative to each other.

1.1.1 Objective

Through observation and lichenometry, the objective addressed here has been *to identify and investigate how several landforms have been developed in time and space within the valley Fosdalen in Nordfjord, western Norway.*

The discussion is outlined from existing theory on possible landforms *in situ*, and possible originative and current influencing processes based on observations. In addition, the results presented are discussed against former research conducted in the area and several suggestions are made.

2. Study area

2.1 Location

The studied valley, Fosdalen, is located in the innermost part of the Nordfjord area in western Norway. Nordfjord splits into three valleys, Strynedalen, Lodalen, and Oldedalen valleys, with azimuth trends SE-NW (fig.2.1). Fosdalen (970-1041 m a.s.l.) is a contributory valley to Lodalen. Fosdalen heads NE-SW, and due to a pass, it is separated from Strynedalen (fig.2.2-2.3)

Fosdalen is approximately 3 km long, and 1 km wide. Fosdalen is shaped as a bowl, with typical glacial characteristics such as a U-form, moraine shapes and debris, and steep mountains above. For this thesis, the southern part of the valley is explored. The mountain south of Fosdalen, Skåla (1848 m a.s.l.) contains what is referred to by Gordon (1977) as a compound cirque, separated by an arête in a steep headwall above. Interestingly, the landforms below the compound cirque are shaped quite differently.

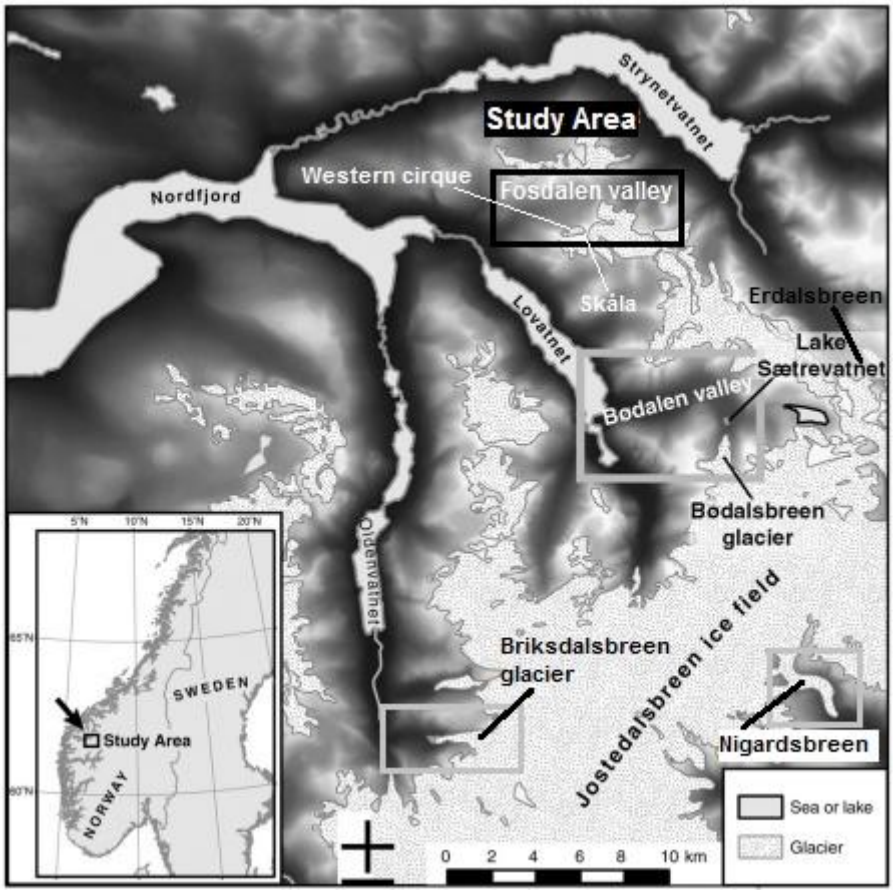

Figure 2.1: Geographic location of the study area and nearby locations

Study area framed in black square (Burki et al., 2009).

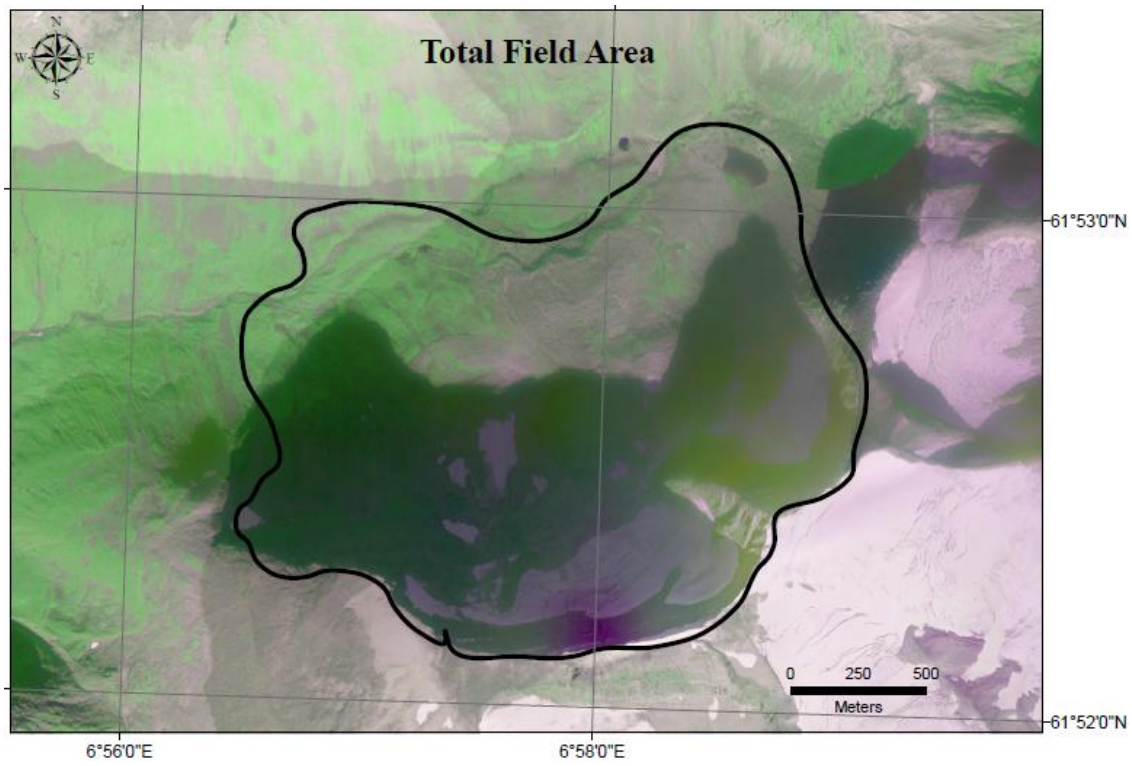

Figure 2.2: Vertical photo of the study area

(Statens Kartverk, 2010).

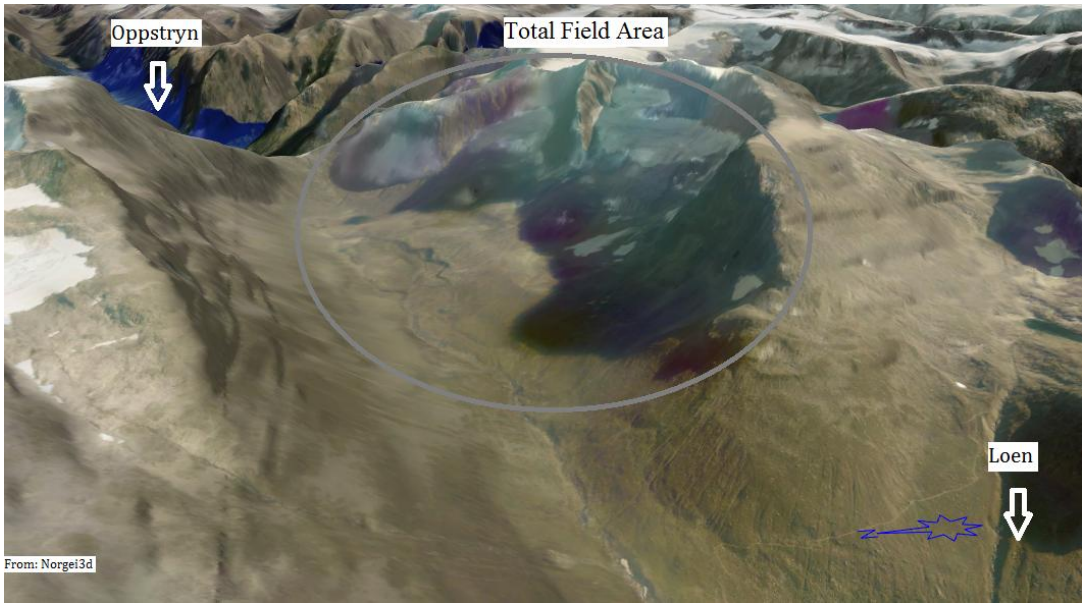

Figure 2.3: Oblique representation of the study area

The darker areas are caused by mountain shadow (Norkart, 2001).

2.2 Bedrock geology

Fosdalen lies in a region which is dominated by gneiss, often referred to as the Western Gneiss Region, and consists mostly of archaean bedrock dated to be approximately 1 - 1,8 billion years old (Nesje, 1995, Nesje et al., 1987), which some places may be affected by the Caledonian Folding (NGU, 2011b). The bedrock geology in Fosdalen consists mostly of quartzmonzonite which some places are transformed into augen gneiss. The western part of the valley consists of granite to diorite gneiss (NGU, 2011a).

2.3 Quaternary geology

The vast fjord and valley landscape in western Norway evolved from a plateau landscape through several intervals of glacial and warmer interglacial periods which took place during the Quaternary age i.e. the last 2,58 million years (Cohen et al., 2013). It is possible however, that glaciation preceded this date (Hewitt, 2000). The last ice age, known as the Weichselian, began 115,000 - 120,000 years ago, and ended around 8,500 before present (NGU and Thoresen, 1997). The last maximum glacial (LGM) extent in Nordfjord during the Weichselian, is assumed to have occurred around 18,000 - 20,000 years ago (Nesje, 1995).

Due to warmer climate in late Pleistocene, the ice sheet slowly diminished after LGM except during Older Dryas 18,000 - 15,000 BP, and Younger Dryas (YD) around 12,800 - 11,500 BP (Muscheler et al., 2008, Nesje and Dahl, 1993, Fareth, 1987), and the cold Erdalen Event in early Holocene, which occurred approximately 9,100 ± 200 BP (Nesje, 1984). It is believed that the Jostedalsbreen icecap that exists today, melted away during the Holocene thermal optimum around 7,400 BP (fig.2.4), and reactivated around 6,100 BP. (Nesje and Kvamme, 1991). It has also been argued that the western and eastern cirque glacier within the compound cirque beneath Skåla did not exist during late Pleistocene and early Holocene. For this reason, one of the moraine landforms in Fosdalen may be a Younger Dryas terminal moraine from the Lodalen valley glacier (Nesje and Dahl, 1992, Nesje and Kvamme, 1991, Thoresen, 1990, Lien, 1985). YD moraines are usually well defined, about 2-10 meters high, curving across the mouth of cirques or across valleys (Andersen et al., 1995)

During the seventeenth and eighteenth centuries, a glacial advance termed the Little Ice Age (LIA) and associated avalanches, rock falls and major landslides caused severe damage to farms in Olden and Loen parishes. The earliest evidence of glacial damage happened in 1684 AD, and at Nigardsbreen, LIA reached its maximum in 1748 AD. However, it has been argued that glaciers west of the Jostedalsbreen icecap reached maximum slightly earlier due to

generally steeper slopes, thus shorter response time (Nesje and Kvamme, 1991, Grove, 1988, Nesje et al., 1991). Nevertheless, Blomsterskardbreen, an outlet glacier from Folgefonni west of Jostedalsbreen did not reach its maximum until around 1940 AD (Tvede and Liestøl, 1977).

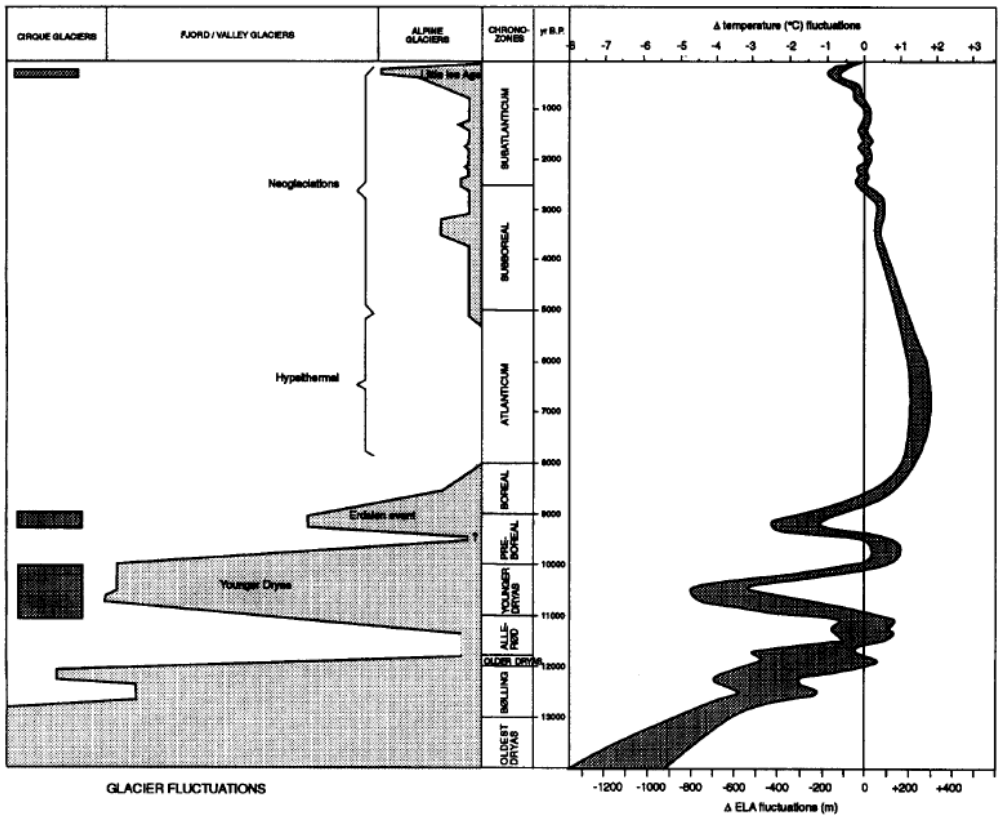

Figure 2.4: Holocene and late Upper Pleistocene ELA fluctuations and associated glaciations

From Nesje and Dahl (1993).

2.4 Climate

Norway lies in the belt of westerly winds stretching around the earth at these latitudes, and therefore the air mass which comes in from the Atlantic Ocean often carry a lot of moisture. The air flows through the fjords and lower coastal areas and then reaches the end of the fjords and valleys where it is forced to rise. Rauber et al. (2008) explains that when this happens, the air cannot contain as much moisture due to the cooling it is subject to at higher and colder altitudes. At some altitude the air becomes fully saturated, and clouds start to form. If cooled even more, the air mass releases moisture in the form of precipitation such as snow, hail or rain.

Although there is no climate monitor in Fosdalen, climate data gathered by Norwegian Meteorological Institute from Loen and Oppstryn suggests that the area has a coastal climate,

with relatively mild winters, cool summers, and a lot of precipitation. The mean annual air temperatures (MAAT), are 5,8˚C in Loen and 5,7˚C in Oppstryn. The annual precipitation levels are 1075 mm in Loen and 1137 mm in Oppstryn (Meteorological Institute, 2014). According to NVE et al. (2014) a coarse interpolation of MAAT equals 0-2˚C for the Fosdalen valley.

Temperatures extrapolated to Fosdalen lie somewhere between the *dry adiabatic lapse rate* (DALR) of 1˚C decrease/100 meters elevation and the *saturated adiabatic lapse rate* (SALR) of 0,5˚C decrease/100 meters elevation depending on the moisture content (Rauber et al., 2008). In her master thesis, Skarsten (2007) compared meteorological data from Oppstryn with data from Erdalen, and as a result used 0,7˚C altitudinal lapse rate. This was confirmed by (A. Beylich, personal communication 2014), who was listed as reference. This temperature lapse rate could according to him also be used in Fosdalen.

Table 2.1: Interpolated MAAT based on the 0,7˚C rate

Roughly estimated altitudes were gathered from several sources. Erdalen event and LIA cirque glacier + Younger Dryas moraine after Nesje and Dahl (1992), and the remaining from Statens Kartverk (2010).

		Oppstryn	Loen
Description	m a.s.l.	˚C/Yr mean	˚C/Yr mean
Erdalen event	900	0,8	-0,2
LIA + Younger Dryas	1000	0,1	-0,9
Terminal ridge	1100	-0,6	-1,6
Eastern Cirque toe	1300	-2	-3
Western Cirque toe	1400	-2,7	-3,7
Eastern Cirque head	1560	-3,8	-4,8
Western Cirque head	1700	-4,8	-5,8
Backwall altitude	1800	-5,5	-6,5

The difference between the coarse interpolation of 0-2˚C in Fosdalen at 1000 m a.s.l. and the 0,7˚C lapse rate interpolation is tiny (table.2.1). The two are still interpolations and should be interpreted with caution. Finally, according to Mernild and Liston (2010), cold katabatic winds originating from glaciers may attribute to even greater differences in microclimatic conditioned places such as the study area.

Former investigations of the discontinuous permafrost lower limit have been conducted by (King, 1986, Ødegård et al., 1996, Etzelmüller et al., 1998). Their research agree in that MAAT is the main influential factor, and that discontinuous permafrost may be present where

MAAT = -4˚C. However, more recent research have estimated the limit to be -3˚C in southern Norway (Etzelmüller et al., 2003, Lilleøren et al., 2012). Furthermore, by using the data, Etzelmüller et al. (2003,1998) modeled distribution of permafrost through a south west - north east profile in southern Norway (fig.2.5).

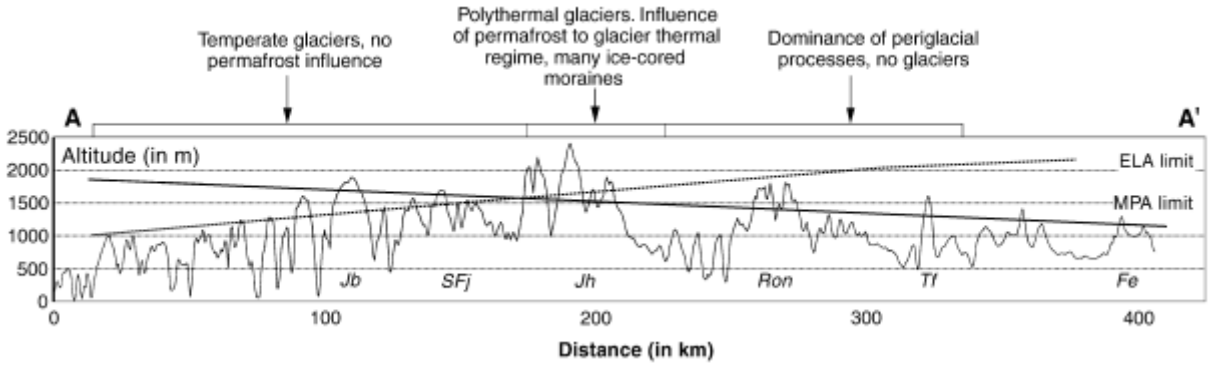

Figure 2.5: Mountain permafrost in southern Norway through a SW-NE profile

Figure shows a profile through southern Norway including the lower altitude of mountain permafrost (MPA) according to the model published by Etzelmüller et al. (1998) and the limits of the ELA. Jb = Jostedalsbreen glacier, SFj = Sognefjellet mountains, Jh = Jotunheimen, Ron = Rondane mountains, Tf = Tron mountain, Fe = Femund mountains. For more information, see Etzelmüller et al. (2003).

According to a study in the valley areas in Møre og Romsdal by Isaksen et al. (2011), the lower limit of permafrost in that area is 1300-1400 m a.s.l. except in north facing rock walls where permafrost probably is present at lower elevations. Differences of lower permafrost limits in north- and south facing rock faces have also been suggested by Hipp et al. (2014) in a pioneer study on the thermal regime of rock walls from Jotunheimen and Hurrungane. The altitudinal difference is estimated to approximately 300 m. Additionally, an increase in MAAT of 2˚C, elevates the limit 400-500 meters. Moreover, they concluded that north-facing rock wall surfaces are < 1˚C warmer than MAAT, while rock wall surfaces that faces south, are < 4˚C warmer than MAAT (Hipp et al., 2014).

Nevertheless, as can be seen in the table above, the discontinuous permafrost limit may be very different in Oppstryn and Loen. Using the 0,7˚C altitudinal lapse rate, Oppstryn may experience discontinuous permafrost at approximately 1500 m a.s.l. while in Loen, this limit may be as low as 1300 m a.s.l. Coincidently the lower threshold of the compound cirque glacier in Fosdalen in 2010 AD based on interpretation from Norgeibilder is 1380 m a.s.l. and 1320 m a.s.l. west and east respectively (Statens Kartverk, 2010). However, if the coarse interpolation by NVE et al. (2014) is used as foundation, discontinuous permafrost is only likely to exist in the upper parts of the headwall.

As can be seen in fig.2.6 below, Oppstryn receives more precipitation than Loen during the year.

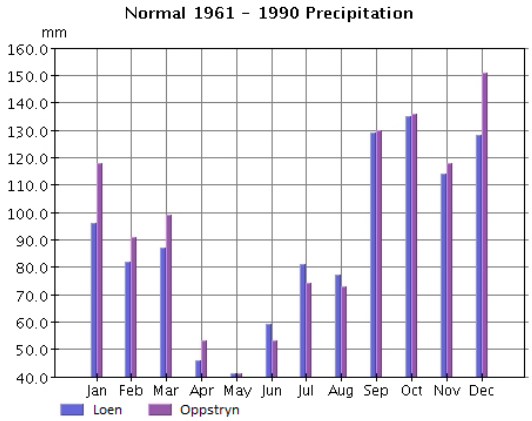

Figure 2.6: N**ormal precipitation in Loen and Oppstryn 1961-1990**

(Meteorological Institute, 2014)

2.5 Vegetation

The study area lies above the tree limit, which varies between approximately 650 - 800 m a.s.l. in the region. Trees can thus be found near the southwestern entrance to the valley. At most places till is covered with heather ling and moss, and black crowberries and blueberries can be discovered in the west. Moving east towards the cirques, altitude increases, and the heathery moors decrease. Rocks containing black moss or the lichen type *Rhizocarpon geographicum* are common where vegetation is sparse, and on solitary boulders. At several sites throughout the area, these lichens were studied in order to provide temporal data for the thesis.

3. Theory

3.1 Glaciers and ELA

Glaciers are large dynamic bodies of ice and snow that moves down slope due to ice creep and gravity. Glacial velocity depends on ice temperature, shear stress, and resisting forces such as the underlying topography and subsurface material. Glaciers gain mass by input of snow, and rain/melt water that freeze onto the glacier, which is known as accumulation. Glaciers lose mass by melting, calving and wind deflation, which is known as ablation. Changes in mass and ice temperatures on glaciers are strongly coupled responses to climate (Benn and Evans, 2010).

The glacier equilibrium line altitude (ELA), is a theoretical construct which is located at the altitude where the annual accumulation is equal to the annual ablation on a glacier. However, due to mountain shadow, wind deflation, avalanching, and debris falling onto the glacier, ELA is not a stable line at a specific altitude. It is the theoretical sum of the equilibrium line positions on the glaciers (Benn and Evans, 2010). ELA is sensitive to climate, mainly summer temperatures and winter precipitation, thus giving TP-ELA which can be used to reconstruct former climate (Nesje and Dahl, 2003, Benn and Ballantyne, 2005, Nesje, 2005).

On deeply incised cirques, TP-ELA may be lower than on plateau glaciers. As mentioned by e.g. Nesje and Dahl (1992), wind transports snow from windward to leeward sides on plateau glaciers, thus not changing the total mass. The situation is different for cirques, as they generally lie in leeward sides, facing their closest pole (Benn and Evans, 2010). Wind accumulate snow onto cirque glaciers, by drift and snow avalanches, thus lowering TP-ELA. This is known as TPW-ELA (Nesje and Dahl, 1992). For simplicity, ELA used for this thesis include both of the former variations.

In a study involving spring and summer temperature reconstructions from western Norway between 1734-2002 AD, Nordli et al. (2002) reconstructed the glacial history of Nigardsbreen, an eastern outlet glacier from the Jostedalsbreen icecap (figure 2.1). The Little Ice Age maximum extent on any individual glacier is known as LIA_{max}. At Nigardsbreen, LIA_{max} occurred in 1748 AD. This has been confirmed by historical documents (Grove, 1988). However, it has been argued that glaciers west of the Jostedalsbreen icecap reached LIA_{max} slightly earlier due to generally steeper slopes, thus higher velocities and a shorter response time (Nesje et al., 1991). The response time of Briksdalsbreen, a steep western outlet glacier from the Jostedalsbreen icecap for example, is five years (Nesje, 2005). However,

Tvede and Liestøl (1977) found evidence of an outlet glacier from Folgefonni not reaching its LIA_{max} until around 1940 AD.

According to the study by Nordli et al. (2002), Nigardsbreen experienced several ELA depressions after LIA_{max}. The most obvious were 1760-1770, 1805-1815, 1825, 1835, 1848-1952, 1860s and mid1870s, 1883-1888, and 1902-1908 AD.

In a study of glacier-front variations of Briksdalsbreen between 1900-2004 AD by Nesje (2005), the glacier advanced during 1901-1910, 1921-1931, and 1956-1997 AD.

3.2 Cirque glaciers

3.2.1 Cirque definition

Due to the variety of glacial bodies which may or may not be defined as a cirque glacier, a cirque definition was agreed upon when 19 geomorphologists participated at the first meeting of the British Royal Geographical Society (BRGS) Small Research Group on Geomorphometry in 1972:

A cirque is a hollow, open downstream but bounded upstream by the crest of a steep slope (' headwall ') which is arcuate in plan around a more gently-sloping floor. It is glacial if the floor has been affected by glacial erosion while part of the headwall has developed subaerially, and a drainage divide was located sufficiently close to the top of the headwall for little or none of the ice that fashioned the cirque to have flowed in from outside. (We might tentatively suggest that part of the headwall exceeds 35°, and the floor slopes less than 20°) (Evans and Cox, 1974).

The definition above indicates that cirques cannot receive much accumulation from other glaciers. However, this definition is problematic for two reasons. The first reason may occur at the early stages of cirque formation. If the hollow is at the margin of a plateau, ice is likely to form onto the high plateau first, at the onset of glacial conditions, and spill over cirque headwalls, thus attributing to their development (Benn and Evans, 2010).

The second problem is that the definition does not account for wind and avalanche accumulation. At the drainage divide south of the compound cirque glacier, snowdrift piles up several meters tall every year. The Skålabreen plateau glacier flows east and south east from this divide, and may contribute to the accumulation with its capacity to store snow throughout

the year which blows over the arête that is separating the plateau glacier from the compound cirque.

3.2.2 Cirque formation

Cirques originate in mountainside hollows which may be due to several processes such as rock slope failures and fluvial erosion. Other processes are snow patch erosion or nivation, which embraces a range of transport and weathering processes accelerated by late-lying or permanent snow e.g. slope-wash, enhanced chemical weathering, debris transport by snow creep or slip, and solifluction, which are encouraged by repeated freeze-thaw cycles and/or abundant melt water during the summer. However, their relative importance under different climate conditions are poorly known. The snow patch is defined as a cirque glacier whenever it is large and steep enough to generate the stresses required for internal creep deformation and basal sliding (Benn and Evans, 2010).

Cirques are often separated by narrow arêtes. Cirques in mid latitudes have a tendency of flowing east due to the accumulation of snow and glacier growth in the lee-side hollows of upland terrains located in the westerly wind belts. Additionally, they have a tendency of flowing towards the nearest pole due to reduced ablation as there is less direct solar radiation (Benn and Evans, 2010).

3.2.3 Cirque development

According to Benn and Evans (2010), glaciers enlarge cirques by subglacial quarrying and abrasion of the cirque floor, while subaerial slope retreat of the surrounding headwall due to overdeepening supplies debris to the glacier surface. If the erosion and down cutting of the floor is going to be effective, the basal ice has to be a least partially temperate. In addition, headwall retreat occurs due to mechanical weathering and mass movements.

Johnson (1904) has argued that cirque development is mainly horizontal. Through his observations in the Sierra Nevada mountains, he concluded that the floor was protected from mechanical weathering due to the ice, while sapping occurred at the headwall through diurnal cycles of freeze thaw erosion. The glacier would through abrasion scour the floor, but this would be to a much less extent than the horizontal headwall retreat.

On the extreme contrary, White (1970) referring amongst other to some Norwegian cirques, stated that arêtes between opposing cirques are so narrow and steep that only slight headwall erosion would cause a breach, thus changing the arête to a pass, or fuse the glaciers.

Nevertheless, the arêtes continues to persist. In addition, avalanche ravines in headwalls would not survive the undermining process of sapping. He concluded that cirque floors are lowered by glacial erosion more rapidly than headwall retreat.

In a Japanese study over a period of 14 years at the Hosozawa cirque, Matsuoka and Sakai (1999) found a correlation between rock fall activity and seasonal snow melt out. 5-15 days after melt out, rock fall activity calculated to 1-3 m^3 disintegrated from the headwall. This is equivalent to a headwall retreat rate of 0.01 mm a^{-1}. Caution of extrapolating the results were advised, due to larger block fallouts of >10 m^3 each decade, which makes the annual headwall retreat rate severely underestimated. Additionally, rock falls did not exceed the crossing terminal ridge. Comparatively, in a study of a former cirque glacier at Kråkenes, western Norway, Larsen and Mangerud (1981) found erosion rates of 0.5-0.6 mm a^{-1} in gneissic bedrock which compared well with other Norwegian studies such as (Østrem, 1975).

A variety of methods have been attempted in order to classify stages of cirque evolution (Benn and Evans, 2010). One approach is to use longitudinal profiles of cirques described mathematically, by the use of logarithmic curves. According to Haynes (1968), a specific logarithmic curve named *k-curve* can be used, and is estimated by the formula:

$$y = k\,(1-x)e^{-x}$$

where *y* is the altitude, *x* is the distance along the profile, and *k* is a constant describing the concavity of the longitudinal profile (fig.3.1). High *k*-numbers correspond to well developed cirques, and low *k*-numbers correspond to an early stage. Cirques with $k = 2$, seem to be deeply enclosed, have steep headwalls, and a well marked lake occupying much of the valley floor. Cirques with $k = 1$, tend to be a bit more open, with less steeply reversed floors. Thus sometimes containing a lake, and sometimes not. Cirques with $k = 1/2$, are usually much gentler, generally scree and vegetation covered, and frequently have gentle sloping floors (Haynes, 1968).

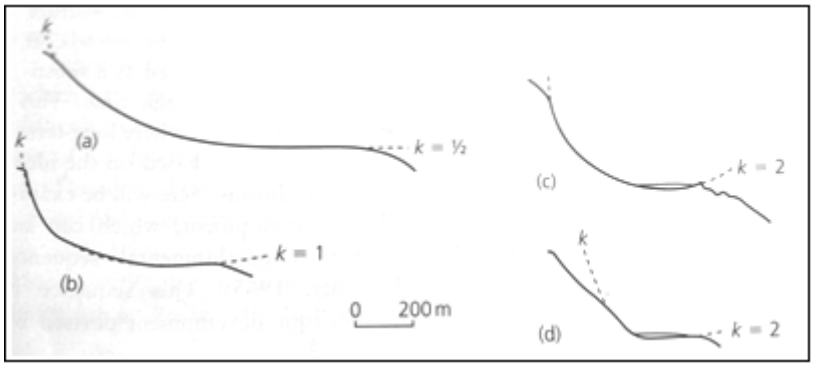

Figure 3.1: *k*-curves fit to longitudinal profiles of cirques in Scotland

After Haynes (1968). However, as shown by (d), not all cirque profiles fit. Collected from Benn and Evans (2010)

3.3 Rock falls

Rock fall is a process involving detachment of boulders and other rock fragments from the headwall and their transport as free fall to the point where they are deposited. This transport includes reconnecting with the slope and further movement by jumping, rolling and sliding down the slope until frictional forces and/or lack of kinetic energy and gravitational forces stops the movement (Evans and Hungr, 1993, Dorren, 2003). Rock fall activity can consist of anything between a singular fragment detaching, to major rock slope failures such as the Loen and Tafjord rockslides (Grimstad, 2005, Dorren, 2003, Blikra et al., 2006), and may or may not disintegrate several times during its course of movement (Evans and Hungr, 1993).

The main factors influencing movement and velocity of rock falls, are related to the slope mean angle of inclination. Debris increase and decrease in velocity at steep and gentle slopes, respectively. Additionally boulder size and form, and moreover the coarseness of the underlying debris, whether it is talus, soil or vegetation affects the velocity (Dorren, 2003).

Rock falls usually produces talus forms that are fall-sorted, with large boulders closest to the toe, and smaller debris such as gravels and sand being deposited closer to the head. This is first and foremost due to the fact that larger objects contain more kinetic energy, and secondly because smaller fragments are intercepted in gaps between larger boulders (Blikra and Nemec, 1998, Pérez, 1989).

3.3.1 Trigger mechanisms

Geology, topography and climate are highly influential factors when it comes to rock falls. Geological processes constitute the foundation of lithological characteristics e.g. crack formation and lithologic strength of the stratum bed. The stability and crack formation in rock walls today are mostly influenced by Pleistocene and Holocene glaciation and deglaciation.

Rock walls previously covered by glaciers and icecaps experiences depressurizing when the ice melts, which increases crack formation and growth, thus rock fall activity is boosted during and immediately after deglaciation (Ballantyne, 2002, McCarrol et al., 1998), often referred to as paraglacial activity (Curry and Morris, 2004).

Several studies has provided evidence that changes in temperature influence the stability in rock walls where freeze thaw mechanisms contribute e.g. (Davies et al., 2001, Gruber and Haeberli, 2007, Matsuoka and Murton, 2008, Blikra and Nemec, 1998). Direct shear box tests made Davies et al. (2001) claim that the strength and stiffness of a joint filled with ice, is a function of both temperature and normal stress. Their research indicated that a decrease in temperature from the freezing point caused more strength of an ice filled joint if the closure pressure was sufficient. A lack of sufficient closure pressure however, resulted in less strength. Consequently, if the slope stability is preserved by ice-filled joints, its reliability decreases with increasing temperatures.

One of the discussions within the subject of rock fall activity is whether it is mainly a paraglacial or periglacial process. In a Canadian study, Luckman and Fiske (1995) found that rock fall rates throughout Holocene were too low to cause the investigated talus forms. Thus, they concluded that the forms had to be paraglacial, caused by depressurizing immediately after deglaciation.

In contrast to the Canadian study mentioned above, McCarrol et al. (1998, 2001) discovered increased rock fall activity in Jotunheimen, southern Norway, throughout LIA, and claimed talus forms to be the result of frost weathering. They rejected the paraglacial interpretation, and concluded that it was mainly a periglacial form, thus the visible expression of periglacial processes.

Climatic fluctuations such as the temperature decrease during LIA in the 17th and 18th centuries may thus contribute to enhanced rates of rock fall. According to Nesje and Kvamme (1991), and Nesje and Dahl (1993), the decrease in mean summer temperatures in western Norway was approximately 1˚C compared to present.

While Grove (2004, 1988) based on historical sources found the highest concentration of rock fall activity to be between 1650-1760, and the research mentioned above by McCarrol et al. (1998, 2001) supported this historical approach, Skarsten (2007) found increasing rock fall activity on a talus in Erdalen, Norway, the past 100 years, compared to rates during the LIA.

3.4 Rock Slope Failures

Rock slope failures (RSF) involves detachment of larger mass than those of rock falls (> 10.000 m^3), and generally leads to rock avalanches (Hewitt, 2009). Several RSF in western Norway seem to have happened during the latter half of Holocene. They are mostly localized in inner fjord regions and is believed to be the result of earthquakes. Major slope failures in these areas are expected to occur 1/1000 yr for each locality (Blikra et al., 2006).

When RSF occur in glacier basins its emplacement geometry is affected by movement over ice, as ice yield less friction than bedrock. Conversely, if the glacier has a lot of crevasses, entrapment of debris is likely. Furthermore, the glacial system may be impacted by such an event. For instance if the debris cover is thick, it may prevent the active layer of penetrating into the glacier, thus reducing ablation. It is also possible that such events may lead to glacial surges (Hewitt, 2009).

If debris is moved further down slope by the glacier, and the glacier melts, an open-work structure is left behind. This structure is usually dominated by angular and subangular debris, clast-supported debris with few fines, small clasts piled up on larger, and non-mixed lithology. Some areas with thick ridges may be common, but they usually disappear when the ice vanish. Some areas might contain thick, dense debris with debris veneers that become obscured by vegetation after several years. The depths of these open-work structures are often irregular, typically 1-5 m. The margins are sometimes marked by a talus 5-10 m high instead of ridge-shaped moraines. However, if rock falls occur repeatedly, the topography can be greatly modified (Deline, 2009).

In a study from Jotunheimen, Wilson (2009) interpreted an extensive accumulation of rock debris as the deposits of a rock slope failure (RSF). The body is composed of large boulders and displaced masses of bedrock. Due to different r-values provided by the Schmidthammer, there had probably been more than one event. He concluded that there are probably more RSF deposits in Jotunheimen, and pointed to the necessity for more research.

3.5 Weathering

André (2003) advised caution about the belief that temperature related freeze thaw cycles, i.e. mechanical weathering is the dominant weathering agent, and points to the lack of investigation on the matter. Instead, she suggested investigation of several agents such as biological and chemical weathering. Hall et al. (2002) addressed the necessity for research on erosion rates caused by chemical weathering compared to rates caused by mechanical

weathering, and to compare rates caused by chemical weathering in periglacial environments with other climatic environments.

3.6 Rock glaciers

3.6.1 Rock glacier definition

Defining what a rock glacier is, has been a prolonged and persisted challenge due to the variation in genetic origin known as *equifinality*, exemplified by talus-derived, and glacier-derived rock glaciers (Berthling and Etzelmüller, 2007, Haeberli et al., 2006, Potter, 1972, Whalley and Azizi, 2003, Østrem, 1971, Lilleøren and Etzelmülier, 2011, Humlum, 1988).

While Potter (1972) in his definition focused on a morphological genesis, Haeberli (1985) argued that rock glaciers only reflected the genetic processes. Later, Whalley and Azizi (2003) contributed by introducing rock avalanches as part of the possible genetic processes. Recently Berthling (2011) proposed a new definition. A rock glacier is:

The visible expression of cumulative deformation by long-term creep of ice/debris mixtures under permafrost conditions.

This latter definition seems a better alternative, as it semantically may account for both present and historic expressions i.e. active, inactive and relict rock glaciers, and similarly, climate variations. Thus opposing Haeberli (1985), who emphasize steady-state creep conditions.

3.6.2 Rock glacier formation

Rock glaciers may originate from glaciers, talus and rock avalanches. In addition, they may develop from ice cored moraines, protalus ramparts and/or other debris forms (Østrem, 1971, 1964, Lilleøren and Etzelmülier, 2011). The essential point is that ice/debris mixtures starts to creep over several years due to local permafrost conditions, and deforms the landform from its original state. According to Ikeda and Matsuoka (2006), talus derived rock glaciers appears to originate from snow banks buried with deposits of large rock falls from the rock wall.

Ice cored moraines are moraines that contain ice cores within. According to Østrem (1971, 1964), ice cored moraines are taller than normal lateral moraines, usually indicating former glacier surface. They are generally regarded as a permafrost conditioned landform, and if the debris cover is thicker than the active layer depth, they may survive for several thousand years. Without permafrost conditions they are unstable and decay within decades, usually transforming into hummocky moraines (Lilleøren and Etzelmülier, 2011). Ice cored moraines

can be transformed into rock glaciers if the deposits start to creep. Furthermore, if the deposit is not moving, it must be classified as a moraine (Østrem, 1971). Protalus ramparts is according to Lilleøren and Etzelmülier (2011) representing an early stage of rock glacier development, and may thus be categorized as rock glaciers.

Another type of rock glaciers are pebbly rock glaciers. Morphologically they have a less rough surface, and a layer of rocks that are tilted on the steep front. Pebbly rock glaciers are rare, as they seem to originate from easily weathered rock types. Presumably they originate from groundwater freezing (Ikeda and Matsuoka, 2006).

Rock glacier morphology is characterized by rough surfaces, steep down-slope fronts at the angle of response, and ridges, furrows and flow lines that are visible expressions of movement as their bodies includes both compressive (ridges) and extensive flow (furrows). If they are still active, they are supersaturated with ice. If they are inactive, they still contain ice, but deformation has stopped. (Lilleøren and Etzelmülier, 2011, Haeberli et al., 2006).

In southern Norway, the lowest elevation of a mapped active rock glacier exist at about 1500 m a.s.l. the same altitude as discontinuous permafrost is assumed to exist. However, several of the intact permafrost landforms in western Norway are situated below this limit. Interestingly, this is an indication of permafrost landforms in marine environments at higher MAAT than expected. (Lilleøren and Etzelmülier, 2011).

In addition, the rock glacier formation zone in Norway seems to have risen in elevation compared to early Holocene. Today, no areas seem to justify neither talus derived rock glacier growth, nor formation. Talus derived rock glaciers may thus represent a period with higher slope activity and weathering rates such as during paraglacial recovery and/or depressurizing, and originate from landslide-influenced deposits which could shorten their formation period. Consequently all current active rock glaciers are glacier derived, and relict talus derived rock glaciers are presumably the oldest rock glaciers (Lilleøren and Etzelmülier, 2011).

Relict rock glaciers generally have the same morphological characteristics as active rock glaciers. However, the quantity of ice is absent, and they are heavily vegetated. In southern Norway, the lowest elevation of a mapped relict rock glacier is 1000 m a.s.l. Moreover, all the permafrost landforms in southern Norway are situated within the YD lateral moraines (Lilleøren and Etzelmülier, 2011).

It should be noted that, using a null-hypothesis approach to rock glacier recognition in the British mountains, Jarman et al. (2013) found that all 28 cases investigated could be explained by different origins, such as rock slope failure, incremental deposits, moraines, protalus ramparts, and coarse debris veneers on bedrock and depositional forms. Thus they concluded that there are no relict rock glaciers in the British mountains.

3.6.3 Rock glacier development

As rock glaciers are considered to be landforms that develop from ice-debris accumulation systems provided by permafrost conditions, they are regarded as cryo-conditioned landforms. Rock glaciers are hence controlled by interactions between ground and surface thermal regimes with a sub-zero diurnal, seasonal or long-term pattern, and earth surface processes (Berthling and Etzelmüller, 2011). Consequently, MAAT low enough to cause permafrost is a necessary condition, although abundance of debris supply is necessary in order to maintain a continued development, i.e. growth.

In a study of Murtèl rock glacier in the Swiss Alps, Kääb et al. (1998) assuming a steady state condition, found that development of transverse ridges took several thousand years, and that wavelengths of approximately 20 m corresponded to a relative age difference of 300-400 yr. Although there might be several additional contributors to ridge development, they attributed compression of flow which occurred below the point of change in average surface slope as a main factor. Assuming a horizontal compression of 0.001 a^{-1} - which prevailed in the zone where the ridge grew - a block of incompressible material of 2 m thickness over the time of 3000 yr, gave a total vertical growth of 6 m. Conclusively they stated that the ridges moves at the velocity of creeping permafrost.

In another study of the Muragl and Murtèl rock glaciers by Frauenfelder and Kääb (2000), the velocity of surface ridges on Murtèl was calculated to approximately 0.05 m a^{-1} (fig.3.2). This is highly different from a recent study on the Sachette rock glacier in the northern French Alps, as it showed surface displacement rates of 0.6-1.3 ± 0.6 m a^{-1} (Monnier et al., 2013).

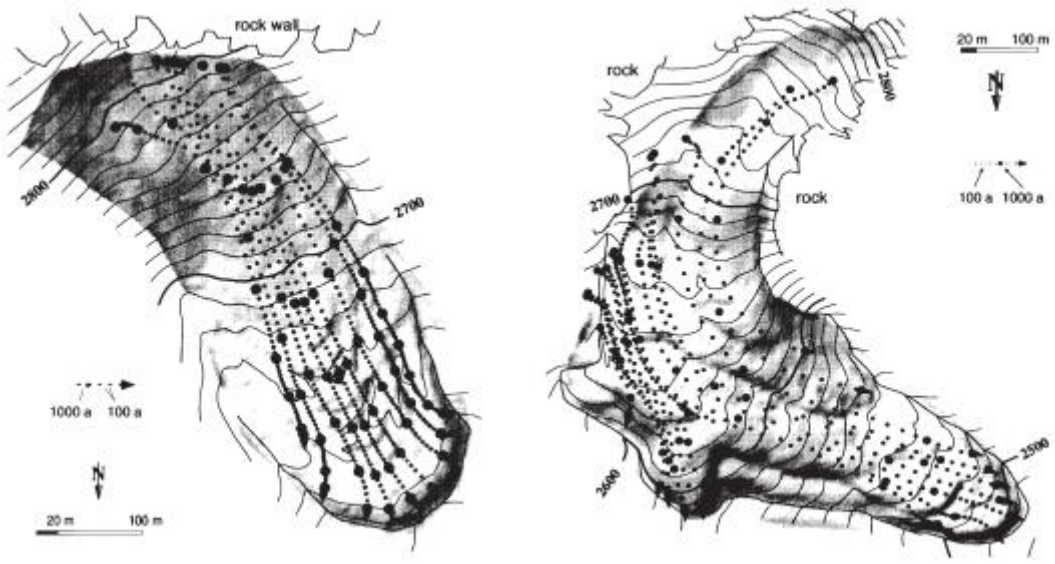

Figure 3.2: Surface velocity flow lines of Murtèl and Muragl rock glaciers

Murtèl to the left, and Muragl to the right. While the small dots represent a time span of 100 years, the large dots represent a time span of 1000 years. Flow lines are based on steady-state conditions (Frauenfelder and Kääb, 2000).

Rock glaciers may according to Frauenfelder and Kääb (2000) be the visible expression of a dynamic history. Areas that involve complex and non-coherent shapes, rich in horizontally and vertically distinguishable creep systems might indicate a complex story. On the contrary, areas with uniform creep streams may represent a history of less dynamic variations.

Rock glaciers may also be part of more complex ice/debris mixture forms, such as suggested in a recent study from the foreland of Cerro Tapado glacier in the Chilean Andes by (Monnier et al., 2014).

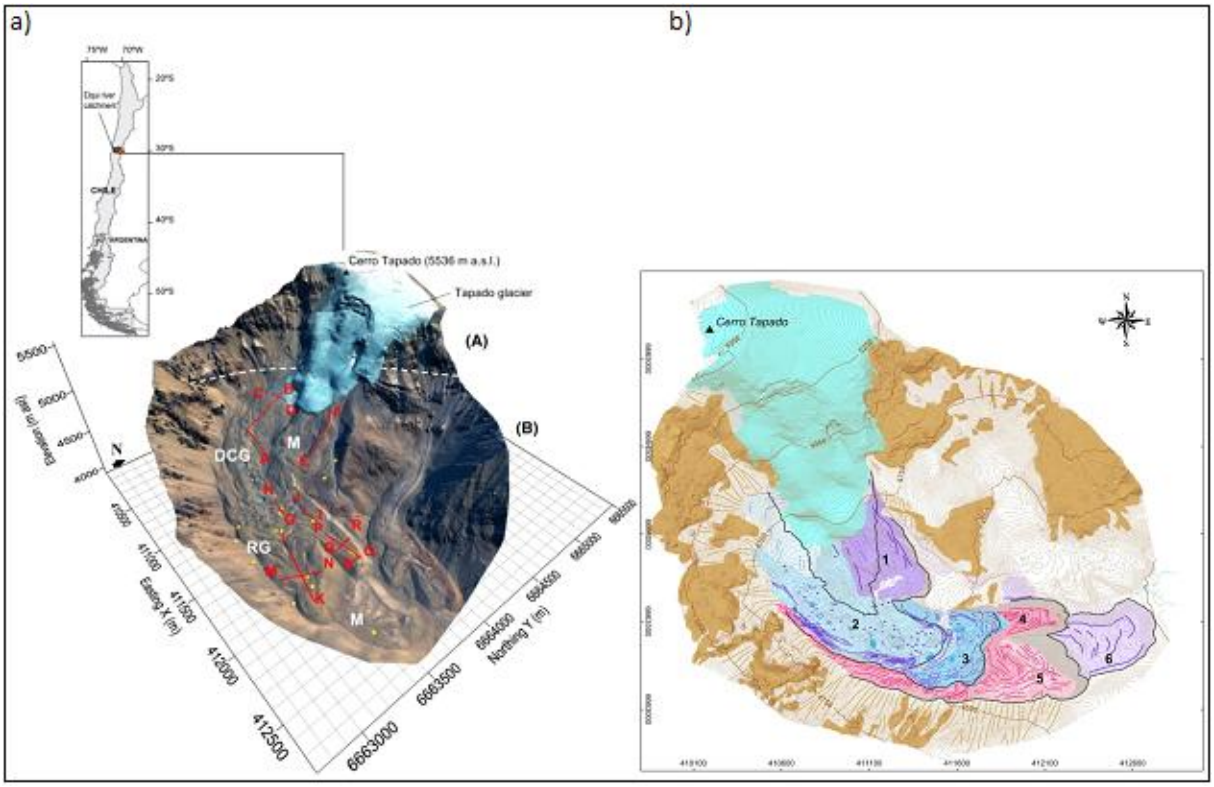

Figure 3.3: Complex ice/debris mixture forms below Cerro Tapado glacier in the Chilean Andes

a) present glacier and the complex landforms below. b) the distribution of different landforms. 1 is the upper latero-frontal moraine complex, 2 and 3 are debris covered glaciers, 4 and 5 are rock glaciers, and 6 represents older moraine constructions. From Monnier et al. (2014).

They drew several conclusions. First that there is no genetic continuum between the upper debris covered glaciers and the lower rock glaciers, as the rock glaciers were overlapped by the debris covered glaciers and do not derive from them. Second, the assemblage of landforms have been constructed through several episodes, with the youngest upper landforms having developed onto the lower landforms. In addition, all landforms except the older moraine constructions have moved down slope since 1956 AD. During the same period, the front of the Cerro Tapado glacier above retreated 400 m. The debris covered glaciers experienced a vertical lowering of more than 10 m, while the rock glacier fronts experienced a rise in elevation, probably due to down slope migration and compressive forces (fig.3.3).

4. Method

4.1 Observation

This thesis is mostly built on observations, which are affected by pre-conceived ideas, and furthermore, interpretations. With regards to observation, Rhoads and Thorn (1996) argue that we are affected by the time we live in including the current and previous paradigms, and thus our observations are to some degree theory-dependent. This is known as the social constructivist perspective.

The fieldwork has been carried out through three fieldtrips. The articles read and applied in between field trips, and all those that eventually were tossed away have without a doubt affected the observations. This is due to the fact that for each trip, the author has discovered new landforms although the route was approximately the same.

From a naturalistic perspective, the aim of observation in contemporary geomorphology is to collect information about an element i.e. landform or process through a causal chain between the observed and the observer. A short chain refers to the sense perception, mainly the eyes. A long chain refers to the use of remote sensing devices and then the eyes (Rhoads and Thorn, 1996).

For this thesis, both short and long chains have been applied. Short chains (eyes), were used during the three field trips, while long chains were used between and after the field trips by means of orthophotos, maps, datasets, and virtual globes. Photographs taken during field trips represent long chains that are based on short chains because the photos represent whatever the eyes initially observed. However they may also be regarded as long chains without this basis due to later re-interpretation which may have caused other observations and interpretations.

Geomorphologists describe the earth by classifying landforms. However, there is no justified definition of what a landform truly is, although there are several perceptions. This is a peculiar phenomenon, as landforms provide the basis for scientific investigations, and the results from the investigations redefines our ideas about the landforms (Rhoads and Thorn, 1996, Berthling, 2011)

In order to separate different landforms, geomorphologists classify them on the basis of being discrete elements. The problem with classification is that this concept requires borders between respective topographic elements. However the reality of nature is more complex (Berthling, 2011).

4.2 Lichenometry

Lichenometry is a well known and traditional geomorphologic dating method, which was first introduced in the 1920s (Sammut and Erskine, 2013), and further developed by the botanist Roland E. Beschel during the 50s and 60s. In essence it is based on measuring the diameter of distinct species of lichens, which is an association between a fungus and an algae. Lichens colonize rock surfaces, and their size gives information about how long the substrate has been exposed to the atmosphere (Beschel, 1950). The most common lichen used for research in alpine areas is *Rhizocarpon geographicum*. It is easy recognizable by its color which is yellow-green, punctuated by black, on siliceous rock (Jomelli et al., 2007).

The more precise description of lichenometry is made in two steps. First of all the diameter of thalli is measured at a surface where the age is known nearby the area of interest e.g. several tombstones with identical lithology and inscriptions if available (Sammut and Erskine, 2013). This determines a relationship between the diameter of the thalli, and time since exposure. If there are no known surfaces, and time is no limit to the researcher, one can record growth rates at the area of interest over several years. Either way, the result can afterwards be transferred to the area of interest where the age of the thalli is unknown (Jomelli et al., 2007).

Growth rates of *Rhizocarpon geographicum* have been investigated by many, and different solutions have been proposed. Early research by Beschel suggested a sigmoid curve (Beschel, 1961). Andersen and Sollid (1971) concluded that the growth was only linear. O'Neal and Schoenenberger (2003) also discovered a linear growth face between 20 and 145 yr. They did however also suggest a rapid growth phase from 8 to 20 yr, and a slow growth phase of unknown duration after 145 years which has resemblance to that of Beschel. Erikstad and Sollid (1986) found that a linear curve gave a better fit to the fixed points than a semi logarithmic curve on the Nigardsbreen glacier which was the only glacier in their study that did not lack fixed control points. However, this curve only fit the LL, not the 5LL method. In contrast, research conducted by Mottershead and White (1972) showed close relation to an exponential function. The different proposed growth curves may be due to the expansions lichenometry has been through since Beschel.

To this day the lichenometric method includes four main categories. Largest Lichen/5 Largest Lichen (LL/5LL), Fixed-Area Largest Lichen (FALL), the Size Frequency approach (SF), and the Lichen Cover approach (LC). There are other lichenometric techniques e.g. Winchester (1984), but they are considered to be modifications of the original methods mentioned above

(Bradwell, 2009). The first dating method used by Beschel in the fifties and sixties, was Largest Lichen (Beschel, 1961). This approach measures only the largest sample of a specific lichen on a homogenous surface, e.g. a terminal moraine. Unlike its successors, the LL/5LL is applauded due to its simplicity and user friendliness (Bradwell, 2009).

Lichenometry as a method provides quantitative results within a short amount of time, and is well suited for decoding Late Holocene glacial histories in high latitude and alpine settings. At high altitudes and latitudes vegetation is often scarce, and above the timber-line, trees are absent which makes dendrochronology impossible. Thus lichenometry can provide valuable results where other methods are difficult or impossible to perform (Bradwell, 2004, 2009).

The LL approach developed by Beschel, is based on his assumption that on a homogenous surface, only the largest thalli i.e. the lichen with the largest diameter is an age indicator. Thus, the largest lichen would indicate optimal growth condition, and minimum exposure time at the given substratum (Webber and Andrews, 1973).

The approach applied for this paper were 5LL which was developed in the seventies as a modification of LL in order to avoid reliance of potential lichen anomalies. The mean of the five largest lichens found on a homogenous surface were measured (Bradwell, 2009).

5LL has been criticized due to the assumption made by Beschel mentioned above (Webber and Andrews, 1973), however several researchers have successfully used average of thalli with the 5LL method e.g. (Evans et al., 1999, Mottershead and White, 1972). On the contrary, there is no evidence that more than 5 lichen enhances the result (Bradwell, 2009). Furthermore there are a lot of variables which influence the growth rate of lichens, especially microclimate and altitude. In addition other flaws can occur due to misinterpretation of lichen species and substrate lithology (Sammut and Erskine, 2013).

4.3 Data acquisition

4.3.1 Field research

Most of the studied area are usually covered by late lying snow, thus a time limit of at most 3-4 months during the summer is generally possible. The fieldwork was carried out July 23rd 2013 (photographs and observation), August 7th 2014 (terrestrial laser scan and observation with tutor), and August 23rd 2014 (lichen measurements and observation). A planned trip in October 2013 was canceled due to early snowfall.

4.3.2 Acquisition strategy

The tool used for measuring lichen size were a Cocraft Digital Vernier Caliper with a range up to 150 mm. For specimens >150 mm, a finger was placed at 150 mm, and the caliper was reset at that point. Specimens >300 mm were not measured.

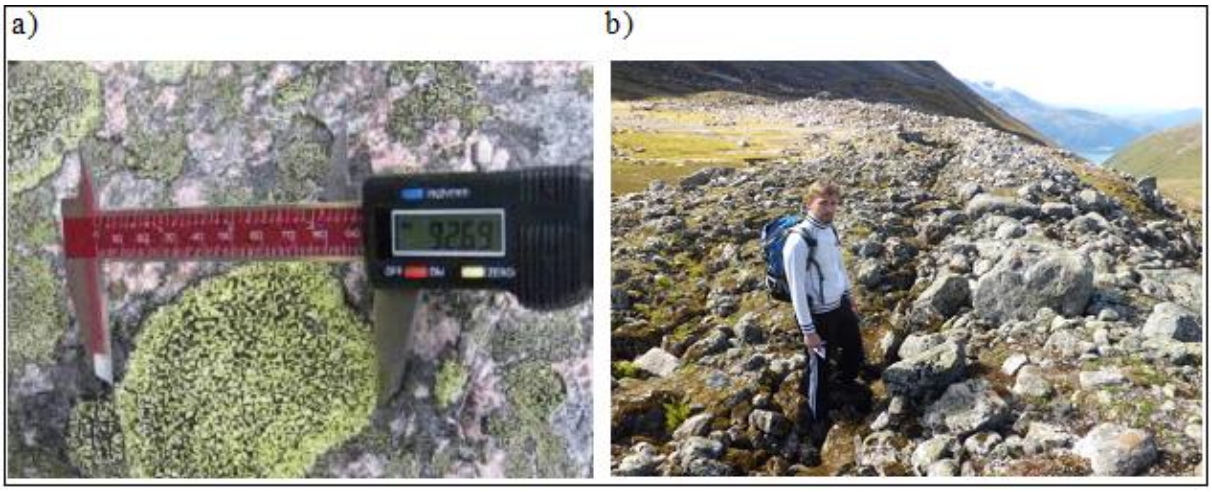

Figure 4.1: Digital caliper and lichen measurement position

a) A digital caliper was used to measure the axis of the thalli. Photo: Silje Skarsten (2007). b) A lateral moraine to the right, and hummocky moraine on the inside. Measurements were carried out on the proximal side of the lateral moraine. Photo: Arvid Gjørven.

Schmidthammer dating was considered as an alternative or amendment to the lichenometric dating method. Due to the highly weathered rock surfaces, and the lithological challenges gneiss induced to R-values (Matthews et al., 2013), the method was rejected.

A terrestrial laser scanner (TLS), was used to scan the valley at six positions in order to provide high resolution pictures. The goal was to gain a more accurate knowledge of landforms than could be interpreted by aerial photos and orthographic photos. However, the time needed to process the raw data into meaningful data that could be used for interpretation exceeded the time frame for this paper. This caused exclusion of the TLS data.

For the lateral moraines identified by Nesje and Dahl (1992), and additional push- and lateral moraines identified during this research, lichens on the proximal side were measured (fig.4.1). The reasons for this is that according to Erikstad and Sollid (1986) the lichens on the distal side of a lateral moraine is older than the proximal side, and this paper aim to discover whenever the glacier started to retreat. The amount of specimens measured depended on available thalli. Two people searched the same surfaces in order to avoid overlooking specimens. Below the western cirque a minimum of 10 specimens were measured on the

moraines due to high availability. The lateral moraines were also easy to identify, with one exception. The M2 moraine had an even upper surface (chapter 5.2.1.3). Thus lichens were measured close to the top, and additionally a couple of meters onto the proximal side in order to confirm or invalidate a homogenous age. Below the eastern cirque less specimens were available, and also the lateral moraines were harder to identify due to redistributed debris. For other landforms, lichens were measured wherever the largest specimens could be found, mostly on large boulders.

The criteria for lichens to be measured were first of all that they were separated from other specimens. Secondly, they had to have a somewhat circular shape. Those that were subjectively recognized as too elongated were not measured. And lastly, the specimens had to grow on a somewhat flat surface. Those that grew across different sides of their respective substrates were disregarded. In accordance with Erikstad and Sollid (1986), the black ring surrounding the lichens was included in the diameter.

The measurement was carried out during late summer on a partly cloudy day at around 12˚C. The substratum was dry except near drainages streams, the two ponds and the small lake in the valley. Lichens in wet areas were not measured.

4.3.3 Limitations

Although lichenometry is an easy to use technique which requires little use of time and involves low costs, it has as well as other techniques its limitations and uncertainties.

To begin with, problems occur at sites where rock falls, snow avalanches, debris flows and other processes are regular and ongoing. The distribution of new debris and redistribution of older debris may burry or crack boulders that could contain valuable and representative specimens of lichens (McCarrol et al., 1998). This may cause both overestimating and underestimating of the temporal result depending on the origin of the debris.

A second problem with lichenometry is the possibility of "snow kill", which means that the substrate receives too little sunlight and moisture because of late lying and/or thick snow cover. This extends the colonization period, and reduce the growth rate of lichens (Matthews, 2005, Innes, 1985). In this particular field, the mountains deflect a lot of possible sun radiation. In addition, snow avalanches throughout the field occur every year, causing late lying snow. This may cause severe underestimation of the surface age.

Thirdly, when measuring the longest axis of a thalli, there is a chance of measuring fused lichens as one specimen (Innes, 1985). Additionally not all lichens grows with a circular shape, but may be elongated, and questions can be raised whether measurements of these forms are accurate. In both settings, the surface age may be overestimated.

Next, if weathering is too strong, the surface of the substrate will not be stable, and lichen growth will be delayed. Moreover, if the substrate is polished it stays wet shorter which reduces growth (Erikstad and Sollid, 1986). In both situations ages may be underestimated.

Furthermore, McCarroll (1994) found a correlation between boulder size, and lichen size. Meaning that if there are few large boulders, ages may be underestimated.

Finally, establishing the growth curve in an area is a difficult process as seen earlier (chapter 4.2). It requires several accurate control points, and precise historical information (Matthews, 2005, Erikstad and Sollid, 1986), and as demonstrated by McCarroll (1994), there is a correlation between boulder size and lichen size.

Skarsten (2007) tried to establish a local growth curve for Erdalen by using tombstones in Oppstryn (5 km north east of Fosdalen). However, the lack of older control points made this impossible. Even with success, Fosdalen lies about 1000 meters higher, which may cause a lag before colonization can occur, and growth rates may also be influenced. Thus statistical results if compared may not have been reliable. As previously commented by Erikstad and Sollid (1986), using regional growth curves does not solve this problem. However, when comparing several regional growth curves, one might be able to choose the one best suited for a specific field. Regardless of the accuracy of the curve chosen, relative ages between forms can be estimated which is valuable information.

4.4 Analytical techniques

4.4.1 Lichen growth curve

Matthews (2005) compared several former growth curves in western Norway, and applied new subregional growth curves within Jotunheimen. His research indicated a decline in growth rates from west to east, and he argued the results were due to more precipitation in the west. Erikstad and Sollid (1986) made a curve for the Nordvestlandet region based on 5LL: $\ln(y+90) = 0{,}0119x + 4{,}6086$, with a reliability of 0,9981. The curve is based on a semi-logarithmic coordinate system with the following formula:

$In(y+c) = ax+b$

where x = lichen diameter, y = age, and a, b, and c are constants. They did however address the necessity of caution when using this curve as it may underestimate lichen values, due to lack of good quality localities for the control points. In order to fit the curve to the figure by Matthews (2005), the formula was inverted, so that x and y have been swopped:

$x = (1/a)*(\ln(y+c)-b)$

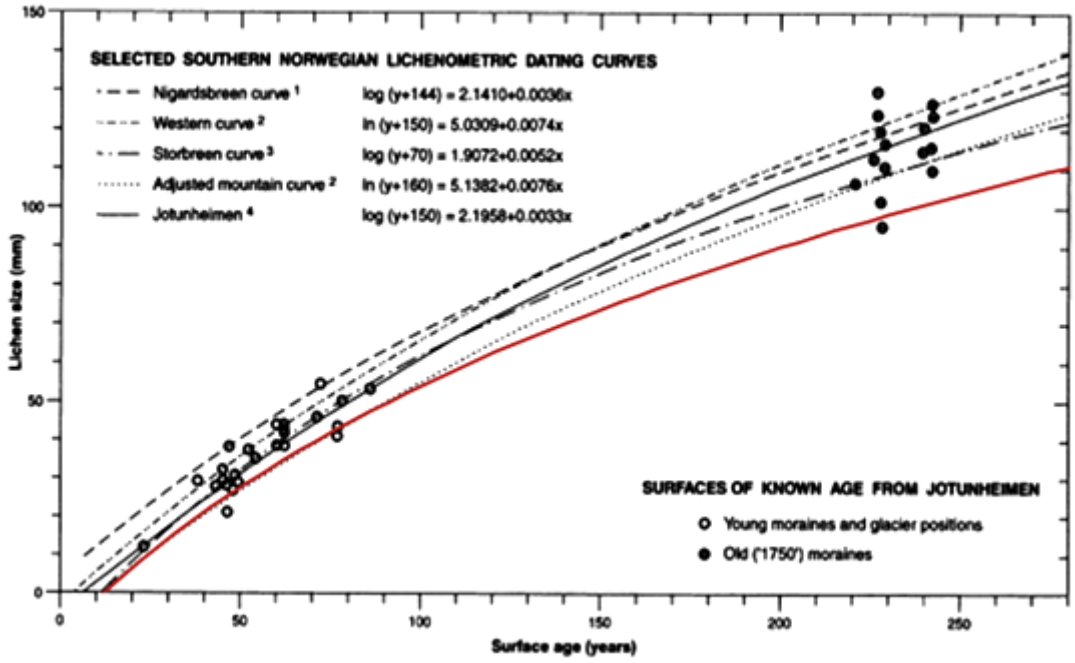

Figure 4.2: Selected published lichenometric dating curves from Southern Norway

Curves are in relation to the lichen sizes on surfaces of known age in Jotunheimen used as control points. Nigardsbreen (Bickerton and Matthews, 1992), Western and Adjusted Mountain (Erikstad and Sollid, 1986), Storbreen (Matthews, 1994) and Jotunheimen (Matthews, 2005). The reddish curve is not part of the original figure. It represents the Nordvestlandet curve by Erikstad and Sollid (1986), and has been sketched and adapted to be compared to the former curves. Figure gathered from Matthews (2005).

The Nordvestlandet curve is applied in Fosdalen, because it is based on control points relatively close to the investigated area (fig.4.2). Compared to the other curves, it seems to overestimate age. However, as this curve is based on the westernmost control points, lichen growth rates may be relatively high, as suggested by Matthews (2005). In addition, the control points in the figure above are from Jotunheimen which lies several miles east. The north western curve is therefore justifiable to use for this thesis. Besides, it will contribute to placing landforms in time relative to each other. For this thesis, the time frame has been divided into 5 year intervals, meaning each landform age estimate is ± 4 yr.

4.5 Existing datasets

4.5.1 Former research

Nesje and Dahl (1992) sketched a map showing their perspective on glacial chronology in Fosdalen (fig.4.3). This map has provided the basis for this thesis.

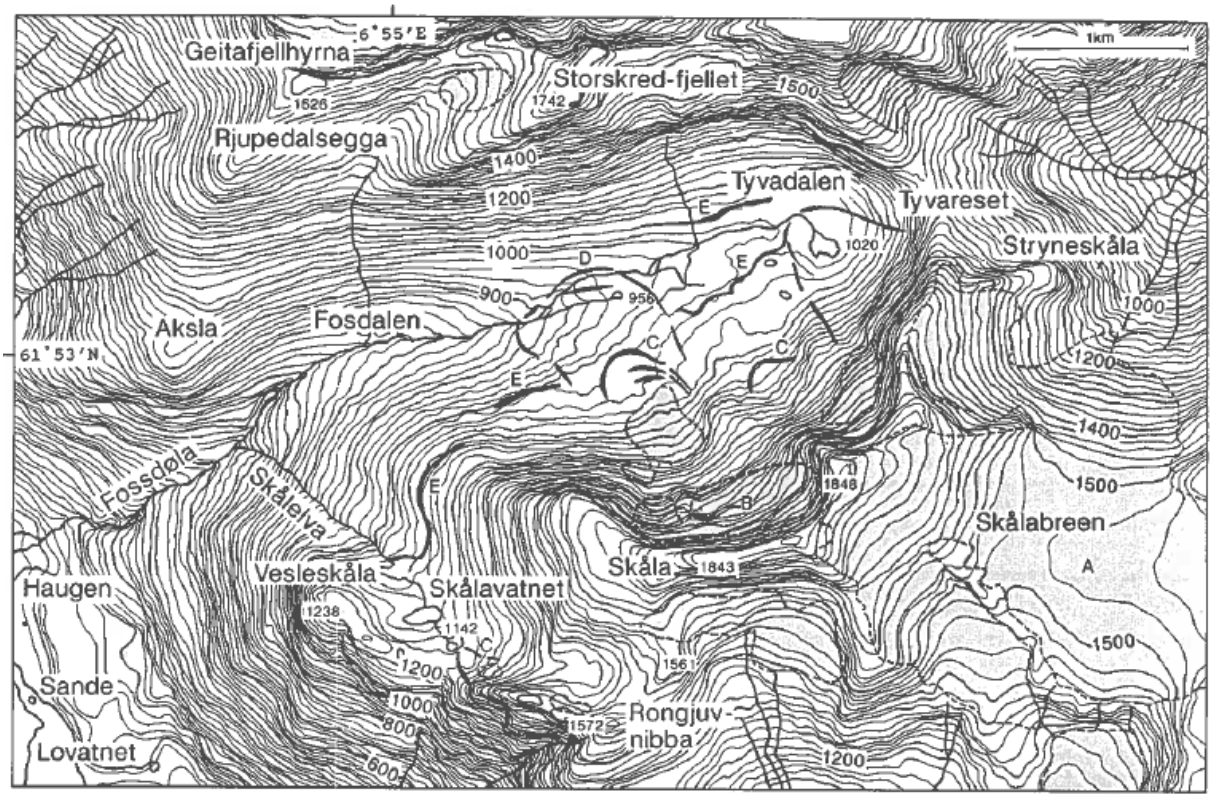

Figure 4.3: Former landform interpretations in Fosdalen

A is the Skålabreen plateau glacier. B is the western cirque glacier in 1992. C is LIA marginal moraines. D is Erdalen Event marginal moraines. E is YD marginal moraines. From Nesje and Dahl (1992).

4.5.2 Maps

Several sets of basic map data were used in this paper.

First, digital maps displayed at www.norgeibilder.no. Datasets were *Sogn 2010* (Statens Kartverk, 2010) and *Sogn 2005* (Statens Kartverk, 2005). The latter was only used for temporal comparisons of snow and ice abundance, and additional interpretation with different light settings. *Sogn 2010* was used for area, length, and altitudinal measurements as well as for landform interpretations.

Second, the virtual globe *norgei3d* was used for landform interpretations (Norkart, 2001).

Third, *Kvartærgeologisk kart over Norge. Tema: Jordarter* by Thoresen (1990) was used to compare deposits registered to the findings in this study.

Fourth, digital maps showing lithological features from Norwegian Geological Survey were used to determine bedrock geology in the study area (NGU, 2011a, NGU, 2011b).

Fifth, a topographic dataset provided by Stryn municipality was used to calculate volumes and longitudinal profiles (Stryn Kommune, 2014).

Finally, a mosaic dataset consisting of digital orthographic photos, with spatial resolution 0.5 m provided by Hans Ola Fredin in a previous GIS course were used for mapping and landform interpretation. The orthographic photos are from the *Sogn 2010* dataset mentioned above (Statens Kartverk, 2010).

4.5.3 Meteorological data

Temperature and precipitation measurements from Loen and Oppstryn parishes were gathered from Norwegian Meteorological Institute at www.eklima.met.no (Meteorological Institute, 2014).

4.5.4 Temperature lapse rate

The temperature lapse rate was established after confirmation from an NGU researcher (A. Beylich, personal communication 2014)

5. Results

5.1 Site descriptions

First in this chapter the study area is divided into five separate sites. The next step is to describe the landforms within each site, and their influencing processes based on observations. In addition, lichen data is presented for each site in order to estimate landform age.

The study area is divided into two categories, and five separate sites. The categories are M-sites which are highly influenced by glacial processes, and R-sites that may be visible expressions of other main processes. The five sites are the following:

- M1 includes evident moraine forms and a plain below the western cirque glacier.
- M2 includes moraine forms and ridges below the western toe of the eastern cirque glacier.
- M3 includes a longitudinal ridge, a plain, and moraines below the eastern toe of the eastern cirque glacier.
- R1 includes the debris-landform systems and river area north and west of M1.
- R2 includes a hitherto unmapped debris -landform system, and a mapped Younger Dryas lateral moraine (Thoresen, 1990).

Whereas the sites M1, M2 and R1 are relatively easy to separate due to their morphologic features, sites M3 and R2 intersect with each other. The split chosen is due to the strategic choice of separating places that clearly have been influenced by glacial activity, to those where other processes seem to be most influential. In this case, a longitudinal ridge seems to be both a lateral moraine (chapter 5.4), and part of a former talus system (chapter 5.6).

Figure 5.1: Panorama picture visualizing the study area seen from north

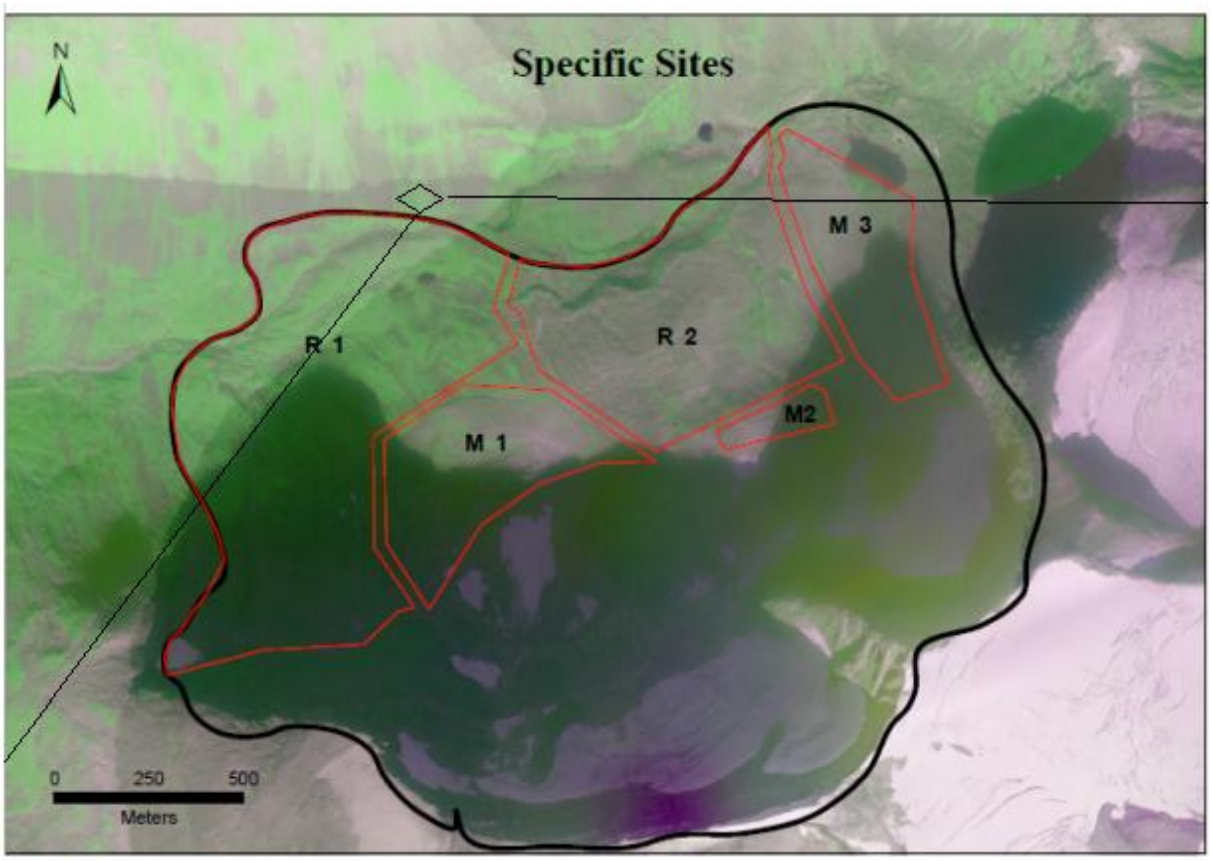

Figure 5.2: Specific sites overview

The five specific sites within the study area where measurements and observations were made are separated by red lines. Green areas are caused by vegetation, and dark areas are caused by mountain shadow. The square show pictorial position for the panorama picture in figure 5.1 above (Statens Kartverk, 2010).

5.2 M1 site

a)

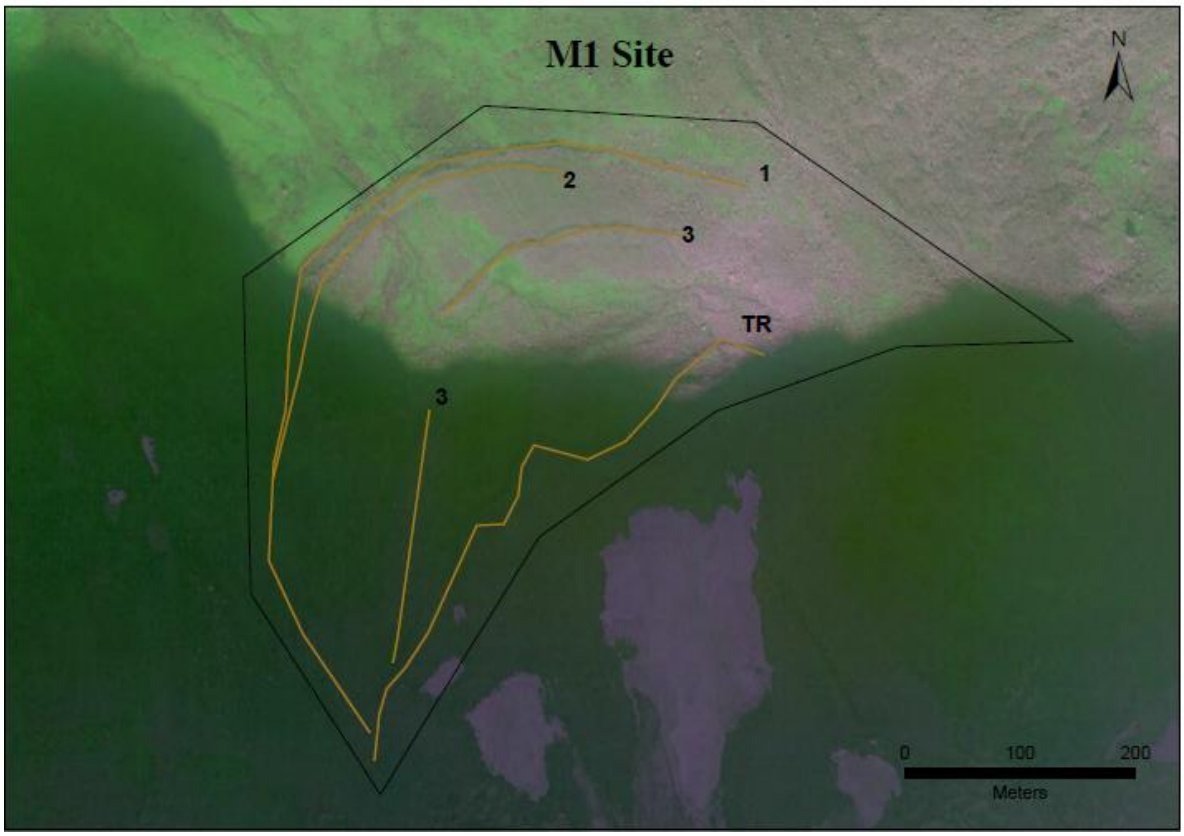

b)

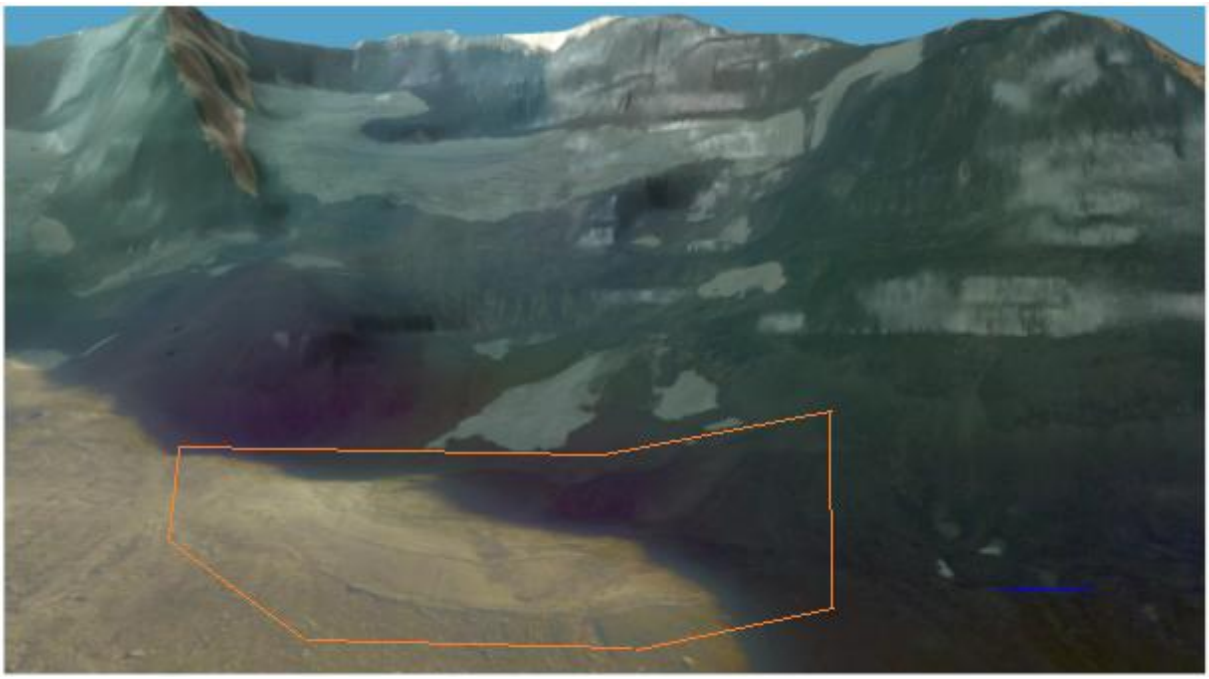

c)

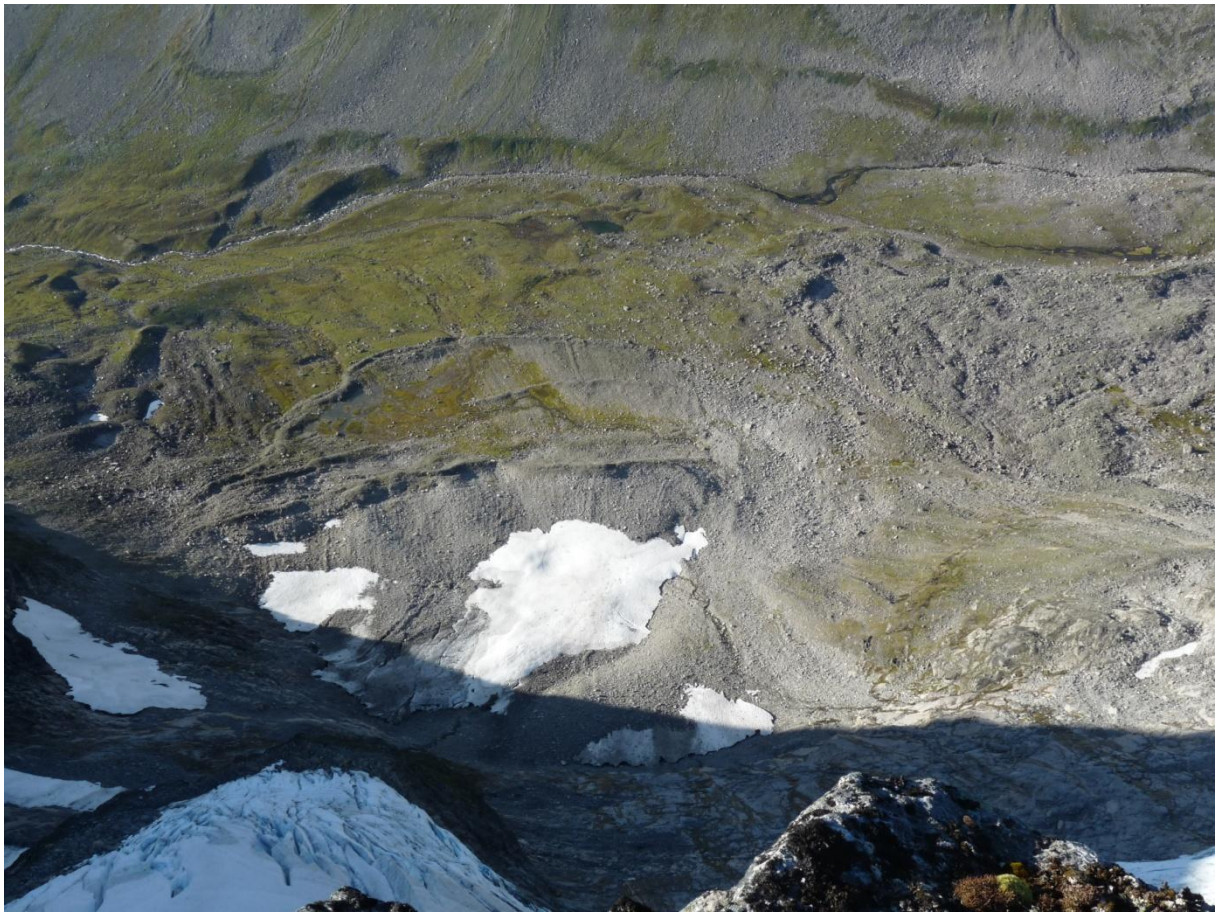

Figure 5.3: M1 site overview

a) Sketched orthographic photo (Statens Kartverk, 2010) M1-1: terminal moraine. M1-2: moraine with an even upper surface. M1-3: moraine interrupted by plain. M1-TR: transverse ridge. b) M1 site sketched (Norkart, 2001). c) picture taken from Skåla. Photo: Ivar Berthling.

5.2.1 Spatial data

5.2.1.1 M1-TR

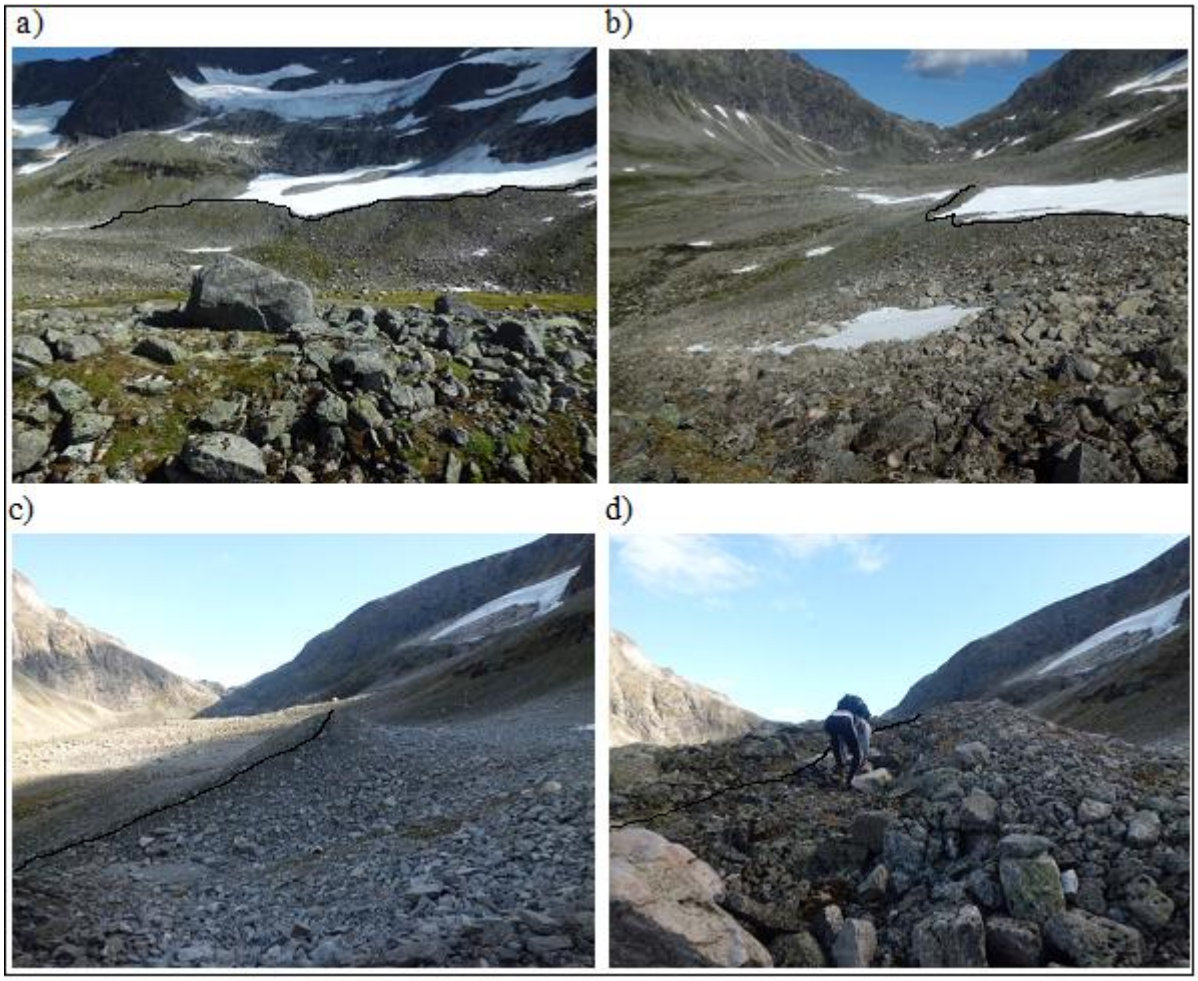

Figure 5.4: M1-TR

Two parallel transverse ridges named M1-TR. a) M1-TR seen from below. Western cirque above. b) M1-TR and late lying snow. c) M1-TR during late summer. d) close up picture of M1-TR, consisting of two parallel ridges. Myself for scale when measuring lichens on the proximal side of the outer ridge. Photo: Arvid Gjørven

M1-TR consists of two parallel transverse ridges that cross the former glacial floor in front of the western cirque glacier (fig.5.4). The outer ridge has a steep distal side, and is about 20 meters tall (fig5.4a). Debris is unsorted and semi rounded. A few large boulders can be seen on the plain in front. The outer ridge has little vegetation, except at the drainage point, where the ridge is pushed slightly forward. The other parallel inner ridge lies adjacent, and consists mostly of unstable angular rocks and boulders (fig.5.4c). Note that lichens were only measured on the outer ridge (fig.5.4d), as it is likely that the parallel inner ridge has worse growth conditions.

Current influencing processes include first and foremost snow avalanches indicated by late lying snow (fig.5.4b). Second, rock fall activity is indicated by debris angularity on the inner ridge. Debris behind the inner ridge is fall sorted, which indicates rock falls are either distributed onto snow, or redistributed by snow avalanches. Third, debris flows indicated by gullies, levees and lobes. Finally weathering indicated by weathered debris on the outer ridge. Debris on the inner ridge is also weathered, though very limited.

5.2.1.2 M1-1

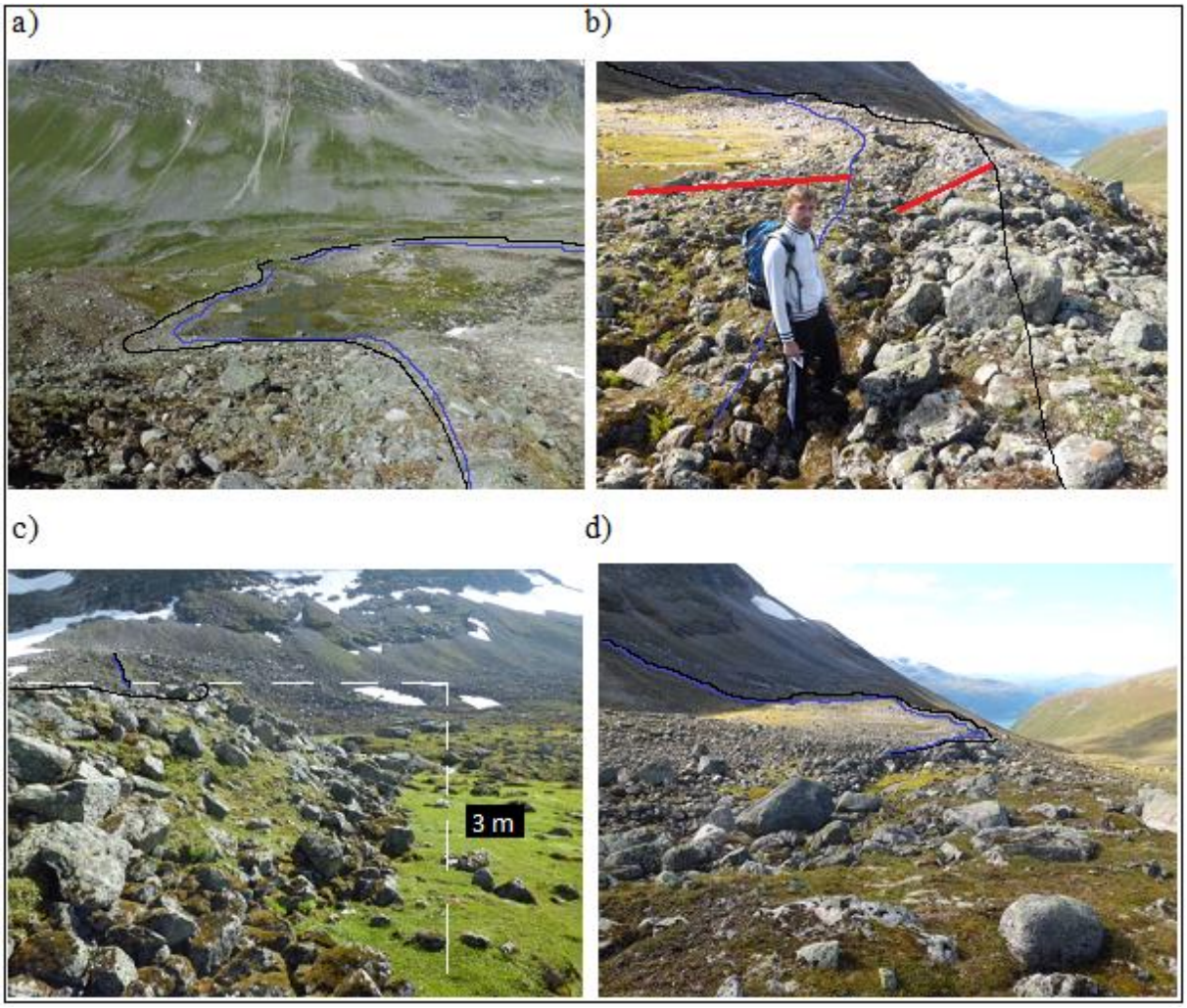

Figure 5.5: M1-1 and M1-2

Black line: A terminal moraine named M1-1. Blue line: Adjacent moraine named M1-2, which is fused with M1-1 where the colored lines lie into each other. Red line: Difference in angle on the proximal sides. a) western and frontal part of M1-1, seen from above. b) M1 and M2 lie adjacent to each other, and that M2 has an even upper surface. c) distal side of M1 and vegetation outside. d) eastern part highly modified, and one of many gullies heading down slope. Photo: Arvid Gjørven

M1-1 is a terminal moraine 2-3 m high, beneath the western cirque glacier. Debris is mostly unsorted and semi rounded, although some boulders are more or less angular. The distal side

of the foremost part is vegetated, and vegetation below the moraine is well developed (fig.5.5c). Debris on the proximal side is partially covered with moss (fig.5.5b). Note that the western part of the lateral moraine lies on top of TR (fig.5.5a,d).

Current influencing processes affect mostly the eastern part. M1-TR above combined with surrounding topography, redirects several of the processes mentioned above to this area and modifies and/or erases that side of the moraine. Direct observations include late lying snow, gullies, and levee channels. The foremost and western part may be influenced by boulders and avalanches crossing M1-TR, and increased erosion from runoff during melt season.

5.2.1.3 M1-2 and plain within

The inner moraine adjacent to M1-1 is named M1-2, although they merge into one moraine several places (fig.5.5a). M1-2 has an even upper proximal surface. Its height cannot be observed because it lies adjacent to the M1-1. Debris on the proximal surface is mostly semi rounded and more vegetated than on its exceeding counterpart. Debris on the distal side is similar to the proximal side of the lateral moraine.

The plain inside contain both angular and semi rounded boulders. Several boulders are partially buried in the vegetated ground, and a few lie on top of it. Most of the boulders are colonized by moss. The plain has moss on top, and a thin layer of soil beneath it. Underneath lies a thick layer of gravel and sand. It is unclear how thick this layer is.

Current influencing processes are few, as most of the processes mentioned earlier are at work further east. Nevertheless, angular boulders without lichen indicate that rock falls occur. However, they may have been transported by avalanches, although no perched boulders were observed. Additionally, runoff streams pass through the plain and may contribute to a thicker layer of sediments.

5.2.1.4 M1-3

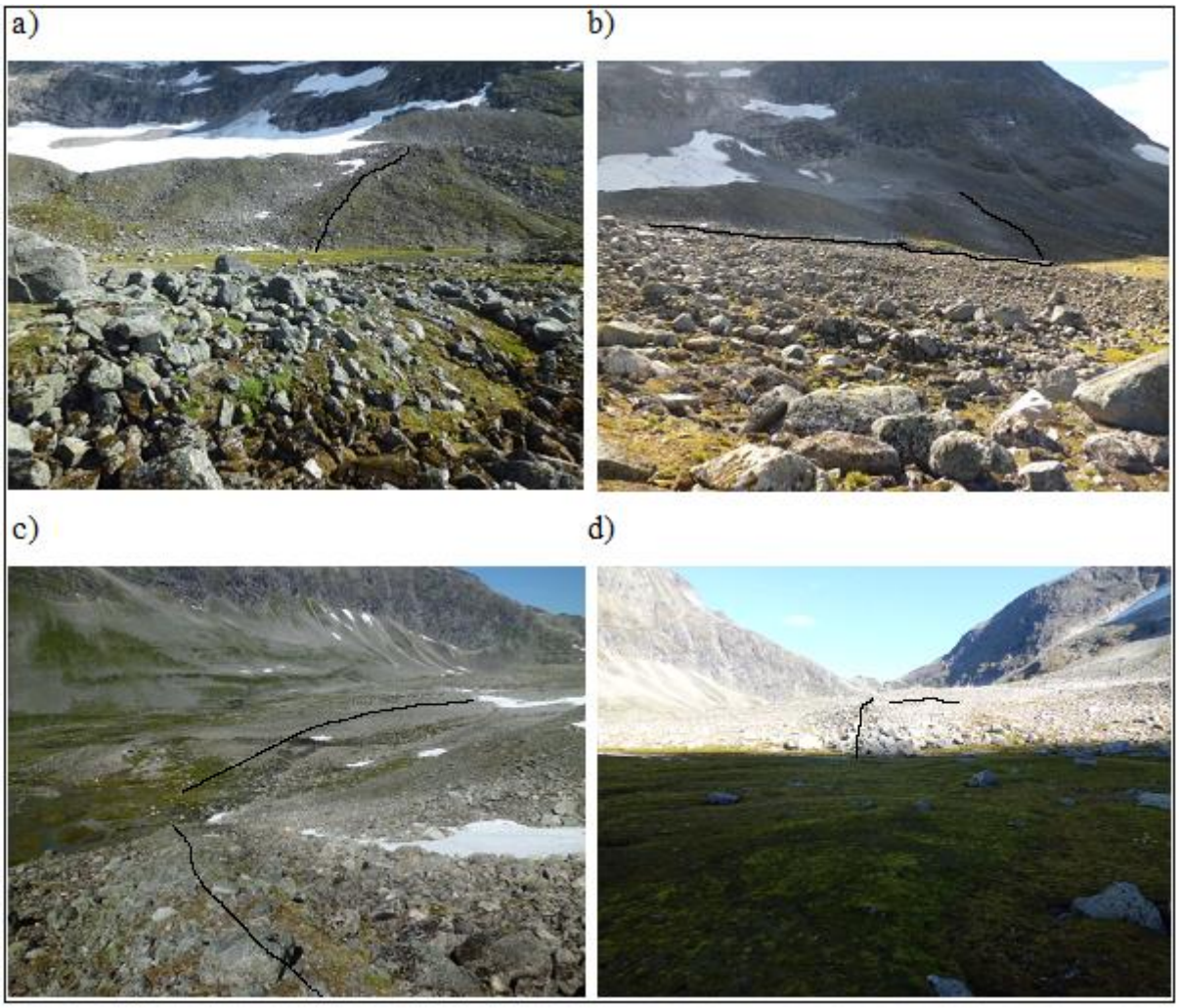

Figure 5.6: M1-3

Black line: M1-3. a) western part of M1-3 disappear into the plain. b) M1-3, seen from north east. Note that south western part of M1-1 (which at this point is fused with M1-2) and M1-3 lie on top of M1-TR. c) M3 seen from above. d) eastern part of M3 disappear into the plain.

M1-3 is a moraine that lies in the middle of the plain (fig.5.6c). It has the same characteristics as the outermost moraines except that is has less vegetation and moss. Moreover the height is only about 1 m. Additionally, the plain interrupts the northwestern part of this moraine (fig.5.6a,d). Note that the western part of M1-3, along with the outermost moraines, lies on top of M1-TR (fig.5.6a,b).

Influencing processes are probably the same as the exceeding moraines. Particularly it seems that runoff increases plain height, thus parts of the moraine is buried underneath it.

5.2.2 Temporal data

The dating curve chosen for the lichenometric data, is the Nordvestlandet curve by (Erikstad and Sollid, 1986). According to this curve and the 5LL method, M1-TR is the youngest of the measured forms within the M1 site. However, based on morphostratigraphy, M1-TR is the oldest landform and the date in table 5.1 thus only indicates the time it was last deglaciated. M1-1 is the second oldest landform, and dates back to 1769 AD. M1-2 dates back to 1819 AD. The distal upper surface of M1-2 was measured twice, but closer to the plain the second time in order to figure out whether the whole distal surface was of the same age. The second measure is named M1-2: Surface in table 5.1, and dates back to 1824 AD. M1-3 is dated to 1874 AD.

Table 5.1: M1 lichen data

Please note that lichen age in this study is divided into 5 year intervals.

	M1-TR	M1-1	M1-2	M1-2: Surface	M1-3
5LL size [mm]	46,2	101	87	86,6	70,6
Age					
BP (yr)	85	245	195	190	140
AD	1929	1769	1819	1824	1874

5.3 M2 site

a)

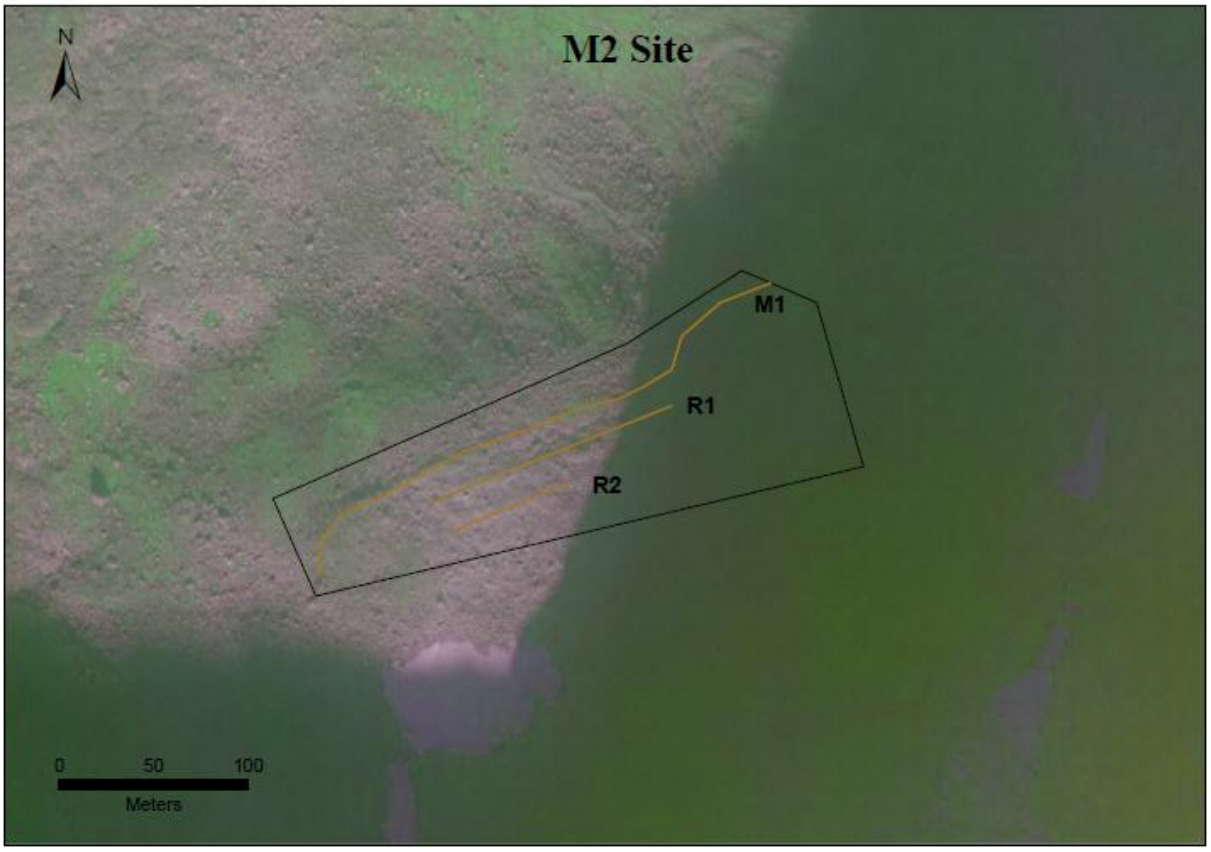

b)

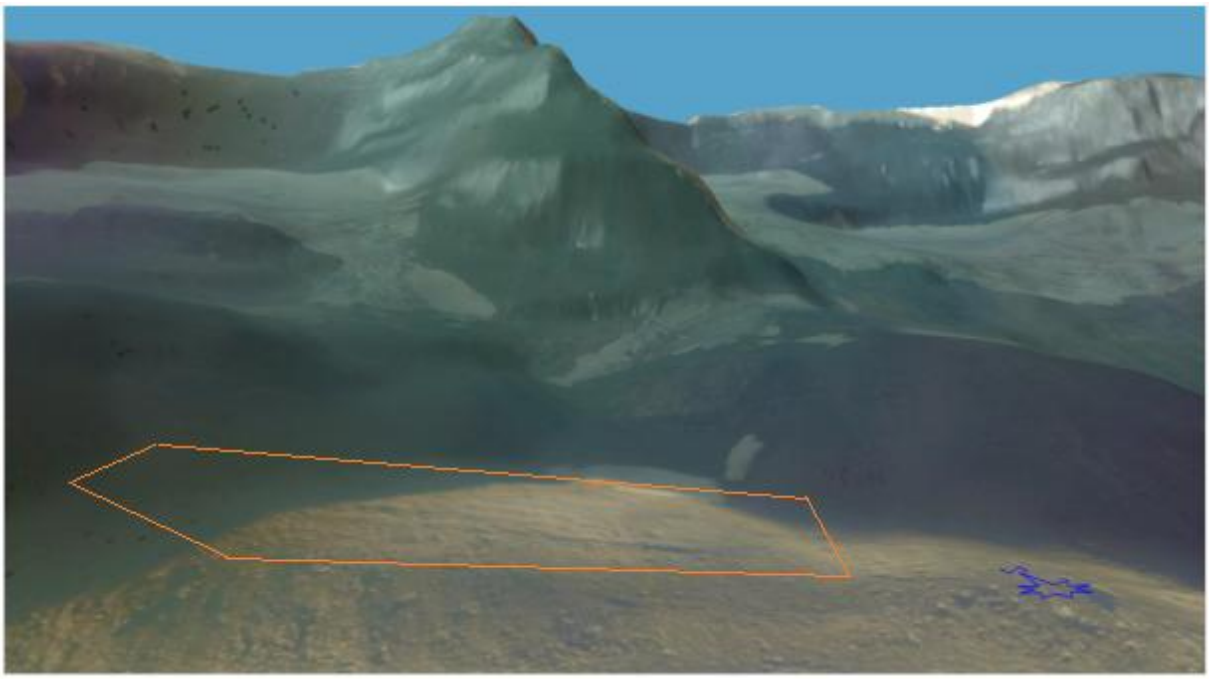

Figure 5.7: M2 site overview

a) Sketched orthographic photo (Statens Kartverk, 2010) M2-M1: terminal moraine. M2-R1: transverse ridge. M2-R2: bump. b) M2 site sketched (Norkart, 2001)

5.3.1 Spatial data

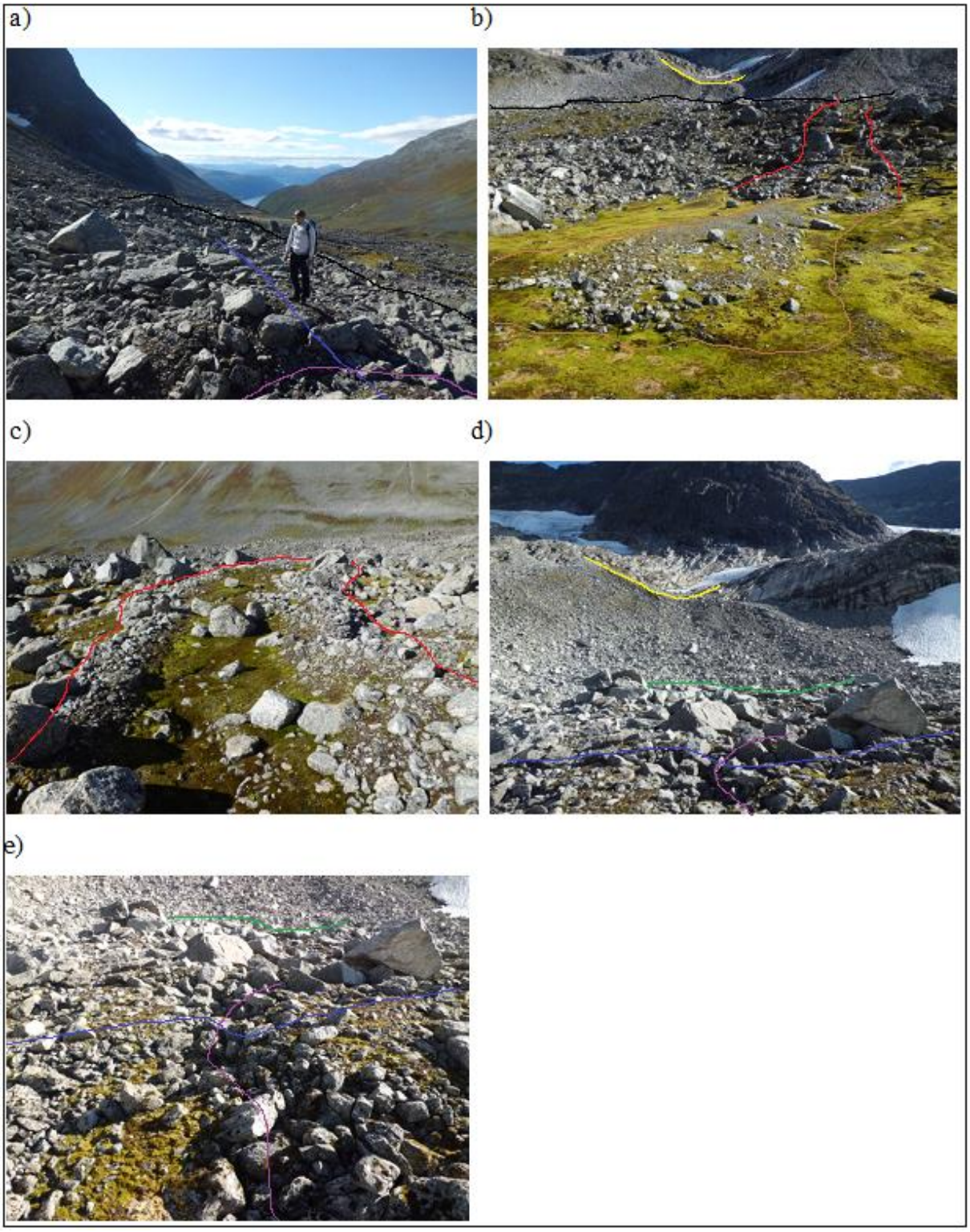

Figure 5.8: M2 site investigated landforms

Black line: M2-M1. Blue line: M2-R. Purple line: Furrow in M2-R1. Green line M2-R2. Red line: Levee. Brown line: Debris flow lobe. Yellow line: Recent moraine, not investigated. a) M2-M1 and M2-R1. Person for scale. b) M2-M1 on

top of the slope. Note the lobe and levee in front. c) levee seen from above. d) fall sorted debris below arête. e) M2-R1 ridge with minor furrow. M2-R2 bump in the back. Photo: Arvid Gjørven.

M2-M1 is a terminal moraine. Along with M2-R1 (ridge) and M2-R2 (bump), they constitute the investigated landforms at the M2 site, and lie in front of the eastern cirque glacier at its western toe (fig.5.7). M2-M1 is 1-2 m high, and its eastern part is mostly buried or destroyed by angular boulders. All three forms consist of semi rounded debris partially covered with angular boulders on top. M2-R1 and M2-R2 have more vegetation than the outermost M2-M1. M2-R2 is so short it might be defined as a bump. M2-R1 is the only one with vegetation. The height of the two latter forms are about 1 m. Debris above is fall sorted without growth.

Current influencing processes are mainly rock falls, based on the fall sorted angular debris. Below the lateral moraine, lie several levees and lobes with pebbles and gravel on their sides and on their front, and finer material in the middle (fig.5.8b-c). These indicate debris flows. At least one stream can be heard flowing underneath, or somewhere within the debris underneath the site. Moreover, perched boulders indicate snow avalanche activity. Finally, the bright area below the arête, was until recently covered by glacial activity.

5.3.2 Temporal data

Lichen data estimates the lateral moraine to 1859 AD. R1 has little or no lichen growth. LL on M2-R2 is less than 40 mm, which means it became ice free no earlier than 1944 AD. Based on morphostratigraphy, it is possible that M2-R1 and M2-R2 are older than M2-M1, but no conclusion can be drawn based on current observations.

Table 5.2: M2 lichen data

	M2-M1	M2-R1	M2-R2
5LL size [mm]	74,5	No growth	< 40
Age (yr)			
BP	155		
AD	1859		

5.4 M3 site

a)

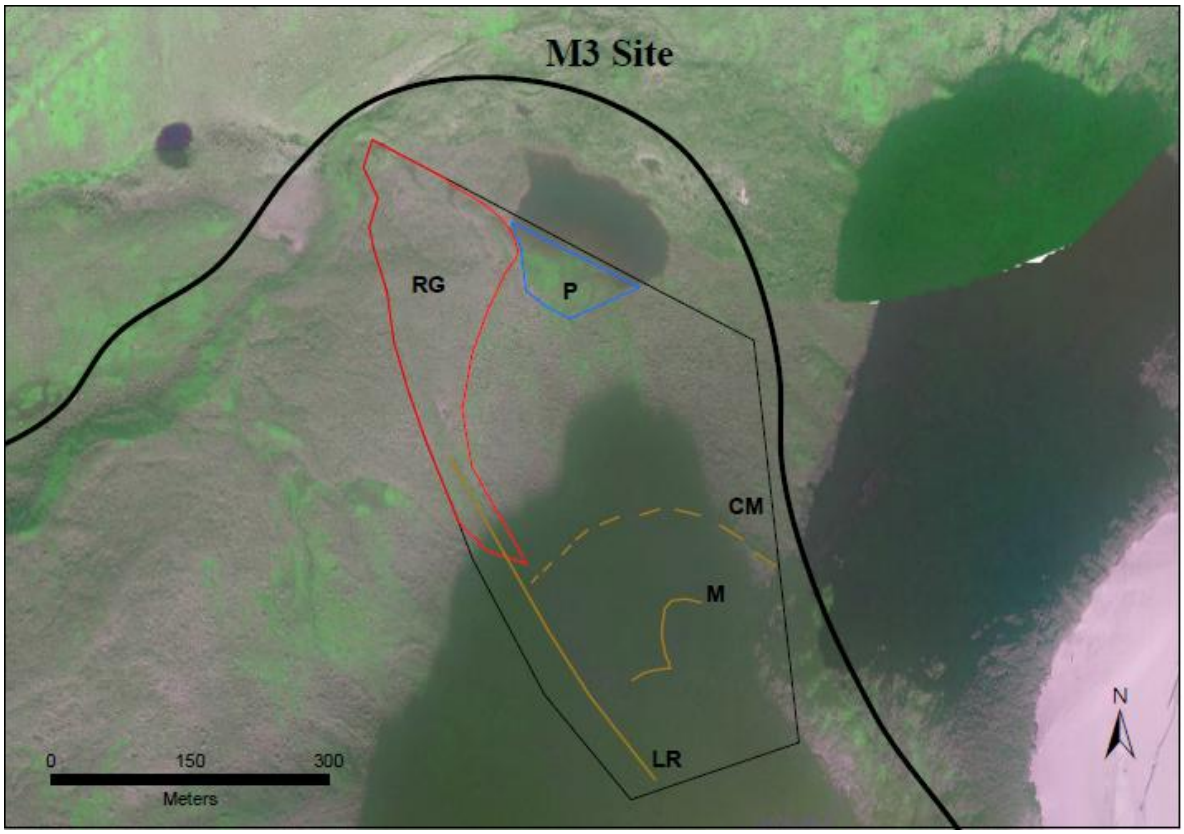

b)

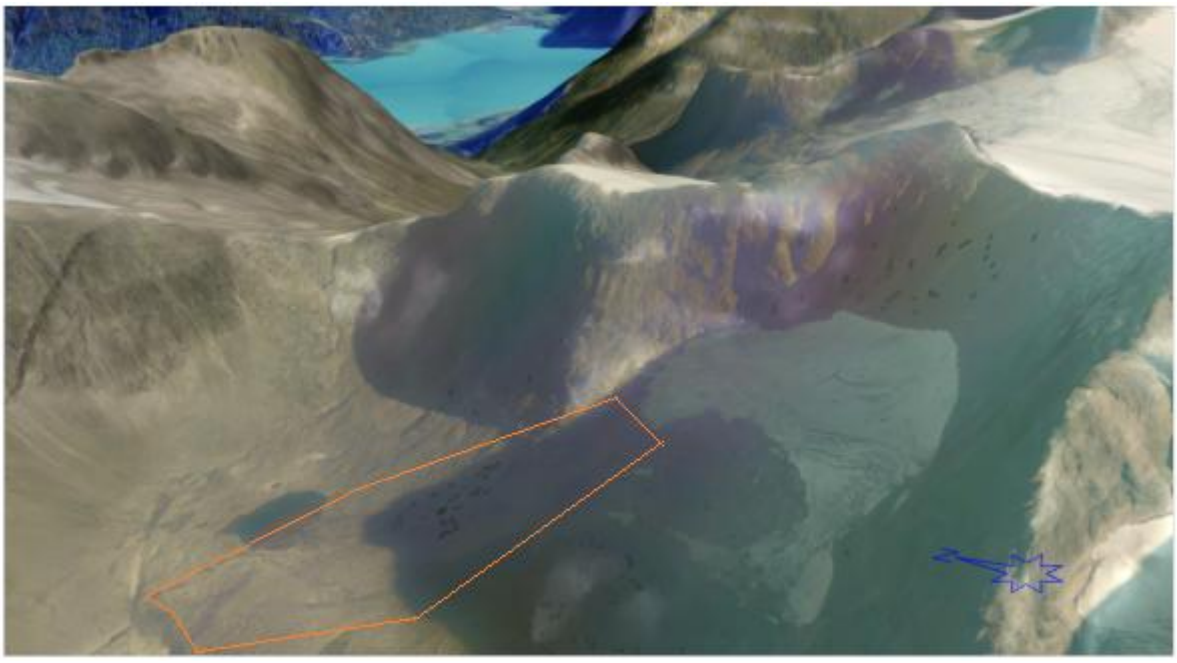

Figure 5.9: M3 site overview

a) Sketched orthographic photo (Statens Kartverk, 2010) M3-M: moraine close to modern glacier. M3-CM: contoured moraine. M3-P: plain. M3-RG: eastern part of the hitherto unmapped debris -landform system. M3-LR: longitudinal ridge. b) M1 site sketched (Norkart, 2001).

5.4.1 Spatial data

5.4.1.1 M3-M

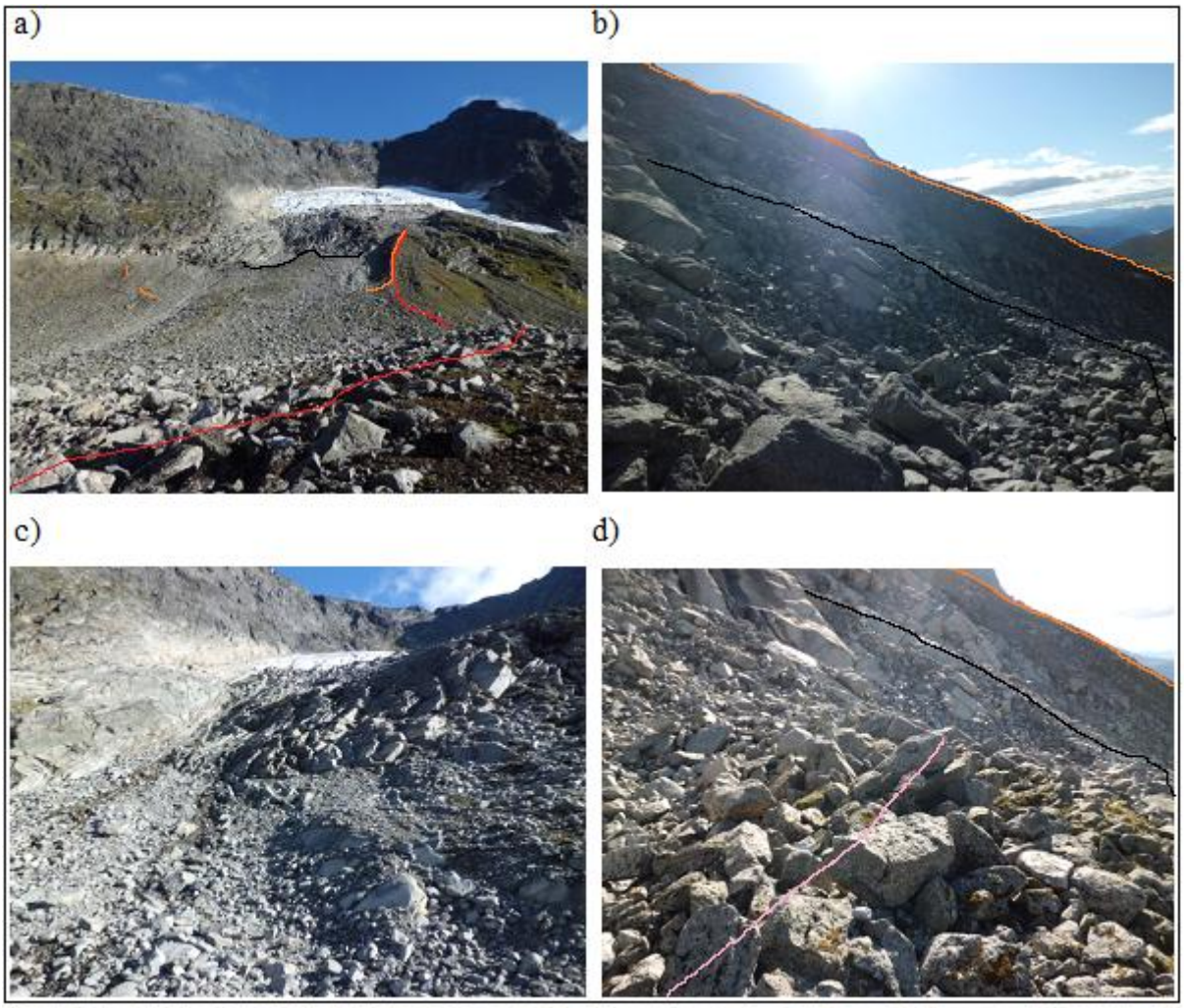

Figure 5.10: M3-M

Black line: M3-M. Orange line: M3-CM. Red line: M3-LR. Pink line: layer of deposits in a weird position. a) eastern cirque seen from below. M3-M close to the glacier, M3-LR heading down slope, and turning east (M3-CM). b) parts of M3-M, and M3-CM. Picture taken from a ridge above M3-M. Note joints, cracks and bedding direction. c) bedding direction. d) ridge behind M3-M. Note layer of deposits in a weird position.

M3-M is a moraine that lies in front of the eastern cirque glacier at its eastern toe (fig.5.10a). The height is difficult to measure as it is lies on top of a large transverse ridge that is invisible on the datasets used due to mountain shadow (fig.5.9). M3-M consists of semi rounded, and angular debris, and is has little or no vegetation. All around the moraine, a lot of angular and highly unstable debris can be observed (fig.5.11). Several boulders found have similar angle of inclination as the stratified bedrock (fig5.10b-c). Also, angle of joints and cracks are generally 90˚ to the stratification.

Current influencing processes are probably enhanced runoff during melt season, snow avalanche activity, and rock fall activity. The bright part of the headwall indicates recent glacier activity in those areas (fig.5.10a, c).

The underlying transverse ridge mentioned above has a front with at least an angle of response, and approximate height is estimated to > 20 m. A layer of deposits within the transverse ridge has a weird direction compared to other debris in the area (fig.5.10d).

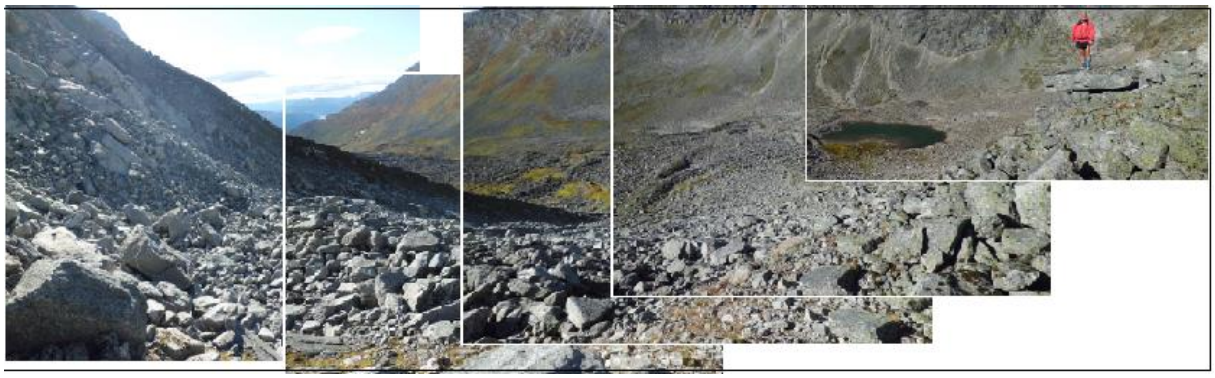

Figure 5.11: Panorama picture visualizing the M3 site seen from south

5.4.1.2 M3-LR

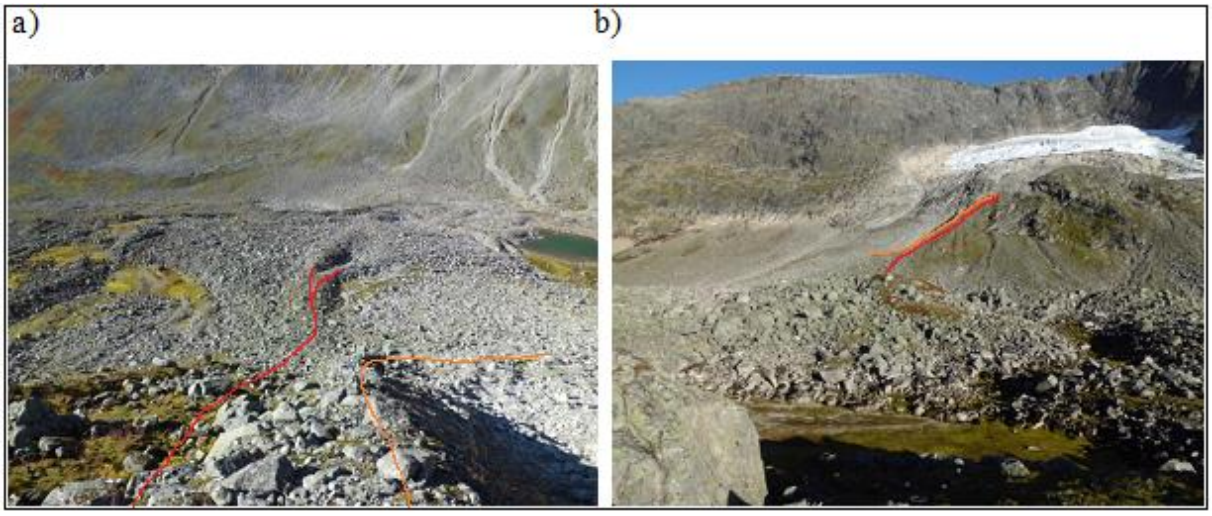

Figure 5.12: M3-LR

a) M3-LR heading down slope, and being part of a larger ridge that continues across the valley floor. b) M3-LR being part of an older talus system.

M3-LR is a huge longitudinal ridge that head down slope (fig.5.12). The west side of the ridge is old, and heavily vegetated. In contrast, the east side has less vegetated debris that lies on top of the old ridge (a). On the east side, debris also shows more variance in angularity. A

longitudinal depression splits M3-LR at the valley floor before it ends in a chaotic, fan like shape, with several ridges and furrows.

Current influencing processes are probably limited. The uppermost part of LR might be affected by enhanced runoff during melt season, avalanche activity and rock fall activity. Due to surrounding topography most processes will evade the ridge, except possibly erosion of the lower east side caused by rock fall and snow avalanche activity. Weathering can be observed on west side debris.

5.4.1.3 M3-CM

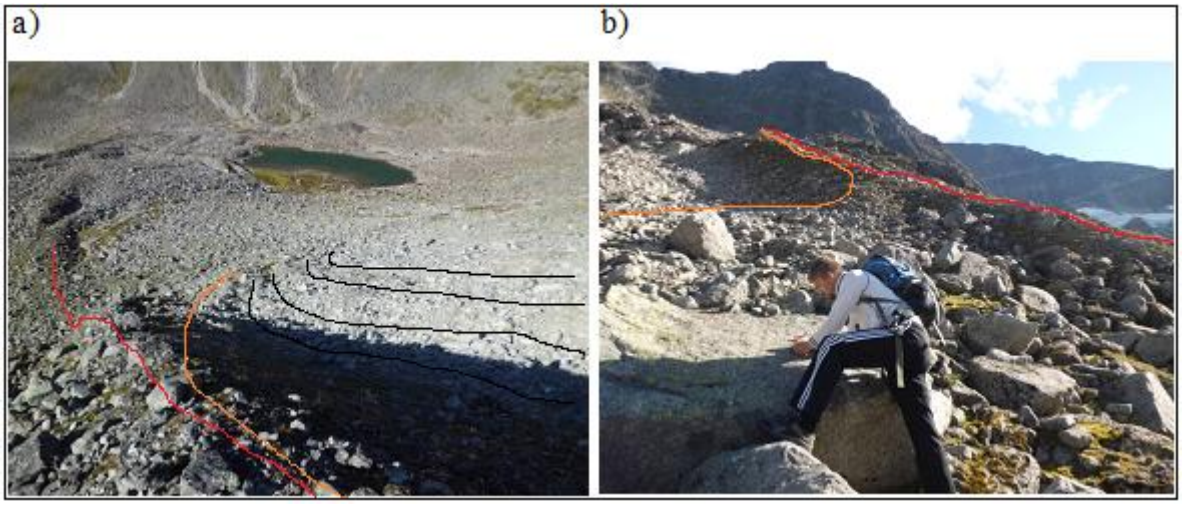

Figure 5.13: M3-CM

Red line: M3-LR. Orange line: M3-CM. Black lines: channels. a) M3-CM turning east, and several small channels inside following the same pattern. b) large boulder measured down slope of M3-CM. Photo: Arvid Gjørven

Halfway down towards the valley floor M3-LR splits, and contours of a former terminal moraine (M3-CM) can be observed (fig.5.13). While most of M3-CM is overridden by a lot of angular debris, the northwestern front is evident. The front contains several rounded and semi rounded debris in addition to several angular boulders. Upslope, several parallel channels follows the same pattern as M3-CM, i.e. longitudinal and then turning east (5.13a).

Current influencing processes are primarily snow avalanche activity, due to a lot of perched boulders and observation of late lying snow. Secondly, rock falls, based on the tendency of fall sorted angular debris.

5.4.1.4 M3-P

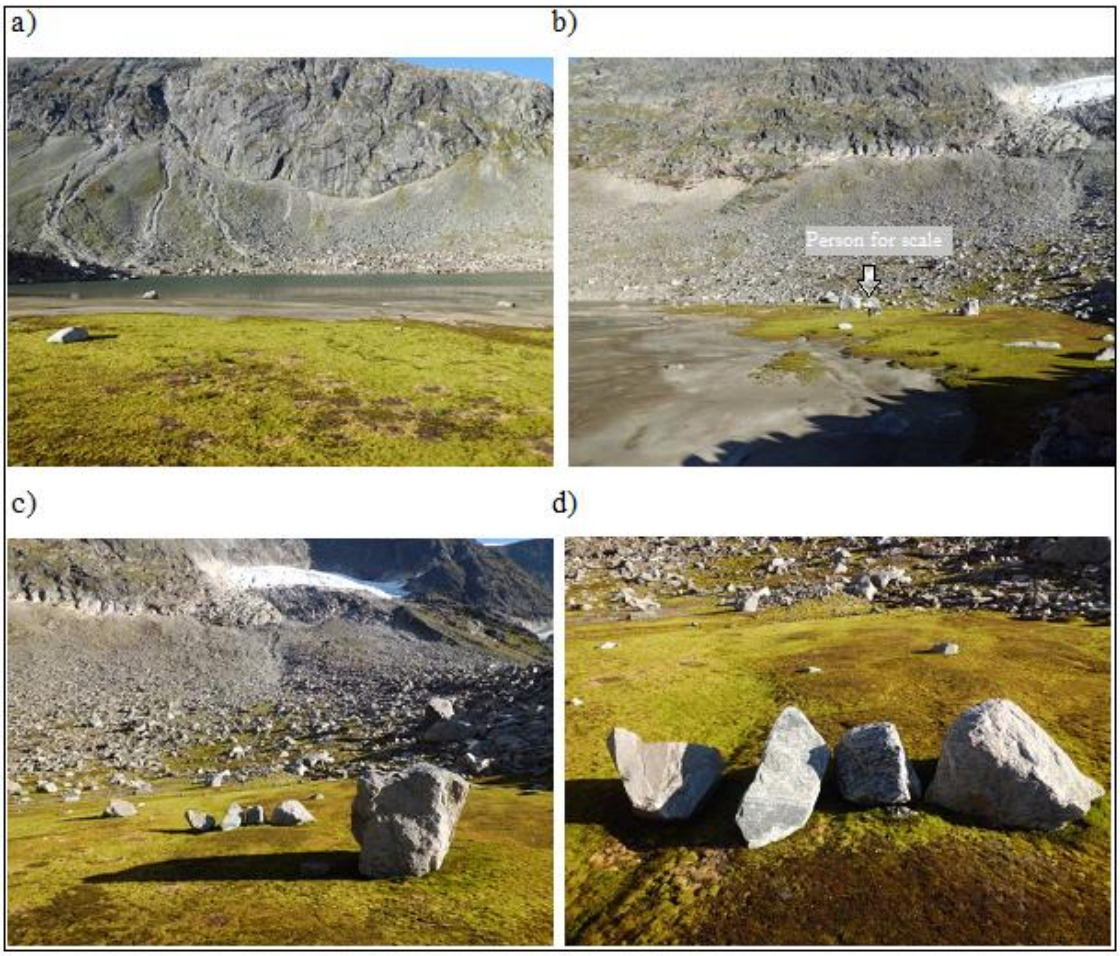

Figure 5.14: M3-P

a) plain and lake below eastern cirque. b) plain with person for scale. c) plain towards cirque glacier. Note height difference from the plain to the debris -landform system to the right. d) rocks with no lichens. Photo: Arvid Gjørven

M3-P is a plain at the valley floor below the eastern cirque (fig.5.14). A shallow lake occupies most of the plain. However, about 1/3 of the area is dry and covered with vegetation, mostly moss. Underneath is a layer of finer debris, whether it is clay, silt or sand. There is no moss close to the lake (fig.5.14b). Several large angular boulders without vegetation lie on top of the moss. In the back, a lobe similar to those described earlier can be observed along with plenty of angular debris, mostly large boulders (fig.5.14c-d).

Current influencing processes may include snow avalanche, and/or rock fall activity. The large boulders on the plane may have been redistributed from higher parts of the slope, or they may have disintegrated from the headwall and fallen, rolled, slid and jumped down to the plain. As there is no trace of the boulders journey in the moss behind them, chances are runoff

is filling the plain rather quickly. Moreover, the lobe indicates debris flows, which supports this argument.

5.4.1.5 M3-RG

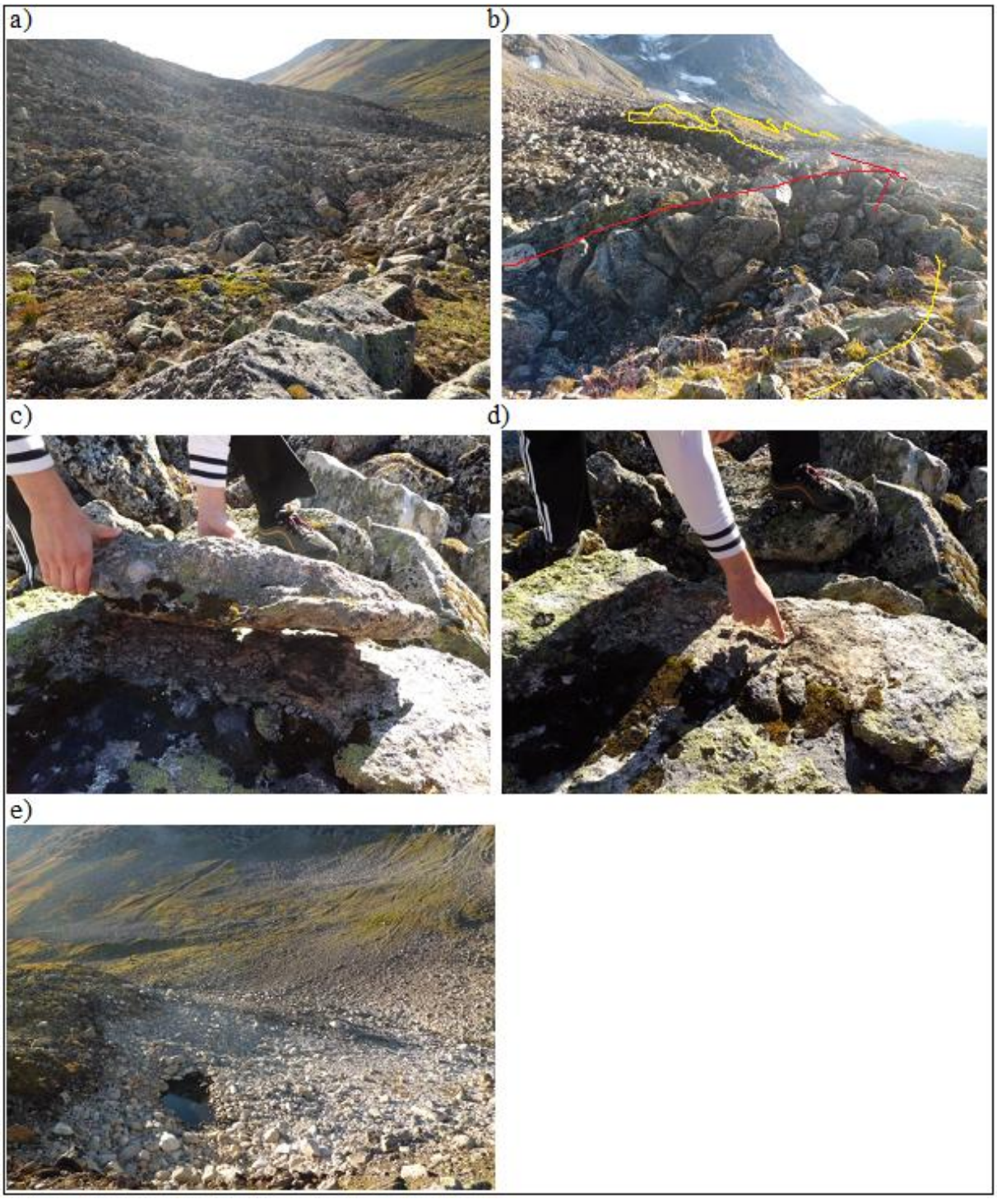

Figure 5.15: M3-RG

Yellow line: Younger Dryas lateral moraine (YDM). Red line: ridge from M3-RG lying onto YDM. a) M3-RG is composed of several transverse, diagonal and longitudinal ridges and furrows. b) M3-RG crashes into and onto a landform previously interpreted and mapped as a Younger Dryas lateral Moraine (Lien, 1985, Nesje and Dahl, 1992,

Thoresen, 1990), and a ridge lying onto the latter (see chapter 5.6). c-d) highly weathered debris. e) north eastern area in front of YDM. Note the color of the boulders. Photo: Arvid Gjørven

M3-RG lies west of the lake and plain. It is a body of unconsolidated debris with several transverse, longitudinal, and diagonal ridges and depressions can be observed. The average boulder size is large close to the Younger Dryas lateral moraine (YDM) at 1030 m a.s.l. compared to further upslope. Moreover, the foremost boulders lie close to, or on top of YDM, and seems to have been pushed onto it (fig.5.15b). Most boulders are at least partially covered with moss, and some of the ridges are almost completely covered (fig.5.15a). The general height of the body is at least 5 m compared to the plain. Moving westward, YDM is approximately 20 m high compared to the smoothed northern area, and the rock glacier about 1-2 m lower at the front. YDM at its easternmost end is about 10 m high, which is similar to the rock glacier height. However, backward heights varies a lot. Finally, the debris is heavily weathered (fig.5.15c-d).

Current influencing processes may be limited to weathering. However, 2005 AD pictures show late lying snow in almost all furrows, which imply snow avalanche activity (Statens Kartverk, 2005). Perched boulders has not been observed, but was not searched specifically for during field investigations, which makes interpretation difficult (see further discussion in chapter 6.4)**.**

5.4.2 Temporal data

M3-LR is estimated to 1904 AD (table 5.3). However, the measurements were made on the proximal side of the longitudinal ridge, which means the result is part of the M3-CM lateral moraine. Thus they cannot be used for estimating age of M3-LR. There is also a tendency of increased lichen size moving down slope. The M3-CM measurements have been carried out on the north western proximal side, as most of the front is destroyed. It is estimated to 1854 AD. However, the general size of boulders are small. According to (McCarroll, 1994), debris size and lichen size are connected. Thus including a large boulder on the distal side probably gives a more accurate age. When this boulder is included, M3-CM is estimated to 1809 AD.

M3-M has very little growth, and in addition, lichens are fused. All specimens are smaller than 36 mm, meaning it became ice free no earlier than 1949 AD. M3-P has no growth on the large boulders lying on top of it. The large boulders lay there in 2005 (Statens Kartverk, 2005), which means that time before colonization of lichens occur is at least 10 years, as there

are still no thalli to be found. M3-RG contain all lichen sizes including several large specimen, but they are fused. Thus M3-RG is estimated to be of an old age.

Table 5.3: M3 lichen data

	M3-LR	M3-CM	M3-M	M3-P	M3-RG
5LL size [mm]	58,4	76/90	< 36	No growth	Fused
Age (yr)					
BP	110	160/205			
AD	1904	1854/1809			

5.5 R1 site

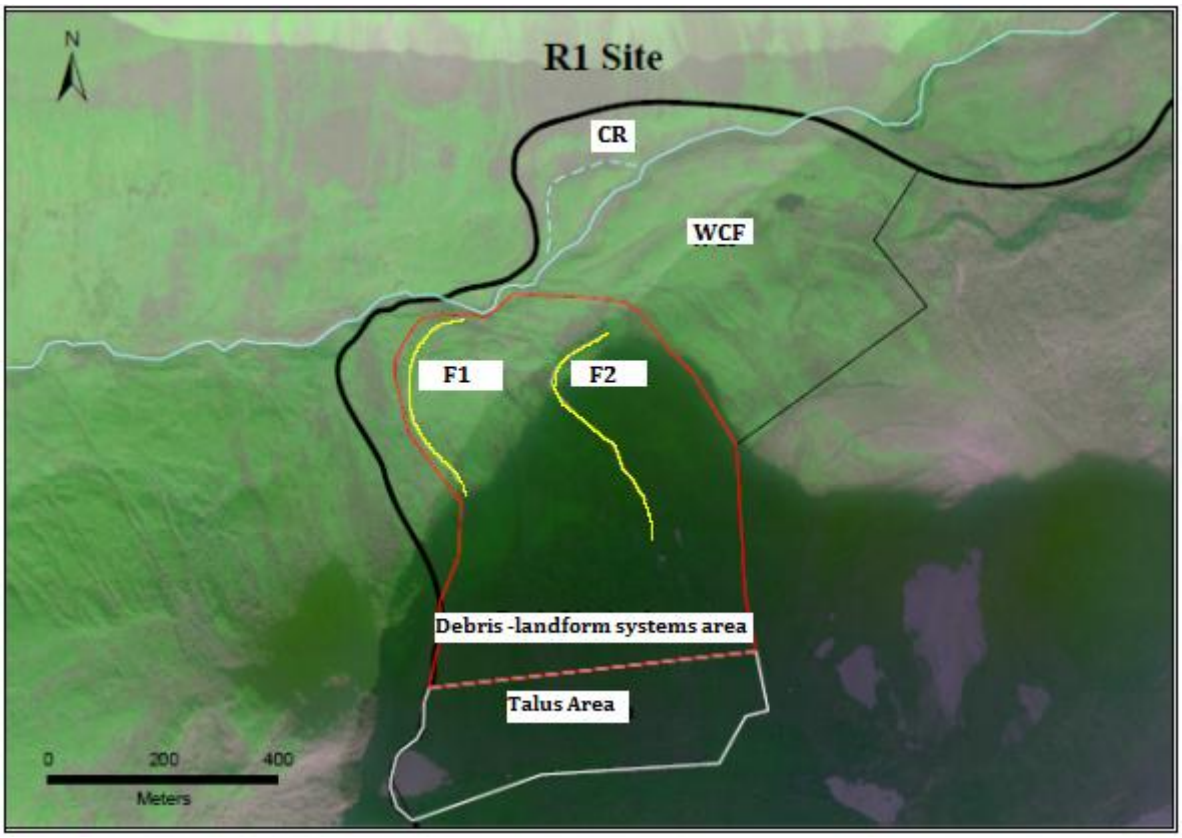

Figure 5.16: R1 site overview

Investigated landforms within the R1 site. Blue line: river. Blue contoured line: CR. Yellow lines: distinct slopes with an angle of response within the Debris -landform systems area. Note that this area is not the same as the debris -landform system referred to in the introduction. CR: ravine. WCF: western cirque glacier foreland (Statens Kartverk, 2010).

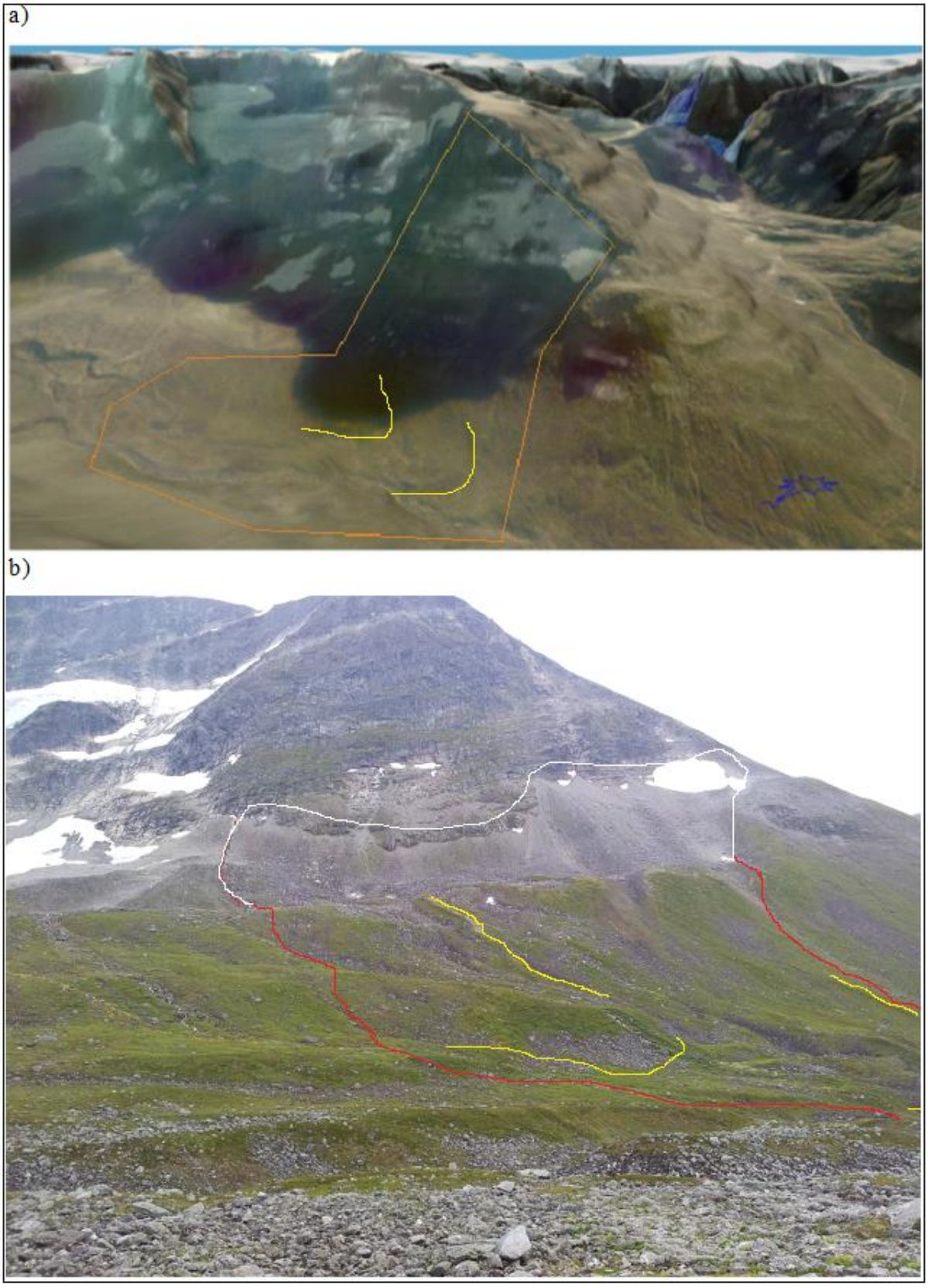

Figure 5.17: Western part of R1 site overview

Orange line: R1 site. Yellow line: distinct slopes with an angle of response. Red line: debris -landform systems area. White line: talus area. a) R1 site sketched (Norkart, 2001). b) western part of R1 site sketched

5.5.1 Spatial data

5.5.1.1 R1-F 1

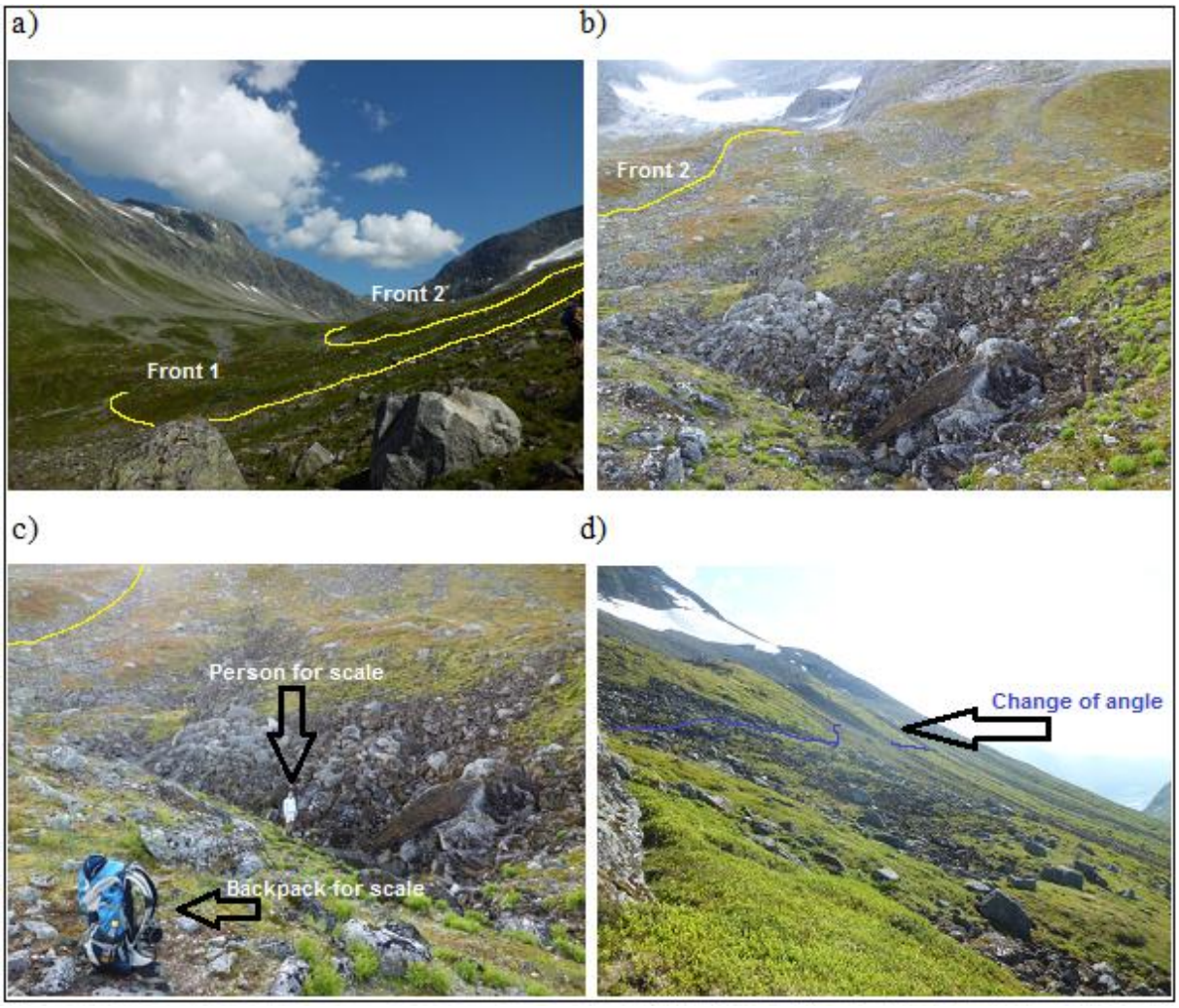

Figure 5.18: R1-F1

Yellow line: landform edge. Blue line: marked change in angle. a) R1-F1 and R1-F2 edges. b) R1-F1 area. R1-F2 marked to the left. c) huge furrows. Note scale elements. d) R1-F1 upslope. Note the marked change of angle. Photo: Arvid Gjørven

R1-F1 is a body of unconsolidated debris that lies west in the study area (fig.5.18a-d). The body is concave, with a steep front at the angle of response which is approximately 20 m high. Several large boulders have been deposited at the bottom of the front. The body contains several ridges, and huge furrows in transverse, longitudinal and diagonal directions (fig.5.18b-d). The body has a vegetation cover that consists of heather ling, and soil underneath. Except within furrows, where debris is almost fully covered by black moss, and additional singular boulders that lie all over the body.

Angle of inclination increase on the upper parts of the body, and additional boulders can be observed where the deviation occur (fig.5.18d). The height of the upslope body is 40-60 m, and the angle is steeper than the angle of response. Above this steep area, the upslope body is concave and ends as an even step (chapter 5.5.1.3).

Current influencing processes down slope are first and foremost weathering, deduced by highly weathered boulders. White angular boulders without lichens observed amounted to less than ten on R1-F1. Thus rock fall occur, but only on rare occasions. The lack of perched boulders indicate that potential avalanches stops at the even step above.

5.5.1.2 R1-F 2

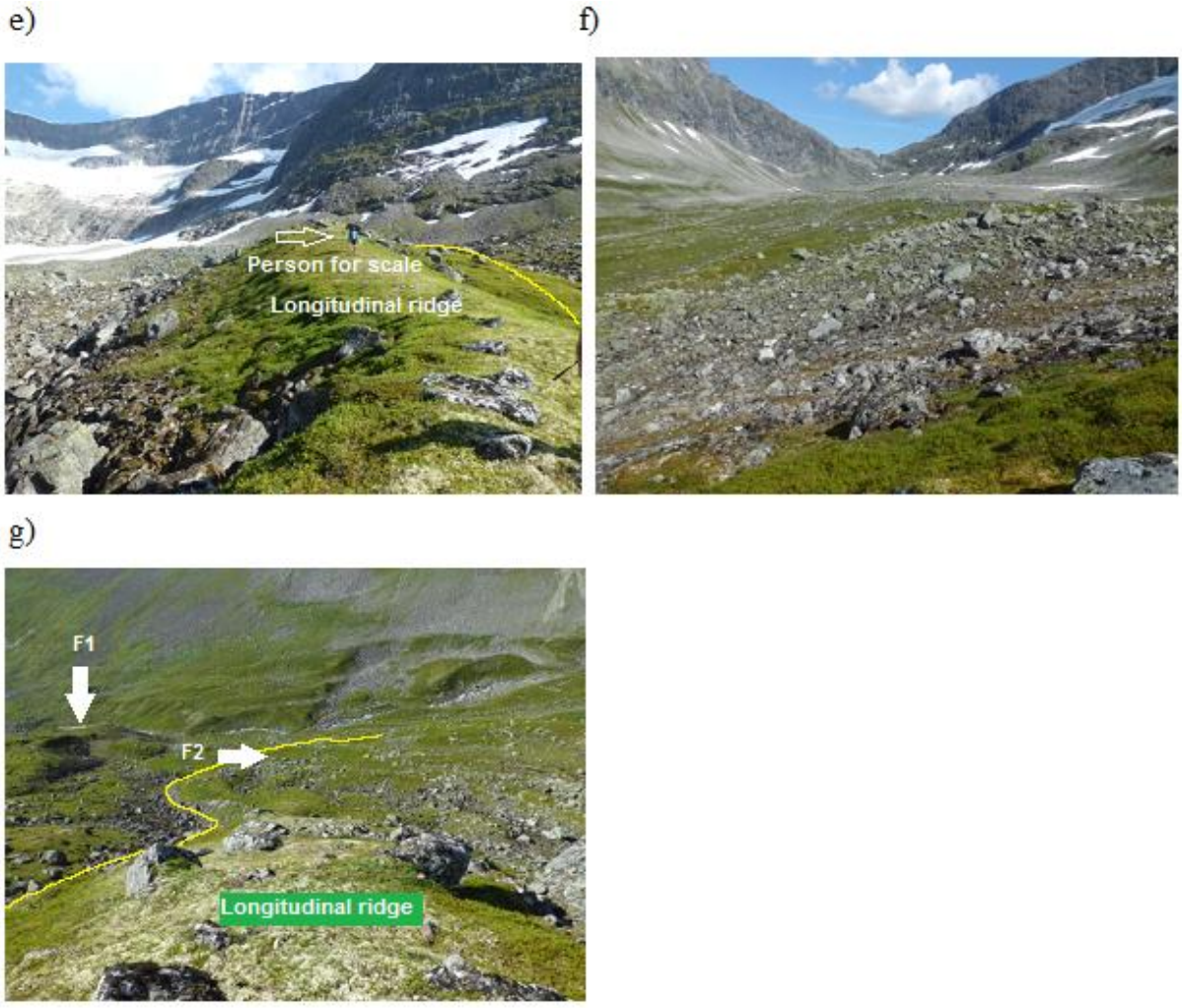

Figure 5.19: R1-F2

Yellow line: edge of R1-F2. Pink line: lobe-shaped form. a) longitudinal ridge being part of R1-F2. b) R1-F2 front, and person for scale. c) possible eastward direction of R1-F2 d) several ridges and furrows. Longitudinal ridge in the middle. e) longitudinal ridge with person for scale. f) distinct differences between the area close to the ridge, and further east. g) longitudinal ridge seen from above.

R1-F2 is a second body of unconsolidated debris that lies east of the previously discussed R1-F1. The form is, as its predecessor, concave with a steep front at the angle of response which is approximately 20 m high. Several large boulders have also been deposited at the bottom of this front. The body contains several ridges and furrows in transverse, longitudinal and diagonal directions (fig.5.19b-d). The body has a vegetation cover that consists of heather ling, and soil underneath. Except within furrows, where debris is partially covered with moss, and additional singular boulders that lie all over the body. In addition, the upper area close to the longitudinal ridge seem less covered by vegetation (fig.5.19f).

The longitudinal ridge on the west side of this body is convex shaped at the upper level, and concave shaped down slope towards the steep snout (fig.5.19a, d, e, g). Similar to the rest of R1-F2, the longitudinal ridge has a vegetation cover that consists of heather ling, and soil underneath. In addition, a few semi rounded boulders and large boulders emerge from the vegetation (fig.5.19e, g). Accumulations of large boulders can be observed at the bottom and outside of the ridge as well as the snout. All the boulders are mostly covered with moss.

Interestingly, in the middle of the unconsolidated body a lobe-shaped form with reddish vegetation emerges (fig.5.19d). This particular area is less step than its surroundings, and has boulders on top, and surrounding it. Thus it may resemble debris flows.

Current influencing processes are probably few, as it is likely that the features within the M1 site (chapter 5.2), and the talus and step areas stops most avalanche and rock fall activity (chapter 5.5.1.3). Based on observations, weathering of debris occur. Additionally, the reddish form might be a result of debris flow, due to its morphology.

5.5.1.3 R1-Step and talus area

a)

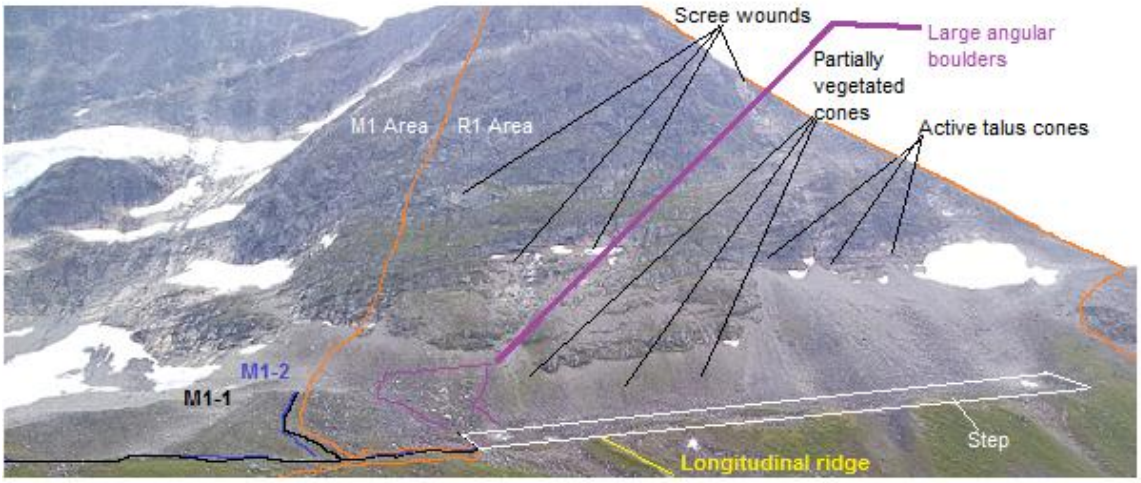

b)

c)

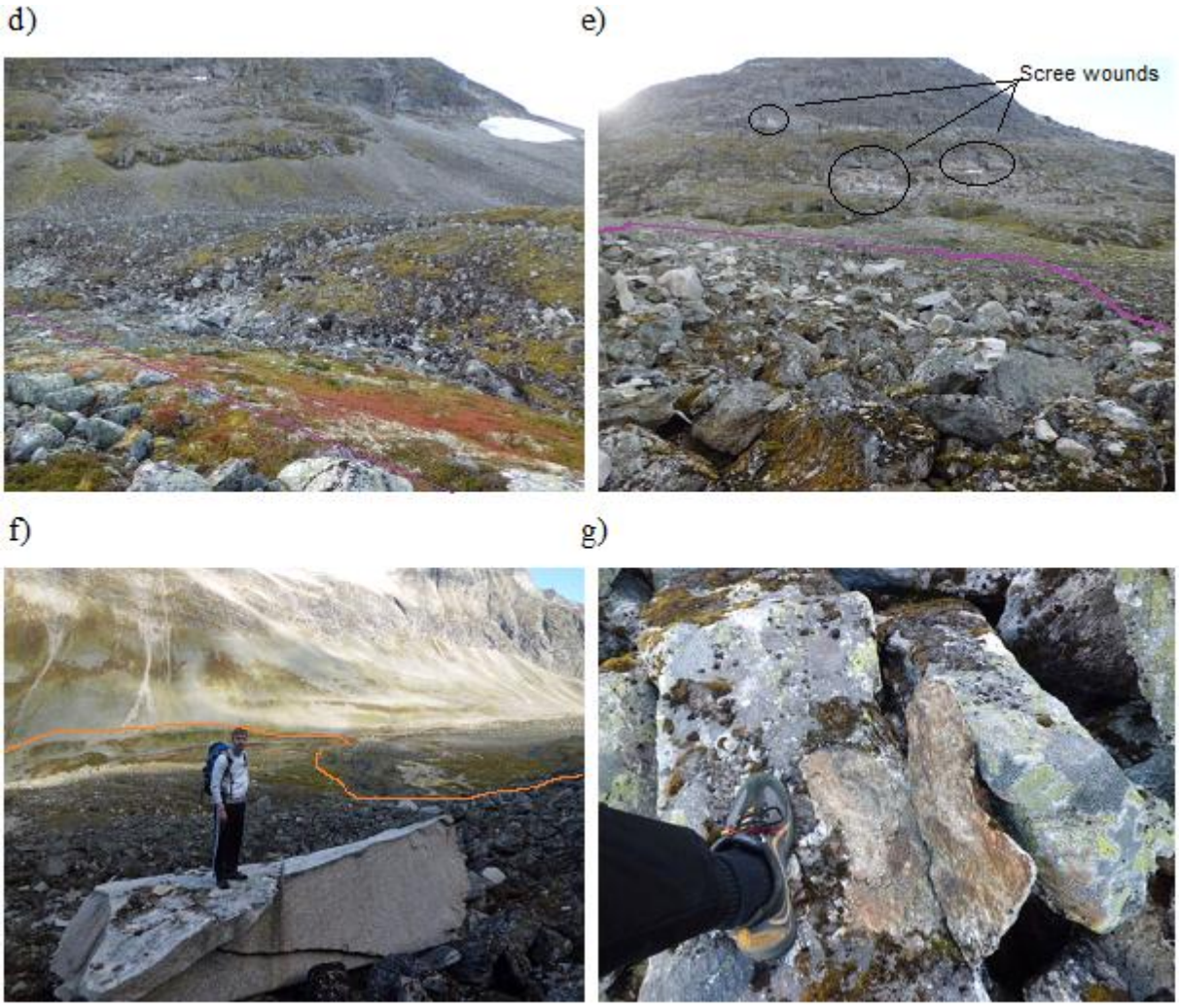

Figure 5.20: R1-Step and talus area

Orange line: R1 site area. a) features on the step, talus area and rock wall. b) western part of talus area, with active talus. Note the diagonal ridges and furrows in the lower parts. c) the step and diagonal ridges and furrows. d) middle part of talus area. Talus cones partially covered by vegetation. Well developed ridges and furrows below. e) eastern part of talus area. Several bright angular boulders and scree wounds in the headwall indicate recent activity. f) the largest boulder found below the scree wounds. This is one of the lowermost recent boulders. Note the perched boulders and pebbles. g) weathered boulder. Photo: Arvid Gjørven

Several coalesced talus cones lie in the south east corner of the study area below a steep rock wall with heights ranging from 100-500 m, west to east respectively (fig.5.20a). Furthermore a pack of snow lies on top the westernmost talus (fig.5.20b). The snowpack contain a small amount of blue ice, and may cause nivation, but is not further discussed in this thesis. East of the snowpack, the coalesced talus consists of angular debris without vegetation, while the eastern talus cones is partially covered by vegetation (fig.5.20d). The talus cones are fall sorted, with smaller particles close to the rock wall, and larger boulders down slope. The eastern talus cones contain several new large and giant boulders with sharp angularity on top

of older heavily moss covered large boulders (fig.5.20e). The angular boulders have not yet been colonized by lichens. In addition, perched boulders can be seen everywhere.

At the bottom of the talus cones, an even surface previously referred to as a step upslope on R1-F1 exists (chapter 5.5.1.1). The step is based 1 m lower than its outer convex and very steep front, and consists of several minor ridges and furrows in diagonal directions headed SE-NW. The minor ridges are approximately horizontal or slightly concave close to the talus. Moreover, a few larger ridges and furrows are situated near the front. While the largest ridges are covered by solid vegetation, it is the other way around for most of the step. Perched boulders have been observed on top of older debris.

Current influencing processes definitely involve rock falls, as a number of talus cones are still active, indicated by none or little vegetation, and scree wounds are still visible in the rock wall above. The step lies at 1020-1040 m a.s.l. and scree wounds are observed at about 1420 m a.s.l. (west), and 1200 and 1300 m a.s.l. (east). The diagonal ridges stand out as minor compared to others in the study area (height = ~0,5 m vs. < 1 m), which indicates either a recent development, or a short-lived duration of development. Second, avalanche activity occur due to perched boulders placed onto older debris (fig.5.20f), In addition, boulders are weathered (fig.5.20g-h).

5.5.1.4 R1-WCF

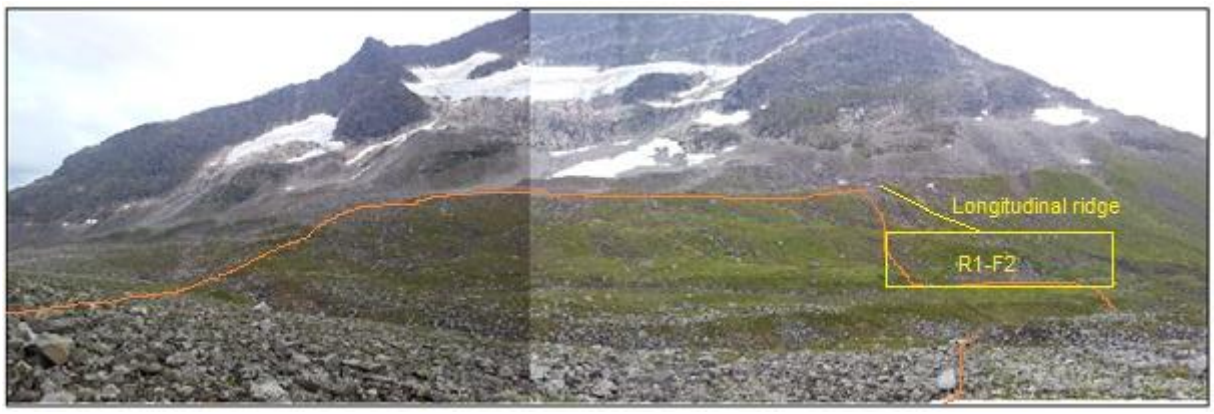

Figure 5.21: Panorama picture visualizing R1-WCF seen from north

Orange line: R1-WCF area. WCF: western cirque glacier foreland

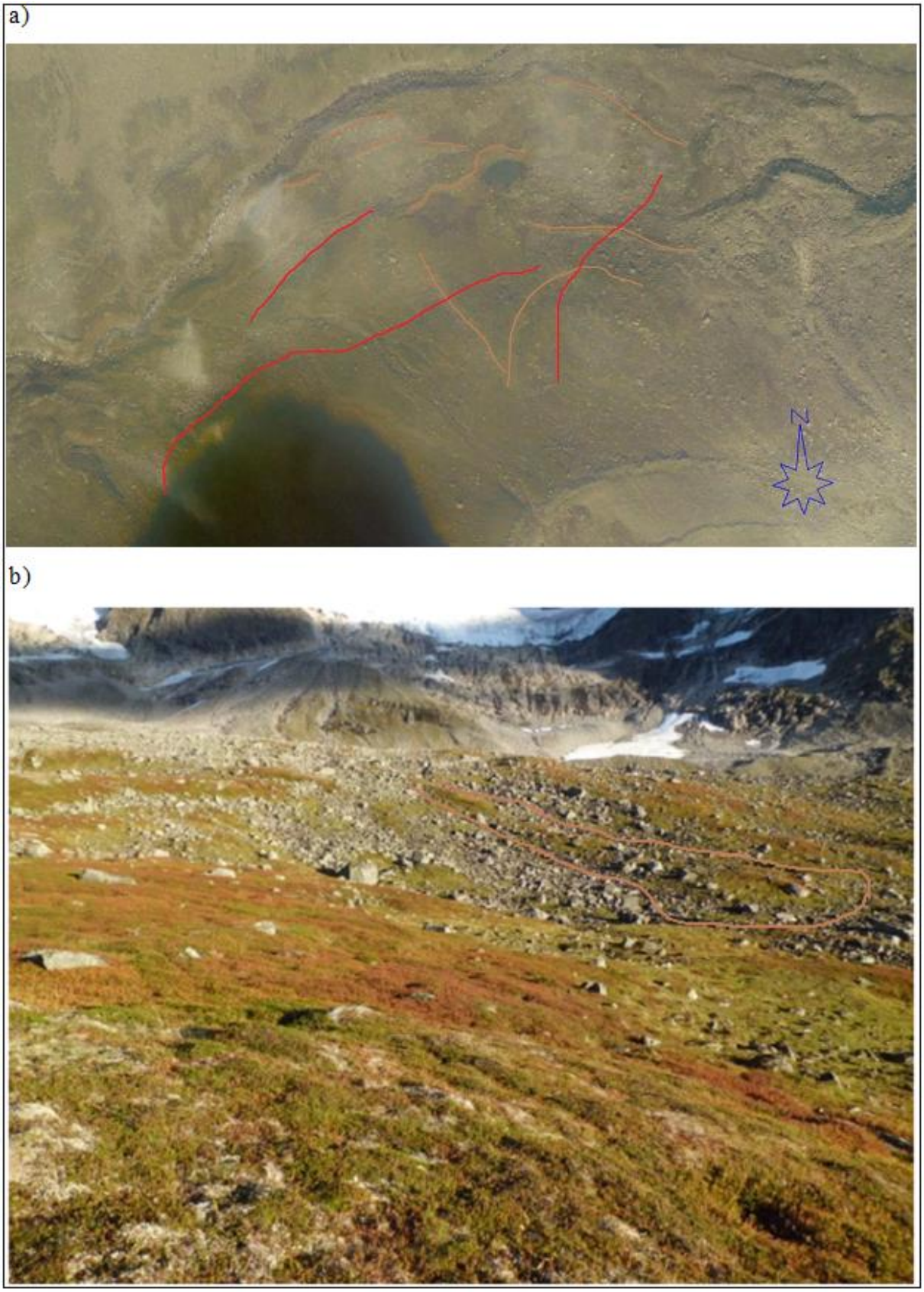

Figure 5.22: R1-WCF investigated features

Brown line: ridges. Red line: distinct altitudinal differences a) R1-WCF site sketched (Norkart, 2001) b) lobe-shaped feature

R1-WCF which is the western cirque glacier foreland, lies north of the M1 site (chapter 5.2). This area includes the eastern part of R1-F2, and additional ridges, furrows, streams, ponds, fronts, and accumulations of boulders below fronts(fig.5.21). Some of the distinct shapes have been attempted identified (fig.5.22c), but in general this place is a mess with non-coherent shapes, filled with horizontally and vertically distinguishable former creep systems (fig.5.22a-b). Additionally, the area is covered with solid vegetation, except within furrows. Thus less attention is addressed to this area as it is near-impossible to provide rational explanations for the spatial and temporal distribution. Finally, there are some forms with surrounding debris and an incline to which resembles lobes formed by debris flow.

Current influencing processes seem to be weathering and erosion caused by runoff.

5.5.1.5 R1-River and R1-CR

Figure 5.23: R1-River and R1-CR overview

Yellow line: edge of R1-F1 and R1-F2. Blue contoured line: ravine. Blue solid line: river.

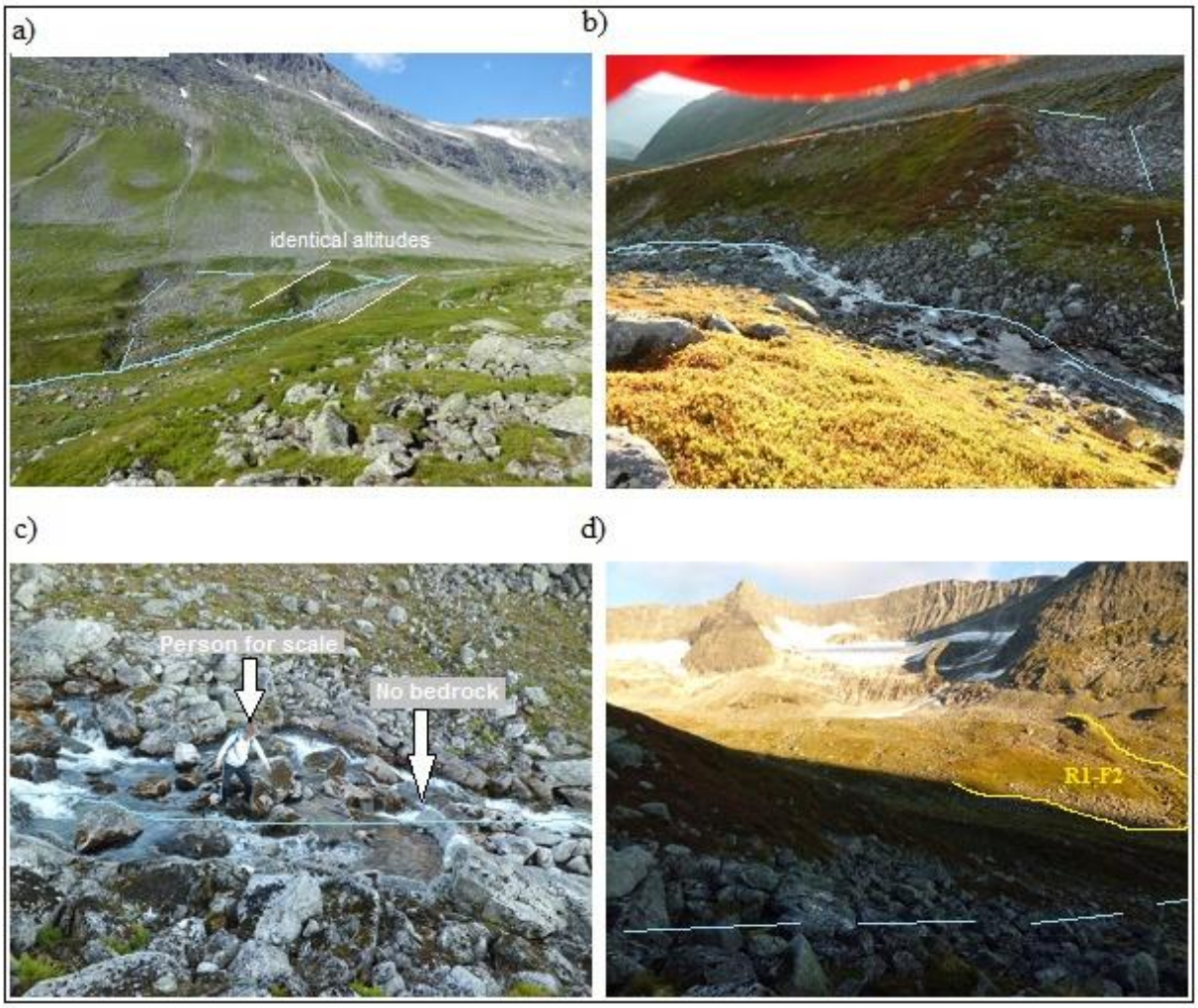

Figure 5.24: R1-River and R1-CR

a) R1-River and R1-CR seen from south. Note gully erosion, levees, and associated debris in general occupying R1-CR. b) R1-River and R1-CR seen from east. c) R1-River. Note that the river has not yet eroded down to the bedrock. d) western part of R1-CR. R1-F2 and parts of WCF in the back. Photo: Arvid Gjørven.

The R1-River and R1-CR area is quite interesting as they lie down slope/north of R1-WCF (western cirque glacier foreland). The peak between R1-River and R1-CR has the same altitude as the northernmost part of R1-WCF. They are both located at 920 m a.s.l with a slight incline towards east (fig.5.24a). The area north/above R1-CR is higher (940 m a.s.l), and shows a similar incline towards east.

R1-River consists mostly of rounded boulders. However, the boulders are more angular than what one might expect in rivers, probably due to the short distance of transportation. Additionally, semi rounded and angular boulders can be observed within the river. Most of the boulders found are partially covered by moss. The river has not yet eroded down to the bedrock (fig.5.24b-c).

R1-CR consists mostly of angular boulders, and additional semi rounded boulders. Most of the boulders are partially covered with moss, and lichens have not been observed. There are also a lot of perched boulders. An underground stream can be heard approximately 1 m beneath the debris (fig.5.24d). Proper rounded boulders have not been observed, even when looking down through space between the uppermost boulders. Moss such as observed on the previously discussed plains lies on top of this underground stream (chapters 5.2.1.3 and 5.4.1.4).

Current influencing processes in R1-River, are accumulation and redistribution of debris by debris flows, snow avalanches and rock falls from the south facing rock wall and adjacent talus north of the study area. At the same time, R1-River transports debris down-valley, and erodes the river bed. R1-CR is exposed to the same processes as the former, except the erosion caused by the current stream which is lower due to less discharge in the underground steam.

5.5.2 Temporal data

Table 5.4: R1 lichen data

	R1-F1	R1-F2	R1-Step	R1-WCF	R1-River	R1-CR
5LL size	No measures	> 230	> 300	No measures	No measures	No measures

The largest lichens found at the Step area is more than 300 mm, i.e. old (table 5.4). The same can be said for R1-F2. Only fused lichens have been observed on R1-F1, thus none have been measured. The Talus/Step, Western cirque glacier foreland (WCF), River, and CR areas seem to be diachronic, which make the 5LL method invalid as it is meant for homogenous forms.

Based on morphostratigraphy, R1-F1 is older than R1-F2, as the latter seems to lie onto the former (fig.5.23). Additionally, the Step area and upslope parts of R1-F1 seems to lie onto R1-F1 (fig.5.18d). Thus the latter seems to be older than the Step area as well. R1-F2 is covered by solid vegetation, while the Step area is not. The Step is also currently influenced by active talus cones and correlated rock falls. However, the outer edge (i.e. the upslope part of R1-F1) is also covered by solid vegetation. Based on LL, the Step area is older than R1-F2. However, as pointed out by (Innes, 1985), (Matthews, 2005) and (McCarroll, 1994), there are several factors that influence lichen growth (lichen reliability is further discussed in chapter 6.2.2). In addition, when lichens are this large, and situated quite differently, they

cannot be used as reliable sources as their growth have been subject to entirely different conditions.

Conclusively the data used in this thesis is not enough to establish a timeline for the R1 site, except the relative position of which R1-F1 is suggested to be older than R1-F2 and R1-F1-Upslope/Step area as they seem to lie onto R1-F1.

5.6 R2 site

a)

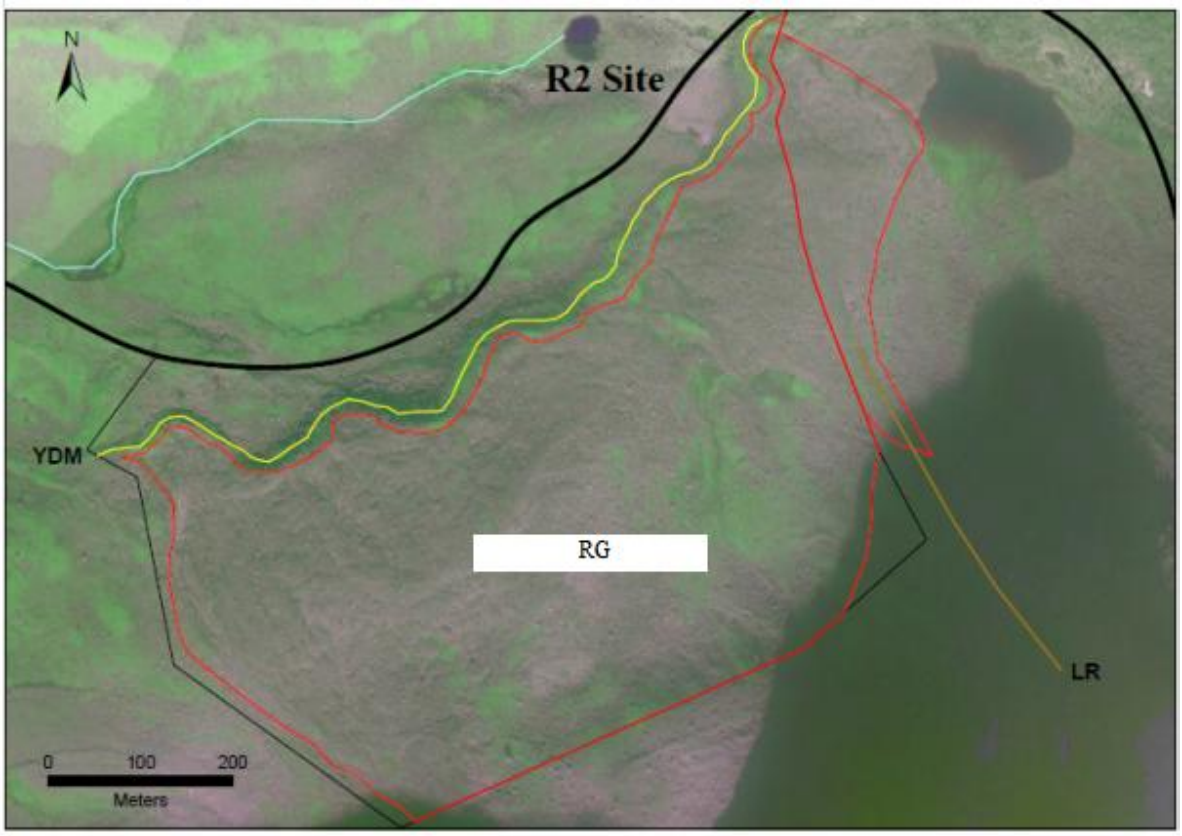

b)

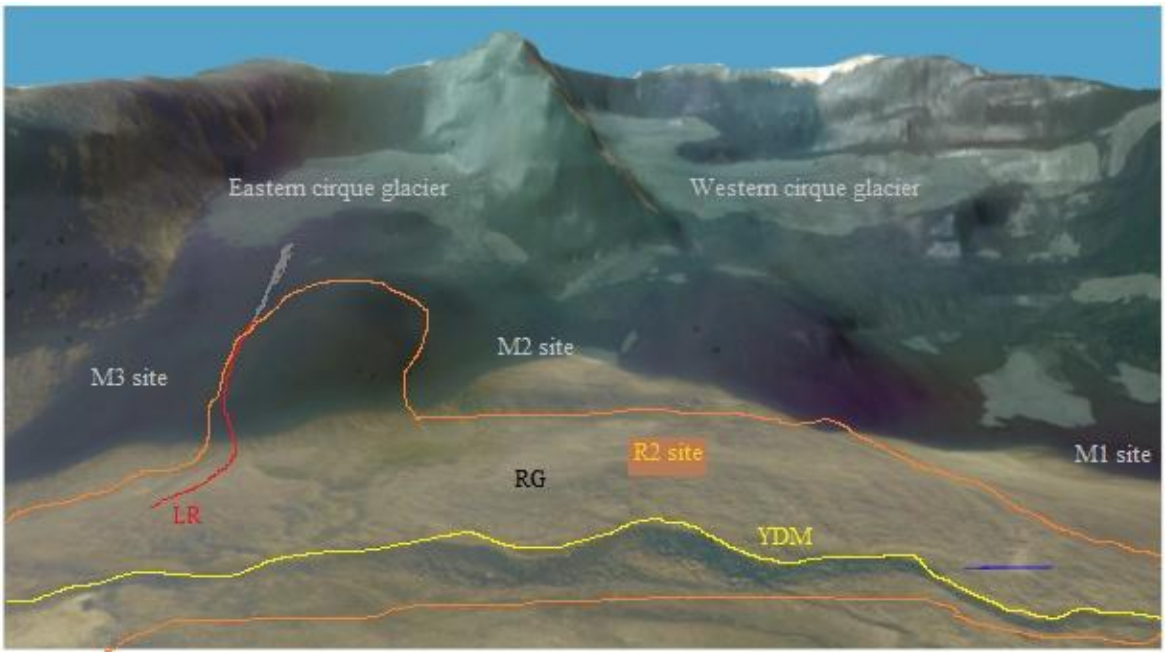

c)

Figure 5.25: R2 site overview

a) Sketched orthographic photo of the R2 site (Statens Kartverk, 2010) R2-RG: unmapped debris -landform system. R2-LR: same as M3-LR longitudinal ridge mentioned in chapter 5.4.1.2. b) R2 site sketched. Note YDM front-system. (Norkart, 2001). c) Picture taken from Skåla. Photo: Ivar Berthling.

5.6.1 Spatial data

5.6.1.1 R2-YDM

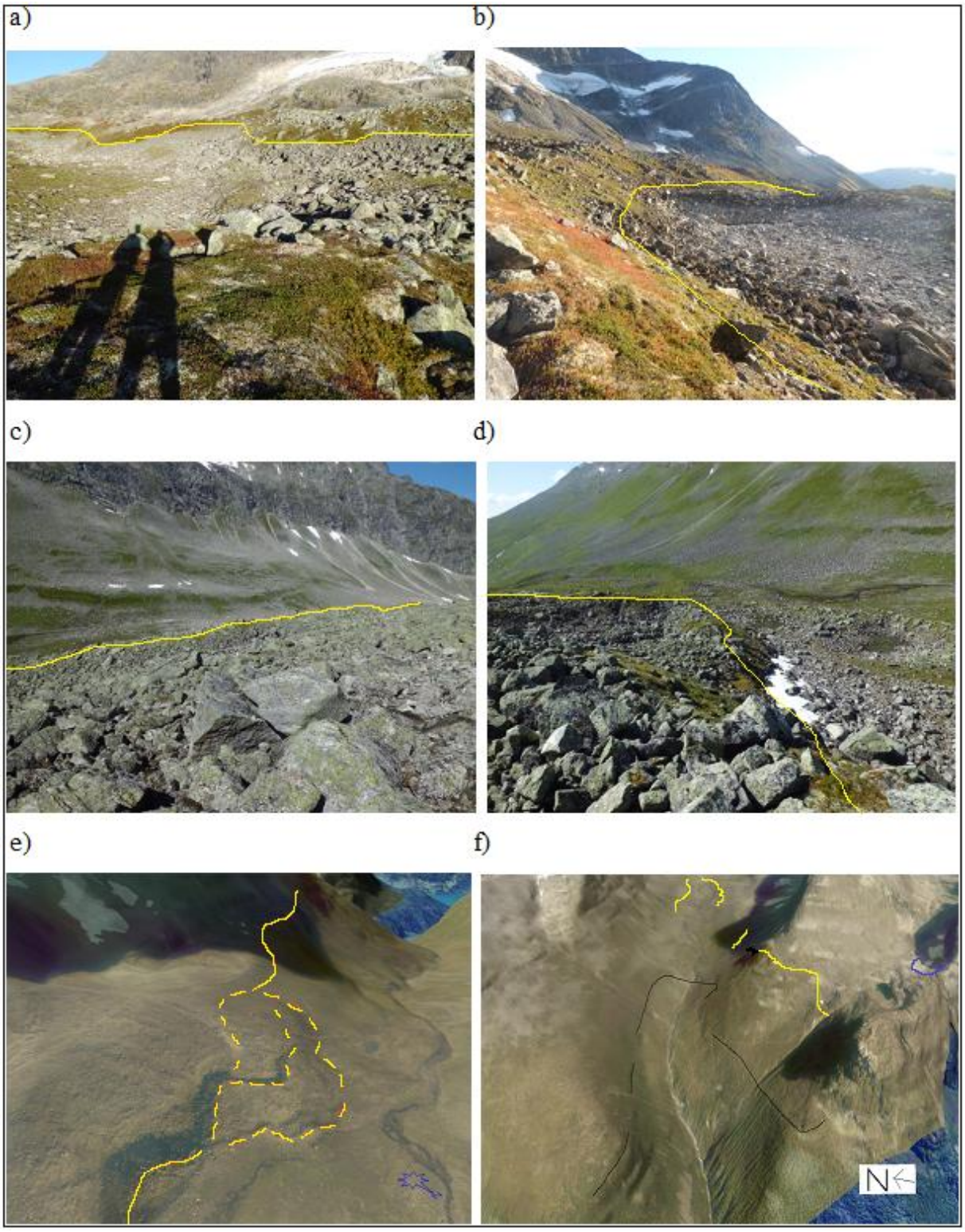

Figure 5.26: R2-YDM

Yellow line: YDM. Blue line: LIA_{max} for a tiny nivation glacier (f). a) and b) YDM. c) The distal transverse ridge is YDM, seen from R2-RG d) Closest, one of the southernmost positions on YDM showing R2-RG at similar altitude as

YDM. Further away, one of the northernmost positions on YDM showing a depression in R2-RG. e) and f) Former research by (Nesje and Dahl, 1992). Reproduced Younger Dryas valley glacier (Solid line), and possible directions in the easternmost part of R1 site based on distinct altitudinal differences (contoured lines) suggested in this thesis. f) Former research by Nesje and Dahl (1992) reproduced. Yellow line = YD Lodalen valley glacier. Suggested alteration for this thesis represented by black line (see discussion) (Norkart, 2001).

R2-YDM is a huge meandering-shaped ridge at the northern limit of the investigated study area. The ridge is covered by solid vegetation and has a steep slope at the angle of response. Accumulated boulders lie at the bottom (fig.5.26a-b). The debris consists of large angular and semi rounded boulders. The northernmost places of R2-YDM are associated with depressions in R2-RG (fig.5.26d), while the latter lies at similar heights at the southernmost places (fig5.26c-d). Several places, longitudinal debris accumulations/ridges cross R2-YDM. Additional ridge-shaped features covered with solid vegetation can be seen north of R2-YDM (fig.5.26a, d). They seem to be partially overridden by the latter.

Current influencing processes seem to be limited to weathering.

5.6.1.2 R2-RG

Figure 5.27: R2-RG

R2-RG sketched (Norkart, 2001)

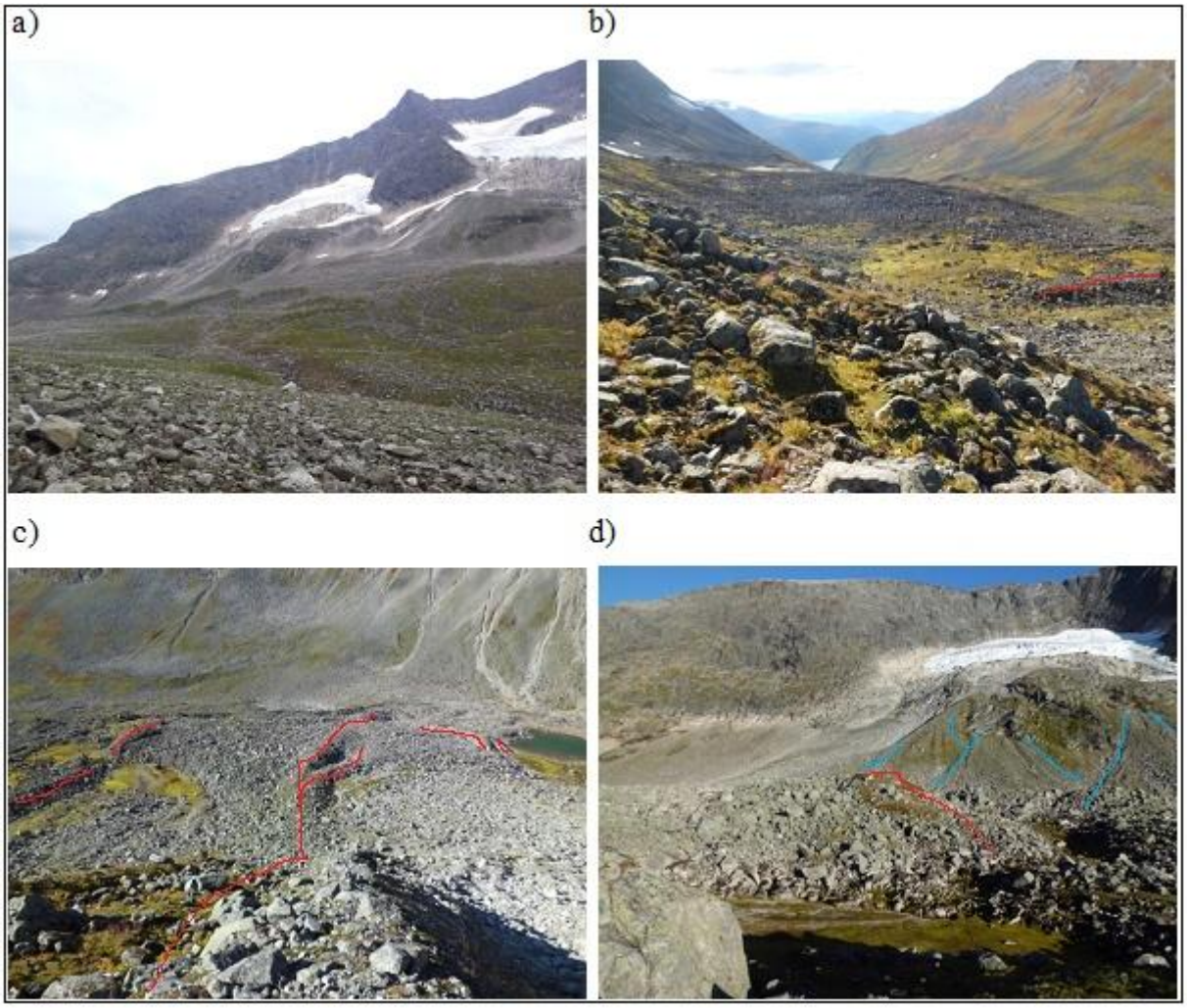

Figure 5.28: R2-RG seen from NW, N and SE

Red line: prominent longitudinal ridges. Blue line: coalesced talus cones. a) R2-YDM as a meandering-shaped ridge and a debris -landform system behind. b) the debris -landform system seen from south east. c) several longitudinal/diagonal ridges. d) coalesced talus cones, former and recent.

R2-RG is a large body of unconsolidated debris that lies below the arête and eastern cirque (fig.5.28a-d). The body is composed of boulder accumulation, and several longitudinal, transverse, and diagonal ridges and depressions. Vegetation type on ridges are mixed. However, there is a tendency of either being a lot of vegetation, a lot of moss, or a lot of fused lichens. Most boulders are semi rounded, although the quantity of angular debris increases towards the back. Furthermore perched boulders and cobbles have been observed towards the back and within furrows.

There are several moss covered areas similar to the plains within M1 and M3 sites (b-d). Due to these areas, patterns which may lead to misinterpretation emerge. In addition, similar transverse and semi circular sediment-filled depressions have been discovered. One of the

semi circular ones has been observed more closely. While boulders in front of the depression are generally small, they are larger upslope.

At the back, R2-RG is fed with debris from both glaciers (fig.5.28a). The largest single boulder found is around 7 m high (fig.5.28i), and several recent large boulders of significant size can be observed (fig.5.28j). An attempt has been made to map distinct furrows and ridges within the body. The transverse ridge (fig.5.28h), can also be seen in the back of (fig.5.28g). The westernmost ridge is fairly covered with vegetation (fig.5.28c-d), but so are others, as seen in (fig.5.28e).

Current influencing processes based on observations are rock fall, snow avalanches, gully erosion, debris flows, and weathering.

Figure 5.29: Panorama picture visualizing R2-RG seen from south

a)


White line = debris routes
Red line = Levees

b)

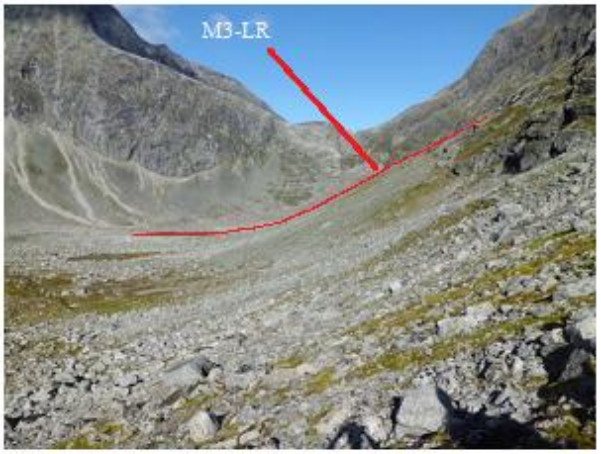
M3-LR

c)


Recent glacier activity

d)

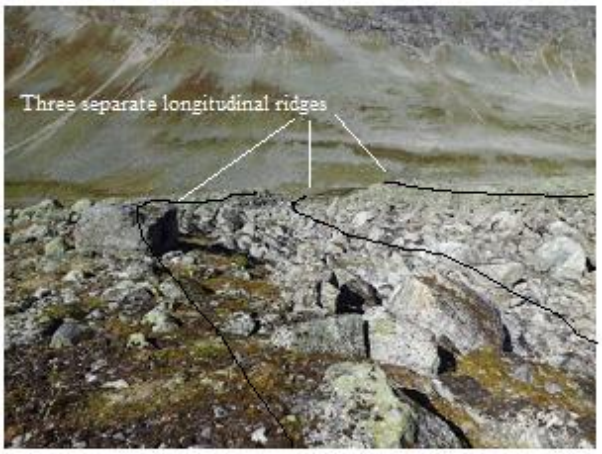
Three separate longitudinal ridges

e)

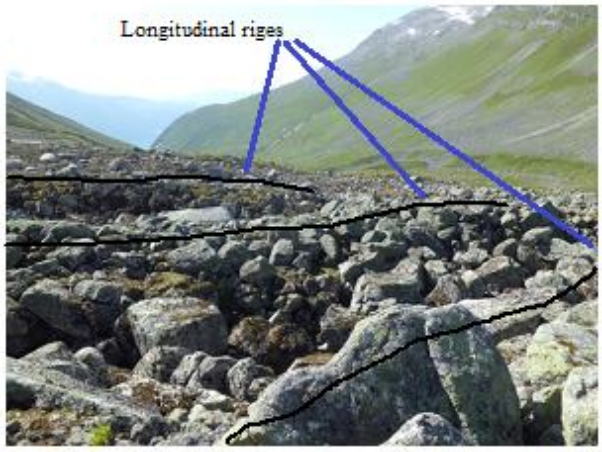
Longitudinal riges

f)

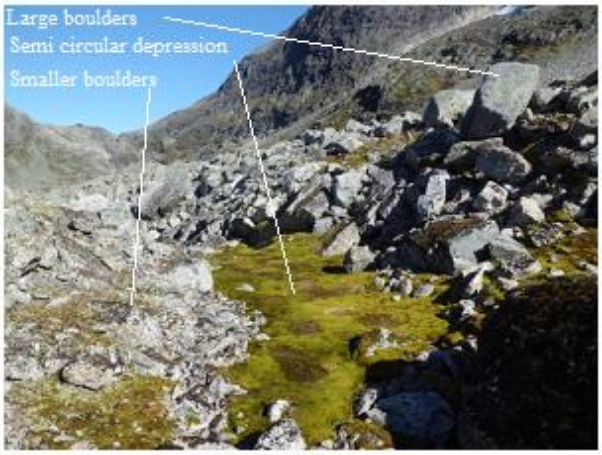
Large boulders
Semi circular depression
Smaller boulders

g) h)

i) j)

Figure 5.30: R2-RG characteristics

a) R2-RG is fed with debris from both cirques. b) former coalesced talus cones and M3-LR c) westernmost ridge with vegetation. d) variation between adjacent longitudinal ridges. The outermost with vegetation, the second with little vegetation and some black moss, and the third with fused lichens. e) well developed ridges with vegetation and furrows. f) furrow partially covered with vegetation. Note difference in boulder size above and below. g) a transverse altitudinal wave higher than the surrounding area. h) giant boulder below the arête covered in fused lichens. i) recently deposited large angular boulder in the north western area RG-R2, without vegetation. j) mapped furrows (white) and distinctive longitudinal ridges (black). Note the transverse black line, which is the same altitudinal rice as seen in (g). R2-YDM is the transverse meandering shadow to the right.

5.6.2 Temporal data

Table 5.5: R2 lichen data

	R2-RG	R2-YDM
5LL size	Fused	> 240

RG-R2 consists mostly of fused lichens. There are also bright angular boulders that indicate recent deposition on the body. For R2-YDM, lichens found on large boulders are mostly fused. The 5 largest are 230-260 mm (table 5.5).

5.7 Lichen growth curve

The Norvestlandet curve displayed below, shows several investigated forms with the 5LL method, as the results are put onto the curve as a function of their size in mm (fig.5.31). According to the curve, all results from the M1 site relate to their distance from the western cirque glacier. The M2-M1 terminal moraine seem to be younger than the M1-1 terminal moraine. At the M3 site, M3-CM seem to have been deposited not far behind the lateral moraine from the M1 site. Based on the curve, M3-LR seems younger than M3-CM, although first probably is the lateral part of the latter.

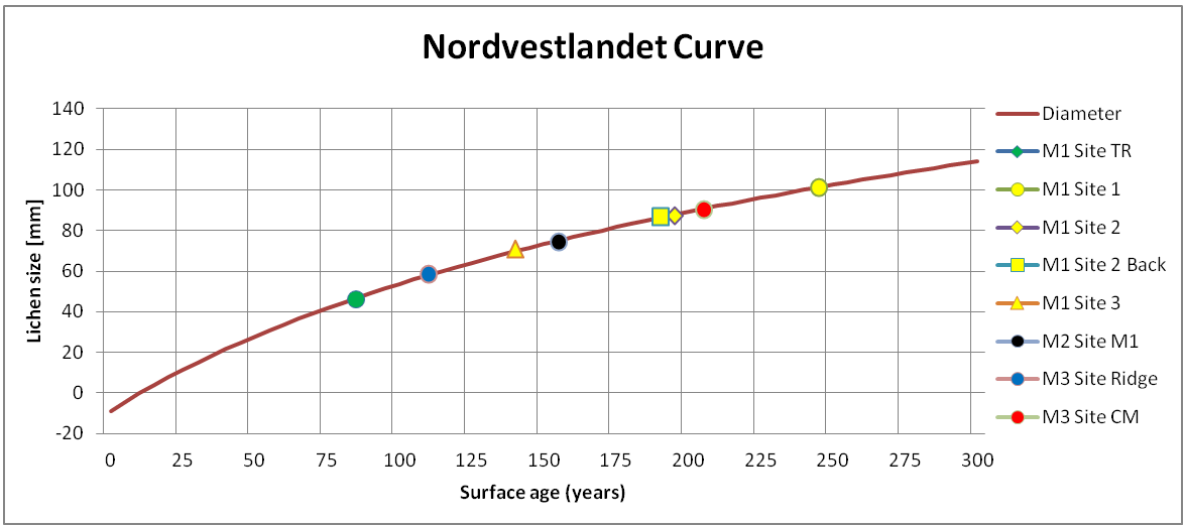

Figure 5.31: Norvestlandet curve

The figure shows selected forms measured by the 5LL method and their respective sites fit to the Nordvestlandet curve by Erikstad and Sollid (1986). The curve has been altered to resemble the curves found in Matthews (2005). Note that "M3 Site Ridge" = M3-LR, and that M3-site CM here is based on the oldest of the two possible 5LL interpretations (chapter 5.4.2).

5.8 Constructed profiles and calculated volumes

The landforms in Fosdalen are many and complex. Several attempted calculations were made in order to try and verify or weaken possible explanations for their present appearance.

- First of all, in order to establish cirque maturity, four longitudinal profiles, based on reconstructed glaciers from Nesje and Dahl (1992), were constructed and compared to *k*-curves after Haynes (1968).
- Second, cirque volumes were measured in order to compare the results with current valley deposits. Thus add to the impression given by the *k*-curves on cirque maturity.
- Third, mass volume of the total study area valley deposit was attempted calculated due to the comparison mentioned above.

- Fourth, mass volume of RG-R2 was attempted calculated, as this has less vegetation than the remaining valley deposits, hence indicating a younger age.
- Finally, two attempts were made to reconstruct a hypothetical former arête than at present, in order to compare the hypothetical volumes with R2-RG.

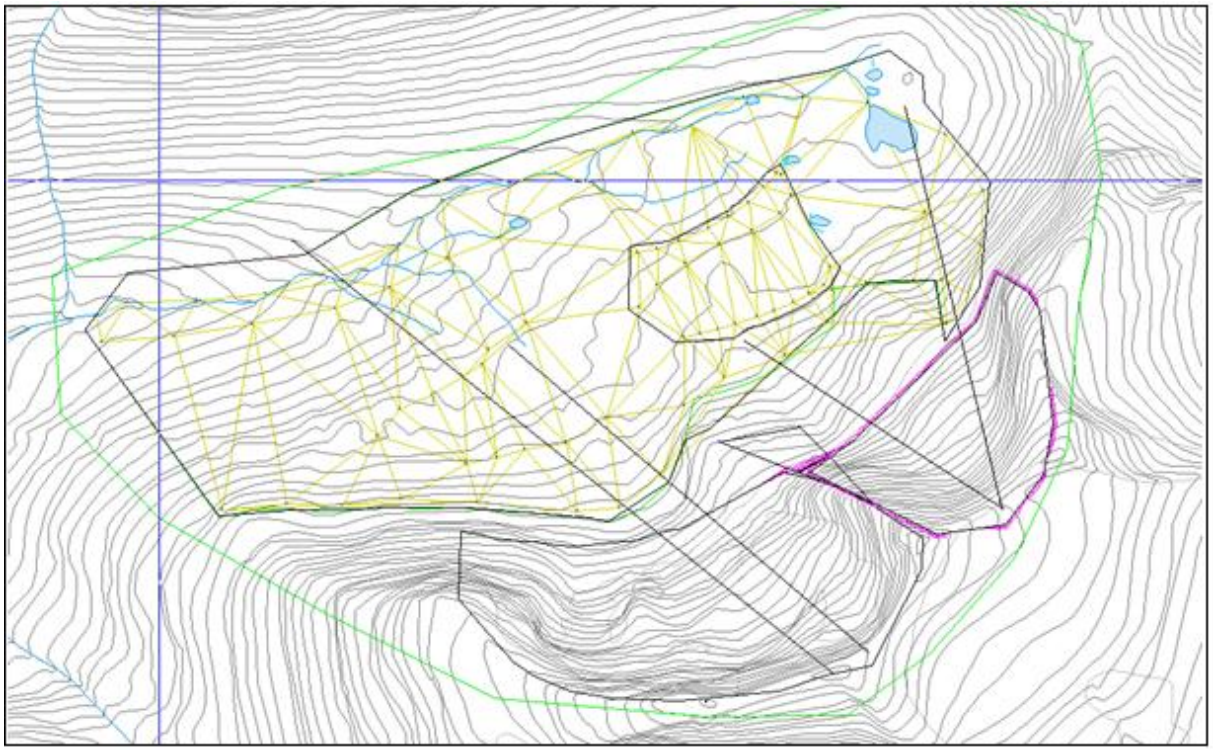

Figure 5.32: Calculations and longitudinal profiles overview

Green line) surrounds the total study area. Yellow lines and black dots) fake simulations of height points in order to make an upside down TIN model based on height contours. Largest black square) total area. Smallest black square) rock glacier in R2 site. Medium black square and purple square) cirques. Black triangle) reconstructed arête. Black lines) Longitudinal profiles. Grey lines) height contours, 20 meter intervals. Blue lines) N-S, and W-E compass directions. Dataset from Stryn Kommune (2014)

5.8.1 Longitudinal profiles

According to Haynes (1968), the use of *k*-curves based on longitudinal profiles can be used to estimate cirque development. It is however, not possible to provide estimated age by this method. When $k = 2$, cirques are well developed. On the contrary, when $k = 0{,}5$, cirques tend to represent an early stage. All the longitudinal profiles in the figure beneath shows close conformity to the ideal *k*-curves. Although none are a perfect match, they all seem to fit closest to $k = 2$, which in turn suggest that these cirques are well developed and of mature age.

It may be argued that the first curve (fig.5.34a) has characteristics similar to *k*-number = 1 (fig.5.33). However, the profile is too steep close to the y-axis. Perhaps a *k*-number = 1,5 would have been a more precise description.

The curves (Fig.5.34a-b) are from the western cirque. However, (fig.5.34a) reflects reconstructed cirque glacier during the Erdalen Event and (fig.5.34b) reflects reconstructed cirque glacier during LIA. Both in accordance with Nesje and Dahl (1992). The difference in interpreted *k*-values may be due to impression given by the length of (fig.5.34a) which is several hundred meters longer than (fig.5.34b), thus giving the impression of having a more even profile. Additionally the longitudinal profiles were constructed approximately 100 meters apart, which may reflect local topographic variations within the cirque.

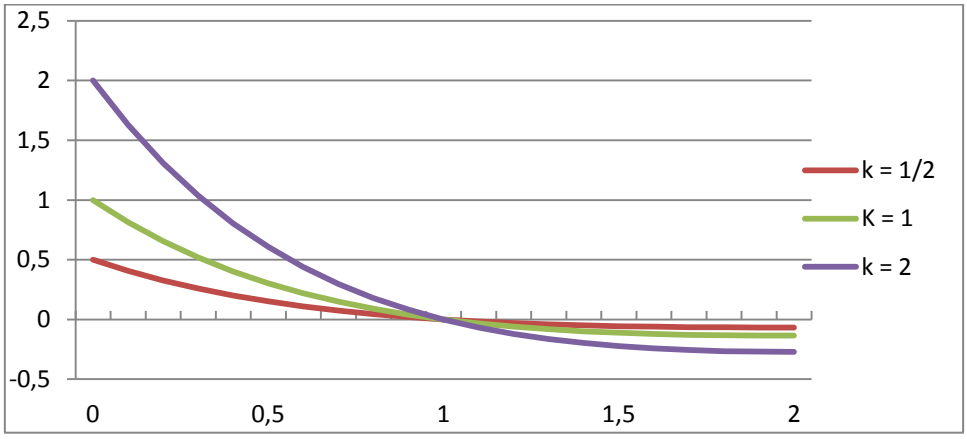

Figure 5.33: Constructed *k*-curves

***k*-curves constructed as directed by Haynes (1968).**

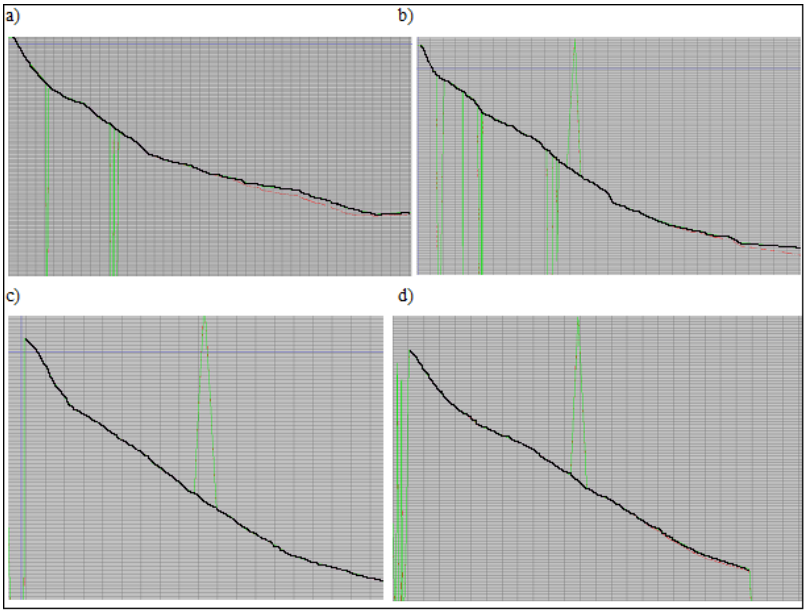

Figure 5.34: Longitudinal profiles in Fosdalen

Black line: longitudinal profile. Green lines that deviate are errors in the topographic dataset. a) reconstructed western cirque longitudinal profile during the Erdalen Event as outlined by Nesje and Dahl (1992). b) reconstructed western cirque longitudinal profile during LIA as outlined by Nesje and Dahl (1992). c) reconstructed western part of eastern cirque longitudinal profile during LIA as outlined by Nesje and Dahl (1992). d) reconstructed eastern part of eastern cirque longitudinal profile to the end of the. Anomalies in the profiles are due to errors in the topographic data used.

5.8.2 Calculated volumes

Because the depths of the valley deposits are unknown, interpolations were made based on assumed depths. These interpolations are only assumptions, and must be treated thereafter. The interpolations were made by building a TIN model on top of existing topography (fig.5.32).

For R2-RG, YDM was chosen to provide the basis for depths at the front, thus 20 m was set. The transverse wave at the middle of R2-RG was also estimated to a depth of 20 meters. Finally, the hindmost area depth was set to 0 m.

When calculating the total valley floor area, the river was used as the northernmost limit. Depth was set to 10 meters in the river due to the resemblance of a flood plain which indicates a sedimentation basin, north of R2-YDM. In addition the river depth increases to at least 10-15 m, west of R2-YDM. Besides, bedrock in the river was only observed west of the study area.

Areas close to the river and rock walls were estimated to a depth of 20 meters. At the rock walls (and cirque headwalls), which were used as the southernmost limit, depths were estimated to 0 meters. Finally, the depths of the areas near the M1-1 front were set to 40 meters, as it is assumed that the valley is deeper in its western areas (fig 5.35).

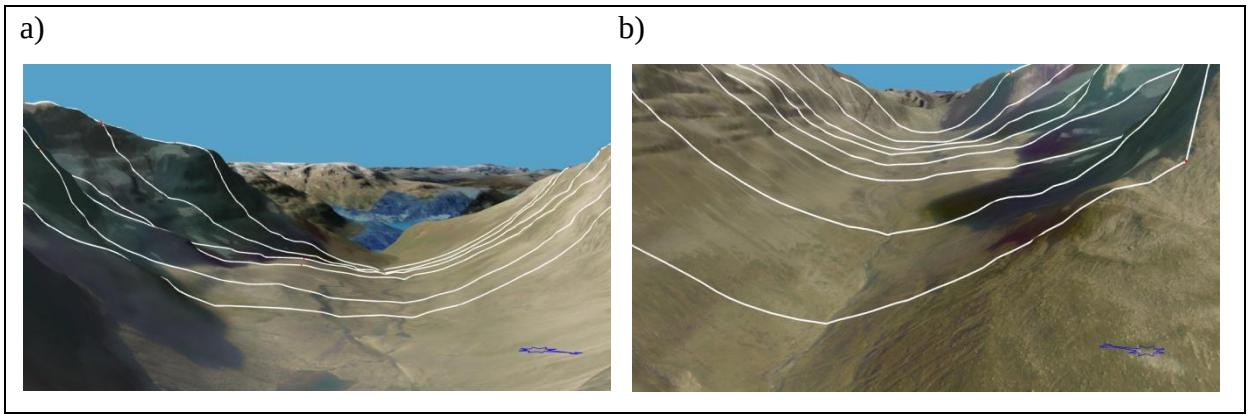

Figure 5.35: Cross sections in Fosdalen

a) Seen from east. b) seen from west. Note that the valley inclines towards the west, while the height of the southern deposits remains relatively stable.

The arête may have been larger than today, as the general width of the valley is smaller than at the arête. A suggested valley width is drawn in the figure the below (fig.5.36a). Two attempts to reconstruct a hypothetical arête were made. Arête thin (fig.5.36c) was reconstructed by assuming it had a vertical front, and a horizontal top. Arête thick (fig.5.36d) was reconstructed with the same angle as the present one. However, the front was moved forward approximately to the cliff as seen on the right side (fig.5.36b).

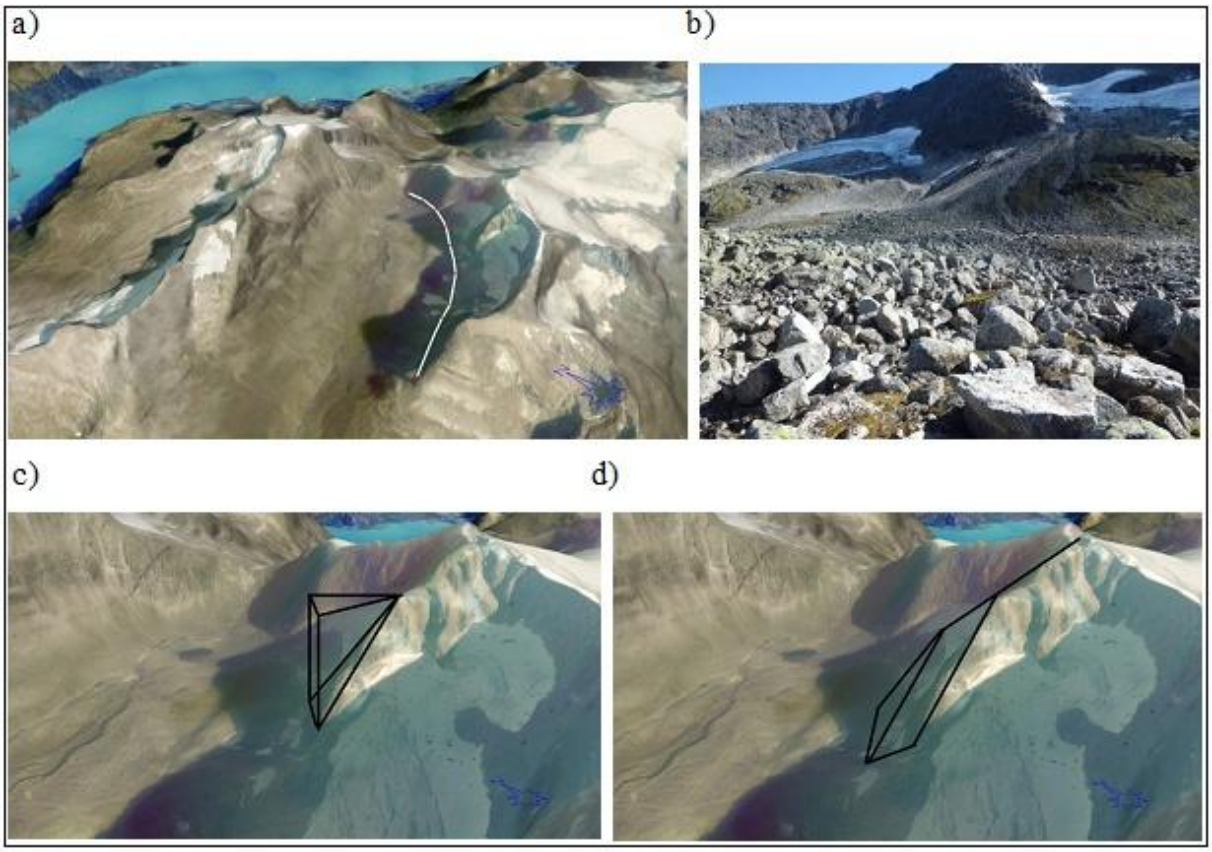

Figure 5.36: Reconstructed Arête

a) white line representing possible former valley width. Note the distance from the white line to the present arête. b) the arête seen from R2-RG. c) arête thin reconstructed. d) arête thick reconstructed.

Integrals were used to calculate approximate cirque volumes. Due to an error in the data, volume of the eastern cirque had to be calculated without integrals. Eastern cirque volume was therefore calculated by oblique floor area and the median of the headwall, and is thus probably underestimated (fig.5.37b). In addition to the whole valley floor mass, R2-RG was calculated. Finally, two varieties of a hypothetical reconstructed arête were calculated (fig.5.37a). All volumes are summarized in figure (fig.5.37c) below.

a)

Form measured:	calculation type:	Balance factor:	Mass:	Unit:	#Integrals:	#Int.valid:	Correlation factor	Corrected mass	Unit:
Western cirque	Volume	1,00	299993349,289	m3	7464464	7462528	1,000003	299993349	m3
								299993349	**m3**
Aretè thin	Volume	1,00	2809381,669	m3	208335	207726	1,000019	2809382	m3
								2809382	**m3**
Aretè thick	Volume	1,00	4433122,822	m3	402451	371781	1,000014	4433123	m3
								4433123	**m3**
R2 Rock glacier	Volume	1,00	2593629,075	m3	3571269	3324234	1,000002	2593629	m3
	Volume	1,00	2322,152	m3	3571269	2813	1,000002	2322	m3
								2595951	**m3**
Total area	Volume	1,00	34880072,182	m3	8544277	7946064	0,999999	34880072	m3
	Volume	1,00	7901,388	m3	8544277	3853	0,999999	7901	m3
								34887974	**m3**

b)

Form measured:	Oblique floor area:	Unit:	Backwall median height:	Unit:	Mass volume:	Unit:
Eastern cirque	353000	m2	280	m	98840000	m3

c)

Form	Mass volume	Unit
Eastern cirque	98,8	mill m3
Western cirque	300	mill m3
Aretè thin	2,8	mill m3
Aretè thick	4,4	mill m3
R2 Rock glacier	2,6	mill m3
Total area	34,9	mill m3

Figure 5.37: Calculated volumes in Fosdalen

a) areas measured with integral. b) area measured without integral due to error in the dataset. c) summarized volumes.

6. Discussion

Below, the discussion attempts to explain the current visible topographic expressions in Fosdalen. First, the age of the compound cirque is investigated. Second, as they are the youngest and therefore most certain landforms, the age of the moraines linked to LIA and post LIA are investigated. Third, the coalesced talus cones and associated present and former landforms west of the western cirque glacier are investigated. Additionally, the possibility of present and former permafrost is discussed. Fourth, the hitherto unmapped debris -landform system is investigated. What it is, and what it is not, is discussed against reinterpreted late glacial chronology in the inner Nordfjord region. Moreover, the time of origin is discussed. Finally, the reconstructed Erdalen Event cirque glacier by Nesje and Dahl (1992) is questioned, and alternative explanations are suggested.

6.1 Cirque age and development

Estimating age of the compound cirque in Fosdalen, is difficult. The use of *k*-curves as suggested by Haynes (1968), for the individual western and eastern cirques indicate that they are well developed cirques i.e. old, but the curves cannot be used for age estimates. However, when comparing total cirque excavated volumes with Holocene erosion rates, and assuming additional steady-state conditions in Pleistocene, an age estimate is possible.

A headwall erosion rate caused by rock falls has been estimated by Matsuoka and Sakai (1999) for the Hosozawa cirque in Japan. Their research indicate a retreat rate of 0.01 mm a^{-1} based on fallouts 1-3 m^3 a^{-1}. Additionally, larger block fallouts <10 m^3 has been estimated to happen each decade. Adding a minimum of 10 m^3 per decade increases the headwall retreat rate to 0.015 mm a^{-1}. Larsen and Mangerud (1981) on the other hand found a greater headwall erosion rate of 0.1 mm a^{-1} on a former cirque at Kråkenes, western Norway. Furthermore they found a total cirque erosion rate i.e. headwall and subglacial erosion combined, of 0.5-0.6 mm a^{-1}.

Hallet et al. (1996) reviewed glacial erosion rates of 20 different types of glaciers in Norway that averaged 0.33 mm a^{-1}, whereas Bogen (1989) found 16 glaciers that have erosion rates ranging between 0.37-4.48 mm a^{-1}. Erdalsbreen, an outlet glacier from Jostedalsbreen about 15 km away from Fosdalen has one of the highest erosion rates of 0.7 mm a^{-1}, and lies within the same bedrock region. Erosion by smaller cirques on similar bedrock is estimated to be an order of magnitude slower (Østrem, 1975, Bogen, 1989).

With this in mind, there seems to be a good chance that glacial erosion rates are somewhere between 0.33-0.7 mm a^{-1}. And as seen by both Matsuoka and Sakai (1999) and Larsen and Mangerud (1981), headwall erosion rates added to subglacial erosion rates are very low (0.015-0.1 mm a^{-1}). Thus the erosion rates used by Larsen and Mangerud (1981) for total cirque erosion simplified by the medium value of 0.55 mm a^{-1} is used for calculating age for the eastern cirque in Fosdalen. Due to lack of sufficient data (oblique floor area), the age of the western cirque is not estimated. But, as it is approximately three times larger than the eastern cirque, and has a similar *k*-curve, the age of the eastern cirque is assumed to provide a minimum age for the western cirque. The eastern cirque in Fosdalen is thus, based on erosion rates by Larsen and Mangerud (1981):

$(m^3/m^2/xa) = a^{-1}$.

where m^3 is the total eroded cirque volume, m^2 is the oblique floor area, *xa* is the age of the cirque provided steady state conditions, and a^{-1} is the erosion rate. Thus giving (98.840.000 m^3/353.000 m^2 /510.000a) = 0.55 mm a^{-1}. What this essentially means, is that if erosion rates were stabile through Holocene and Pleistocene, the eastern cirque glacier developed 510.000 BP i.e. approximately in the middle of Middle Pleistocene 126.000-781.000 BP (Cohen et al., 2013).

However, due to historic climate variations and thus variations within the cryosphere, steady state conditions may have occurred, but only within narrow time limits as seen by the results from Skarsten (2007), Luckman and Fiske (1995), McCarrol et al. (1998, 2001), Ballantyne (2002), Grove (1988, 2004), Nordli et al. (2002), Nesje (2005), Nesje and Dahl (1993). The compound cirque has since estimated time of origin been influenced by several ice ages, where the ice a number of times may have been cold, and thus none to very little erosion have occurred. Following this argument, the estimated age of origin is underestimated.

However, Hallet et al. (1996) found rates between 10-100 mm a^{-1} for large and fast-moving temperate valley glaciers in tectonically active ranges in southeast Alaska. It is not unlikely that western Norway sometimes throughout Pleistocene and early Holocene have experienced similar scenarios, at least in deglaciating periods when MAAT rose. During such scenarios erosion rates may have increased, thus it is possible that the estimated age of origin is overestimated.

Luckman and Fiske (1995) found increased rock fall rates immediately after glaciation in their Canadian study due to paraglacial activity such as depressurizing of bedrock. As there have been several ice ages, and moreover, interstadials, paraglacial activity may have increased headwall erosion rates severely compared to Holocene and present rates. Thus the estimated age of origin may be overestimated.

Apparently, according to former research by Nesje and Dahl (1992), there may have been no cirque glacier activity in Fosdalen during YD, unless the LIA depression were lower than a possible valley glacier entering Fosdalen. If that has been the case several times throughout Pleistocene, the estimated age of origin may be underestimated. However, freeze-thaw mechanisms may have contributed to enhanced rock fall rates even without glaciers being present, depending on whether MAAT lowered the discontinuous- and permafrost limits to an altitude lower than the cirque headwall. In this scenario, stability in the headwall would increase, thus lowering headwall erosion rates, and consequently the estimated age of origin may be underestimated.

With regards to the discussion whether cirques erode mainly horizontally as suggested by Johnson (1904), or vertically as suggested by White (1970), the latter seems to be the winner. This is due to the low estimates of headwall retreat rates (Matsuoka and Sakai, 1999, Larsen and Mangerud, 1981), compared to its counterpart subglacial erosion rates (Larsen and Mangerud, 1981, Hallet et al., 1996).

However, White (1970) argues that his reasoning is due to the persistence of arêtes between cirque glaciers. It is important to note that arêtes are only the visible expression as of now. In a long-term perspective, it is highly unlikely that arêtes will continue their existence, as headwall erosion rates does exist, although being small. Unless permafrost conditions forever will yield the existing arêtes, which is highly unlikely based on historical climate fluctuations and recent climate changes. Thus, his conclusion seems right, while his argument seems wrong.

6.2 Post LIA and associated landforms

According to Grove (1988), and Nesje and Kvamme (1991) Nigardsbreen reached its LIA_{max} in 1748 AD. However, it has been argued that glaciers west of the Jostedalsbreen icecap reached LIA_{max} slightly earlier due to generally steeper slopes, thus shorter response time. In contrast, Tvede and Liestøl (1977) found evidence of an outlet glacier from Folgefonni not reaching its LIA_{max} until around 1940 AD. Finding LIA_{max} and associated age for the western

and eastern cirque glaciers in Fosdalen may provide complementary information that may contribute to the understanding of glacial activity and response since LIA.

6.2.1 Age of western cirque glacier landforms

In front of the western cirque, M1-1 yields the oldest age, 1769 AD. M1-2 and its even upper surface are separated by one 5-year interval, thus they are estimated to 1819 and 1824 AD, respectively. M1-3 is younger, as it dates to 1874 AD. M1-TR seems to be the youngest as it is dated to 1929 AD (table 5.1). However, as can be seen in figure 5.5 and 5.6, the outer moraines are deposited onto M1-TR, which means that they have to have been deposited later than M1-TR. Thus, lichen data for M1-TR only indicates the time it was last deglaciated. Conclusively, the LIA_{max} for the western cirque glacier in Fosdalen is estimated to 1769 AD, which is 21 years later than Nigardsbreen. That leads to questions whether the estimated age is correct.

The western cirque has a steep slope, as seen by the *k*-curves after Haynes (1968). The slope could lead to a relatively short response time, thus indicating that 1769 AD is underestimated, either due to a poor choice of lichen curve, or a reduced lichen growth due to influencing conditions such as late lying snow. The latter however, is unlikely as the inner moraines seem to stop most avalanche activity (fig5.3).

A possible explanation for the estimated age is the difference between TP-ELA on plateau glaciers, and TPW-ELA on deeply incised cirque glaciers. As pointed out by Nesje and Dahl (1992), wind transports snow from windward to leeward sides on plateau glaciers, thus not changing their total mass. The situation is different for cirques, as they generally lie in leeward sides, facing their closest pole (Benn and Evans, 2010). Wind accumulates snow onto cirque glaciers, by drift and snow avalanches, thus lowering ELA (Nesje and Dahl, 1992).

Figure 6.1: Snowdrift on top of western cirque headwall

Photo: Liaset (2006).

Even after Nigardsbreen LIA_{max}, it is likely that snow deflated from the Skålabreen plateau glacier and onto both cirque glaciers in Fosdalen, as this happens at present (fig.6.1). If the general glacial retreat in this area was caused by an increase in summer temperatures, and not so much a decrease in winter precipitation, the 1769 AD estimate is probable.

On the other hand, if the retreat was caused by a decrease in winter precipitation, and not so much summer temperatures, the 1769 AD estimate is less likely to be correct due to the less amount of snow capable of blowing onto the cirque.

In a study of spring/summer temperature reconstruction from western Norway 1734-2002, Nordli et al. (2002) reconstructed the glacial history of Nigardsbreen (fig.6.2). As the compound cirque in Fosdalen lies further west, results from Nigardsbreen should be treated with caution. LIA_{max} at Nigardsbreen occurred in 1748 AD. There were several ELA depressions after this. 1760-1770, 1805-1815, 1825, 1835, 1848-1852, 1860s and mid1870s, 1883-1888, 1902-1908. Similarly, in a study of glacier-front variations of Briksdalsbreen between 1900-2004 AD by Nesje (2005), the glacier advanced during 1901-1910, 1921-1931, and 1956-1997.

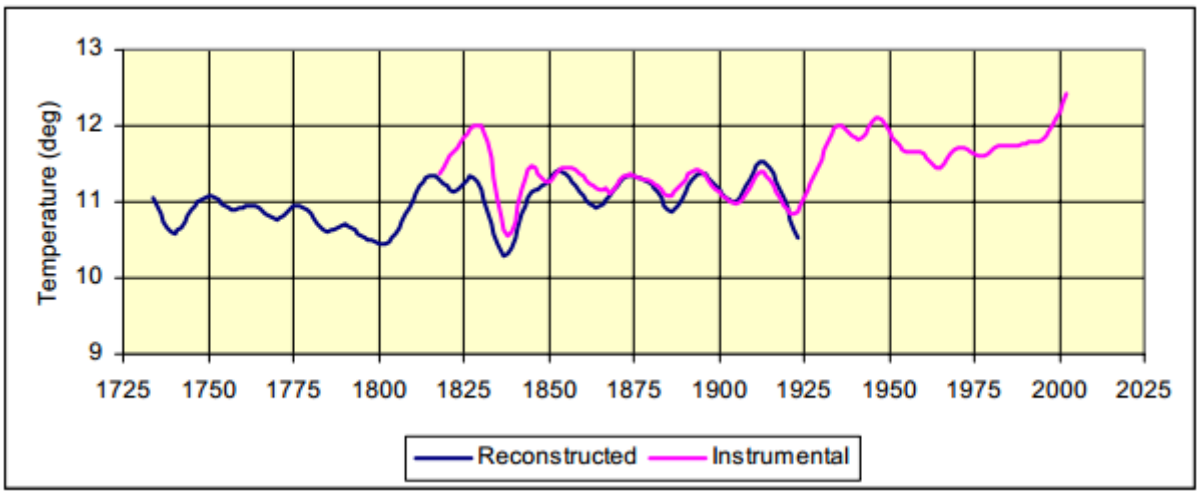

Figure 6.2: Reconstructed and instrumental temperatures

Vestlandet and Bergen series. For more info, see Nordli et al. (2002)

The M1-1 terminal moraine in Fosdalen fits the 1760-1770 advance of Nigardsbreen. According to Nordli et al. (2002), The 1760-1770 advance was dominated by high summer temperatures which is associated with predominating westerly winds that accumulates large amounts of snow. Thus it is probable that the western cirque glacier reached, or preceded its 1748 level in 1769. Conclusively, as age estimates for this thesis were divided into 5 year intervals, LIA_{max} for the western cirque glacier is estimated to 1769 AD ± 4 yr.

M1-2 does not correlate with Nigardsbreen, as the latter preceded the 1819 advance. A possible explanation for this might be the same as for the terminal moraine above, which is the five year interval used for this thesis, thus 1819 ± 4 yr (M1-2) and 1815 (Nigardsbreen) may be the same age. Moreover one cannot rule out the possibility of flaws in the lichenometric data. Another explanation is a delayed response time in Fosdalen. The latter is however less likely, due to the close relation between M1-2 even upper surface in 1824 and Nigardsbreen in 1825.

As summer temperatures were high between approximately 1810-1830 (figure 6.2) temperature data is difficult to interpret. Based on the reconstructed temperatures (blue line), there were two high`s which may have been the years when the deposits were made. However, the instrumental records (purple line) shows only one high late during this period.

M1-3 correlates with Nigardsbreen, and high summer temperatures on both reconstructed and instrumental records. In addition, a huge avalanche in 1868 destroyed almost all the farms at Gjørven in the Strynedalen valley during a winter with heavy snowfall (A.Gjørven, personal

communication 2014). If this indicates a prolonged period of more snow, 1874 ± 4 yr for M1-3 seems to be a reliable estimate due to some years of response time.

M1-TR does not correlate with Nigardsbreen. A marked climatic shift around 1930 increased summer temperatures to levels of which led to a long period of retreat. Briksdalsbreen however, advanced around 1921-1931, and thus correlates with M1-TM.

As for the remaining periods of lowering of ELA on Nigardsbreen, and glacier-front advances for Briksdalsbreen, a more thorough investigation is needed which exceeds the limits for this thesis. One suggestion is, after re-examining pictures from the study area, that there might exist at least one more moraine on the plain between M1-TM and M1-3 (fig.5.3).

6.2.2 Age of eastern cirque glacier landforms

In front of the eastern cirque, at its western toe, M2-M1 yields the oldest age, 1859 AD. M2-R1 has little no growth, and M2-R2 became ice free no earlier than 1944 AD (table 5.2).

In front of the eastern cirque, at its eastern toe, M3-CM yields the oldest age, 1854 AD. However, as the general boulder size was small, lichens on a large boulder lying on the distal side were included, yielding 1809 AD. M3-LR does not provide accurate results, as the measurements were carried out on the lateral moraine of M3-CM (chapter 5.4.2). It is thus only recognized as older than 1809 AD due to morphostratigraphy.

M3-M seems to be the youngest as it became ice free no earlier than 1949 AD based on LL. Boulders found on M3-P had no growth, and as they were observed in 2005 AD (Statens Kartverk, 2005), they were deposited at least 9 years ago. M3-RG had several large lichens, but they were all fused. Thus this form is also only recognized as older than 1809 AD (table 5.3). Both the latter and M3-LR seem to be a lot older than LIA based on vegetation on M3-LR.

Additionally, M3-RG seems to derive from M3-LR, as the latter seems to be part of a former talus system between the western and eastern toes of the eastern cirque glacier (figure 5.4.1.2) and (Norkart, 2001, Statens Kartverk, 2010, Statens Kartverk, 2005).

The terminal moraines below the eastern cirque glacier seem to correlate well, as M2-M1 is dated 1859 AD and M3-CM is dated 1854 AD. Compared to instrumental records and reconstructed summer temperatures (figure 6.2), this period had high summer temperatures, which increases the probability of an interpretation in which these are the terminal moraines

representing LIA_{max} for the eastern glacier. Moreover, present day western toe stretches around 40 m lower in altitude its eastern counterpart. This is approximately the same altitudinal difference as between M2-M1 and M3-CM, which increase the probability of these moraines being deposited at the same time.

It is important however, to consider the possibility that even though both of the terminal moraines correlate well, they may both be incorrect. M2-M1 due to possibly poor growth conditions. As pointed out by Innes (1985) and Matthews (2005), lichen growth rates are affected by lack of sunlight, thus suffering the condition known as "snow kill". This particular moraine lies close to the steep arête and the surrounding headwalls. The mountain shadow can also be seen on datasets covering the site (Statens Kartverk, 2010, Norkart, 2001, Statens Kartverk, 2005).

In addition, the area is highly influenced by redistributing processes (chapter 5.3.1), which according to McCarrol et al. (1998) may cause burying of boulders that could contain representative lichen specimen. M3-CM also experiences mountain shadow, but it lies further away from its surrounding headwalls than the former. It is also subject to avalanches and rock falls (chapter 5.4.1.3) that may have buried representative lichens.

Conclusively, the possibility of snow kill and burying of representative lichens does not outweigh the correlated factors mentioned above, and thus 1859 ± 4 yr and 1854 ± 4 yr is considered to be accurate age estimates. Correspondingly, the possible interpretation of M3-CM being dated to 1809 is excluded.

Compared to Nigardsbreen, the 1854 and 1859 AD results do not correlate. However, temperatures were still high in the beginning of 1850s, and then decreasing, thus suggesting 1854 being more likely than 1859 AD.

In M3-P, several large boulders without lichens lie onto the plain (figure 5.4.1.4). As these boulders were deposited prior to the photos taken in 2005 (Statens Kartverk, 2005), and their large size reduces the possibility of late lying snow and hence snow kill, the time prior to colonization is estimated to >9 yr. Additionally they were deposited far from surrounding rock walls, thus the chance of being affected by mountain shadow is considered small. The Nordvestlandet curve by Erikstad and Sollid (1986) chosen for this thesis thus seem to correlate well, as it estimates lichen colonization to occur 12-14 years subsequent to deposition (figure 4.2). The boulders mentioned should be reinvestigated during the upcoming

years in order to verify the usefulness of the Nordvestlandet curve for the investigated area. Future research should also aim to figure out the exact year of deposition, either by the Be^{-10} method, or by acquiring photos that reveal time of deposition.

6.3 Western rock wall and associated landforms

6.3.1 Present talus systems

As seen in chapter 5.5.1.3. several coalesced talus cones lie below the south western rock wall. Some of them are partially covered by vegetation, and others are not. The ones without vegetation are the westernmost talus cones. However, release areas (in this thesis referred to as scree wounds) can be observed above both vegetated and non-vegetated talus cones (fig.5.20). The difference in vegetation can be explained by the snowpack further west. In 2005, the snowpack stretched further east than today (Statens Kartverk, 2005). If it did so long-term, it would have been difficult for vegetation to establish. If not, the lack of vegetation indicates that these talus cones are active and that rock falls occur frequently. In a recent investigation on rock fall frequency in Erdalen, Skarsten (2007) revealed enhanced rock fall the latter 100 years, compared to LIA, possibly due to a raise in the lower permafrost limit. This increases the probability of the talus cones being active.

The talus cones seem pretty much normal in shape and structure at their heads. On the contrary, their toes transfer into an even step that consists of several minor diagonal ridges and furrows with little vegetation. The front of the step is convex, very steep and the vegetation cover is solid. Also, further down slope, at the place where the angle of the slope declines, several large boulders can be observed. The lichens at the step are mostly fused and tiny, although the largest specimen found is more than 300 mm in diameter, thus indicating a diachronic age (table 5.4).

The steep front is similar to those of relict rock glaciers as they are described by Lilleøren and Etzelmülier (2011), although the abnormal height of >40 m should be mentioned. The step on the other hand, contains little vegetation. This absence is interesting, however not unexplainable due to possibly late lying snow (Statens Kartverk, 2005). Although scree wounds and lack of vegetation on talus cones indicates current rock fall processes, the largest lichen is over 300 mm. The minor ridges themselves were not measured, which in hindsight might had provided evidence of recent development, or undermine such a hypothesis. It is suggested that the FALL approach by McCarroll (1994) is applied on the step and talus cones

in order to figure out the estimated age of the area. This due to the surfaces being diachronous.

6.3.2 The possibility of permafrost conditions

Interpolated MAAT for this area correspond to somewhere between -0.9 ˚C and +2˚C, depending on lapse rate used (chapter 2.4). Relatively recent research by Etzelmüller et al. (2003) and Lilleøren et al. (2012) have estimated that discontinuous permafrost may be present where MAAT = -3˚C, as opposed to the former calculated -4˚C (Etzelmüller et al., 1998, King, 1986, Ødegård et al., 1996). Thus a lower limit of permafrost is estimated to 1500-1600 m a.s.l. this far west (Etzelmüller et al., 1998, Etzelmüller et al., 2003). However, according to Lilleøren and Etzelmülier (2011), several of the intact permafrost landforms in western Norway are situated below this limit, which is an indication of permafrost landforms in marine environments at higher MAAT than expected.

As that may be, Isaksen et al. (2011) estimated the lower limit of permafrost as low as 1300-1400 m a.s.l in rock walls in Møre og Romsdal, and pointed to a difference between north- and south facing rock walls. Hipp et al. (2014) concluded that this difference in altitude between north- and south facing rock walls may be much as 300 m.

The 1300-1400 m a.s.l limit suggested by Isaksen et al. (2011) was measured approximately 80 km north east of Fosdalen. Due to the lower limit increase in altitude towards the west (Etzelmüller et al. (1998, 2003), a minimum of 50-100 m altitudinal increase should be added for Fosdalen. This gives an estimated lower permafrost limit of 1375 - 1475 ± 25 m a.s.l. However, as north facing rock walls may experience permafrost 300 m lower than south facing walls, the altitude mentioned above may be too high, and thus the permafrost limit may be as low as 1075 - 1175 ± 25 m a.s.l.

If the possibility of discontinuous permafrost being present at the talus and step areas is calculated from the extrapolated temperatures from Loen, the optimum conditioned MAAT = -0.9˚C is still 2.1˚C to high (Etzelmüller et al., 2003, Lilleøren et al., 2012). Furthermore, MAAT = -3˚C is found at approximately 1300 m a.s.l. in the north facing rock wall. When 1˚C is added to MAAT as suggested by Hipp et al. (2014), this gives a relationship of -2˚C = 1300 m a.s.l. Consequently, by using the 0.7˚C lapse rate, an altitude of 1450 ± 7 m a.s.l. is required for discontinuous permafrost to exist. If the lowering of 300 m as suggested by Isaksen et al. (2011) for north facing rock walls is accurate, this means discontinuous permafrost may be present at1150 ± 7 m a.s.l. in north facing rock walls in Fosdalen.

Recent rock fall activity occur in the area, as scree wounds are observed at heights approximately 1200, 1300 and 1420 m a.s.l. east-west respectively. The most active talus cones lie beneath the western scree wound. This may indicate that these parts of the rock wall were previously affected by permafrost conditions, and have now become unstable as a result of freeze-thaw mechanisms (Davies et al., 2001, Blikra and Nemec, 1998, Gruber and Haeberli, 2007, Matsuoka and Murton, 2008).

The altitude of the step and upper parts of the talus cones lies between 1020 - 1240 m a.s.l. (Statens Kartverk, 2010). As mentioned above, discontinuous permafrost may be present at 1075 - 1175 ± 25 m a.s.l. This correlates well with optimum MAAT extrapolated to Fosdalen, as it indicates that permafrost conditions are possible at 1150 ± 7 m a.s.l. However, these are the optimum conditions, and as recent scree wounds are located above this altitude, it is possible, but unlikely that discontinuous permafrost occur within the coalesced talus cones at present. As the most elevated part of the step lies at 1060 m a.s.l. and the minor ridges occur at approximately 1020 m a.s.l. it is suggested that permafrost conditions are not present.

Nevertheless, as seen in fig.2.4 by Nesje and Dahl (1993), MAAT was 1˚C lower during LIA, which increases the possibility of discontinuous permafrost existing at that time. Thus, if late lying snow in the area have been a frequent phenomena after LIA, it is possible that the snow cover isolated possible former permafrost from the active layer. This leads to the hypothesis that this landform is a relict rock glacier at an early stage developing during LIA.

As rock glaciers develops from ice-debris accumulation systems provided by permafrost conditions (Berthling and Etzelmüller, 2011), MAAT low enough to cause permafrost and abundance of debris supply is necessary is needed in order to maintain a continued development.

In a study of Murtèl rock glacier, Kääb et al. (1998) found that a block of incompressible material of 2 m thickness over the time of 3000 yr, gave a total vertical growth of 6 m. In addition they found that wavelengths of approximately 20 m corresponded to a relative age difference of 300-400 yr.

The diagonal ridges found on the step are at most 50 cm high, and the distance between them are at most 1 meter. If these ridges can relate to the Murtèl rock glacier, their height indicate that they may have developed within approximately 250 years. Furthermore, if the distance

between them indicates a relative age difference of 15-20 years, and 6 ridges were observed, a short duration such as LIA may have been enough to form a rock glacier.

In other studies of surface velocities, Frauenfelder and Kääb (2000) found surface ridges at Murtèl moving at approximately 0.05 m a^{-1}, while Monnier et al. (2013) found 0.6 - 1.3 ± 0.6 m a^{-1} at Sachette rock glacier.

The approximate length of the step from talus to front is <40 m. If the velocity were close to Murtèl, the time needed for development is approximately 800 yr, while the median of the velocity found at Sachette suggest that a development only took around 40 yr. Hence it is possible that the step is the visible expression of an early stage of rock glacier development.

However, although not found on the minor ridges per se, LL within the step is more than 300 mm. This indicates a deposition prior to LIA. Thus a more likely scenario is that this early-stage rock glacier developed in another cold period, perhaps during the Erdalen Event. Or, a combination is possible. As the front is covered with solid vegetation, it is possible that development started a long time ago, and that the creep processes stopped during the hypsithermal period. Permafrost may then have restarted creep processes during LIA which led to the development of the minor ridges. Although this scenario is possible, the interpretations given here is clearly in need of a more thorough investigation.

6.3.3 Former landform systems

Further down slope, a debris -landform (R1-F1) has the characteristics of relict rock glaciers as described by Lilleøren and Etzelmülier (2011). The surface is covered by solid vegetation except within its huge furrows (chapter 5.5.1.1). The lowermost part of the front is located at 860 m a.s.l.

East and/or onto R1-F1 lies another debris -landform with the same characteristics (R1-F2). The latter differ first of all due to a prominent longitudinal ridge at its upper westernmost edge. This ridge is stretches from the step area mentioned above and down to approximately 960 m a.s.l. At the same time, an element interpreted as a huge debris flow lobe lies some 80 m east of the longitudinal ridge. The lowermost part of the front is located at 910 m a.s.l.

The remaining areas i.e. R1-WCF and R1-River is composed of complex and non-coherent shapes with distinguishable heights and several boulder accumulations, ridges and furrows in transverse, longitudinal and diagonal directions. The peak between R1-River and R1-CR has the same altitude as the topography south of the river.

According to Lilleøren and Etzelmülier (2011), the lowest elevation of a mapped relict rock glacier in southern Norway is 1000 m a.s.l. This thesis challenge this limit, as both R1-F1 and R1-R2 is interpreted as relict rock glaciers. Additionally R1-WCF is interpreted as former creep systems. It is further suggested that the peak between R1-River and R1-CR have been part of R1-WCF and that the R1-CR is a former river course. A possible explanation for the change into the present river course is due to a) melting of ice in the creep systems which eventually the river broke through and eroded down to the its present level b) a GLOF occurring from the plain north of R2-YDM. Both of these suggestions are in need of further investigations.

As for the relative age, R1-F1 is suggested to be older than R1-F2, due to topography and morphostratigraphy as it the latter seems to lie onto the former (fig 5.18). As seen on the foreland of Cerro Tapado glacier where the upper younger landforms have developed onto the lower landforms (Monnier et al., 2014), such an interpretation is considered probable.

6.4 A hitherto unmapped debris- landform system: when, what and how

A hitherto unmapped debris -landform system referred to as R2-RG consisting of several ridges and furrows of unknown origin lies below the eastern cirque. This landform is highly distinguishable from the terminal and marginal moraines below the western cirque. The northernmost meandering ridge has been named R2-YDM . Nesje and Dahl (1992) interpreted R2-YDM as a lateral moraine from the Lodalen valley glacier based on a master thesis from Lien (1985).

In the present thesis, the glacial geology work provided by Fareth (1987) has been reinterpreted, and alternative propositions to the former interpretations by Lien (1985) and Nesje and Dahl (1992) are suggested. First, the deglaciation chronology is reviewed. Later, the R2-YDM is connected to the landforms upslope, and thus reinterpreted along with possible explanations for its current expression.

6.4.1 Deglaciation chronology

Fareth (1987) mapped several prominent moraines in the Nordfjord region. He estimated that 6 readvances occurred after LGM. The youngest which is the Eide stadial, has terminal deposits from valley glaciers located too far east for an ice surface up to 1040 m a.s.l where R2-YDM is located. The second youngest is the Vinsrygg stadial. Although no frontal deposits were located, it is believed that the front was located between Stryn and Innvik. The

lateral moraines observed lies at approximately 300-400 m a.s.l. at Vinsrygg and at the Staurisetra dairy. Thus also indicating that a rapid rise to 1040 m a.s.l. is highly unlikely in such short distance.

During the Nor stadial however, the presence of a valley glacier in Fosdalen seems more likely. Based on maps containing information about the mapped moraines by Fareth (1987), this thesis suggests that the Nor glacier flowed westward, crossing the pass that separates Fosdalen from Strynedalen as it lies at approximately 1260 m a.s.l. The Strynedalen valley glacier is interpreted to approximately 1300-1400 m a.s.l. (corrected for isostatic recovery) at this pass. Consequently the lateral moraine in Fosdalen caused by the Nor glacier must have been at a higher altitude than R2-YDM, and hence been buried or destroyed by processes after its deposition. This is not an unlikely scenario due to the current topography and subsequent processes in Fosdalen. The moraine formation on the north side of Fosdalen is furthermore interpreted as a result of the relict niche glaciers east of Storskredfjellet mountain (fig.4.3). However, a further investigation of the north side moraine is advised as it exceeds this thesis.

Lateral Nor moraines were mapped at 1034 m a.s.l. by Fareth (1987). However these moraines were observed in the Strynedalen valley west of Staurinibba, and is situated more than 6 km west of R2-YDM. Hence they add to the argumentation of a Nor moraine in Fosdalen situated at a higher altitude than R2-YDM. This suggestion also leads to a possible error in the main ice-drainage routes for the late Weichselian maximum ice sheet proposed by Rye et al. (1987).

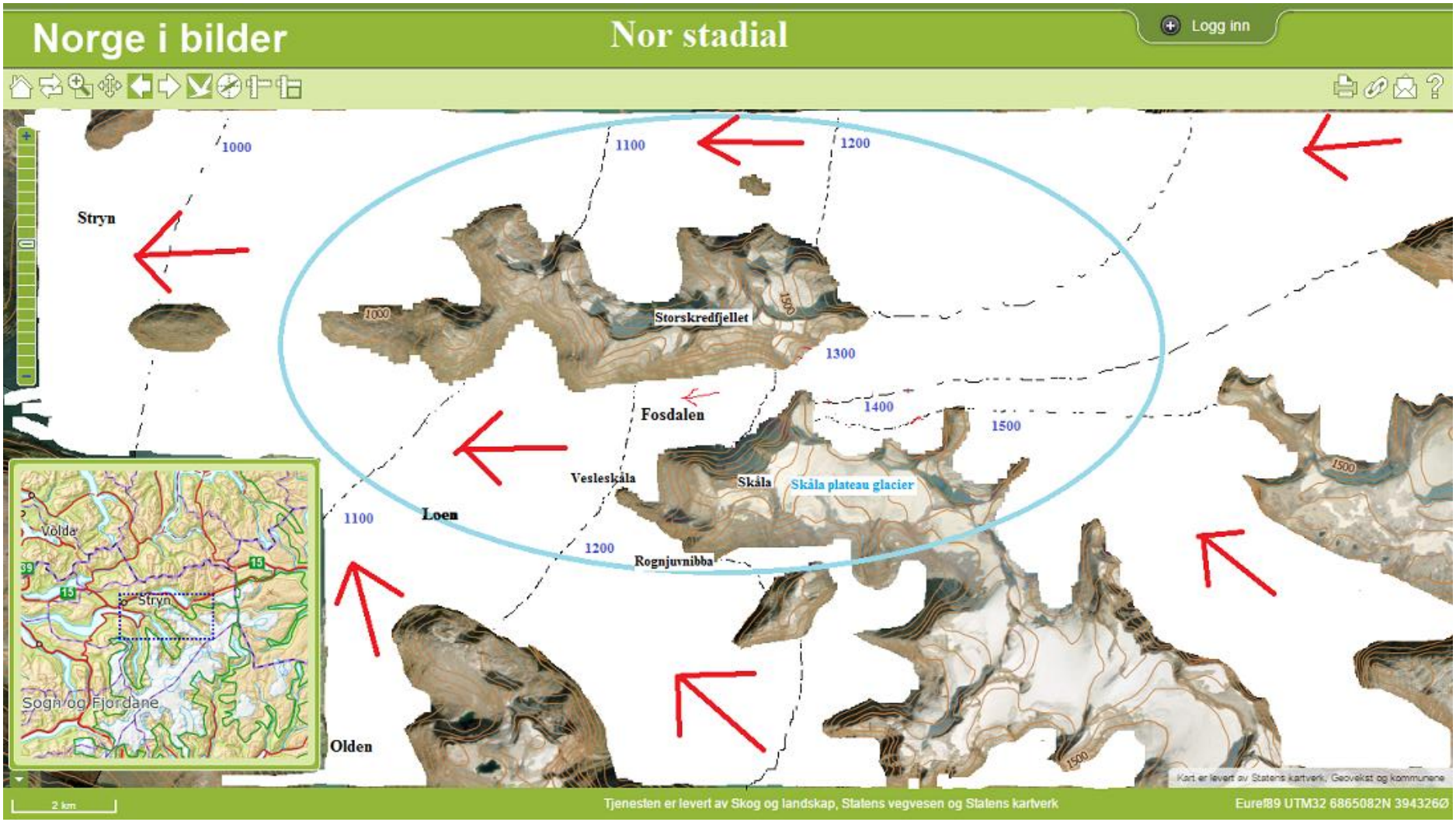
Norge i bilder
Nor stadial
Logg inn
Stryn
Storskredfjellet
Fosdalen
Vesleskåla
Skåla
Skåla plateau glacier
Loen
Rognjuvnibba
Olden
Volda
Sogn og Fjordane
1000
1100
1200
1300
1400
1500
2 km
Tjenesten er levert av Skog og landskap, Statens vegvesen og Statens kartverk
Euref89 UTM32 6865082N 394326Ø

Figure 6.3: Suggested glacial flow direction during the Nor stadial

Red arrows: suggested flow direction. White layer: Reconstructed glacial cover. Blue circle: More accurate mapping than the rest of vertical extent of the glacier. Black contour lines: 100 m interval of vertical extent. Blue numbers: m a.s.l of reconstructed ice sheet corrected for isostatic recovery. The map is based on the Pl.2 map from Fareth (1987) sketched onto Statens Kartverk (2010)

In addition to the R2-YDM shape reconstructed in Nesje and Dahl (1992), the step at the R1 site was interpreted as the same Younger Dryas lateral moraine system caused by the Loen valley glacier. And finally, the last landform included in this system is a moraine which is situated at approximately 1160 m a.s.l. below the Skålavatnet lake. If the latter is a YD lateral moraine, an almost vertical drop of 120-140 m down to the step seems highly unlikely (fig.5.26f).

The present reinterpretation of Fareth (1987) is in agreement with the latter being a YD moraine. However, the possibility of this being a moraine from a former plateau glacier at the westernmost limit of Skåla cannot be excluded. This due to the lowered moraine altitude near the Skålaelva river, as this has been observed near the drainage points at M1-1, M1-2 and M1-TR, thus indicating a westward direction of the moraine. In addition, the general topography between Skåla, Vesleskåla and Rongjuvnibba favours such a glacial formation. All things considered, the present cirque glacier south of Skåla is thus tentatively proposed to have been a plateau glacier stretching westward before turning into a cirque glacier at a later stage.

The final topographic curiosity is the subglacial till in the westernmost part of Fosdalen. Observations through Statens Kartverk (2010) indicates an even level at approximately 840 m a.s.l. on the east side of the valley entrance. Furthermore, approximately where a stream from a niche glacier west of Storskredfjellet enters the river from Fosdalen, the bedrock can several places be observed between 840-880 m a.s.l. The stream has eroded through a thick terrace of subglacial till that gently slope westward. Eastward, the terrace seems to stop where the altitude reaches 840 m a.s.l. Additionally, The R1-F1 lower limit lies next to this position at 860 m a.s.l (fig.5.23). This is not believed to be a coincident, and it is therefore proposed that a valley glacier from Lodalen did in fact flow into Fosdalen (fig.5.26f). However, contrary to former interpretations it is suggested that this occurred at a later stage than the Nor stadial. Presumably during the Vinsrygg stadial, or a hitherto unknown stadial between the two, and at a lower altitude than the former interpretations. As the R1-F1 stops next to this position, it is assumed that this relict rock glacier developed around the time of the Vinsrygg stadial. These suggestions need further investigations. In particular, attention should be addressed

towards the 840 m a.s.l. level, as the suggestions made here may contribute to an altered deglaciation chronology than is hitherto known.

6.4.2 Assembling landforms into one multi-temporal system

The debris -landform system from this point of the discussion include R2-YDM, R2-RG, M3-RG, M3-LR and M3-P (fig.5.25). The system consists of several ridges and depressions in every direction, semi rounded and angular debris, levees, gullies, lobes, a shallow lake and a plain. The vegetation cover ranges from totally absent to solid. Thus, provided permafrost conditions, the system shows some resemblance to active or inactive rock glaciers. However, the problem with such an interpretation occur mainly at the front (R2-YDM). The front has as previously stated been mistaken for a YD lateral moraine.

The hypothesis for this thesis, is that the front is connected to the westernmost longitudinal ridge within the system, and as a result works as the outer frame of the debris -landform system. The westernmost longitudinal ridge is covered with solid vegetation, and has previously been interpreted as a lateral moraine from the western cirque glacier during the Erdalen Event by Nesje and Dahl (1992).

Similarly, Jarman et al. (2013) argues that there are no relict rock glaciers in the British mountain. This due to all the systems, which he refers to as discrete debris accumulations (DDAs), can be explained from other originating processes. For instance rockslides that are being deposited onto a glacier, and then moved and redistributed further down slope by the glacier.

According to Hewitt (2009) RSF involves detachment of larger mass than those of rock falls, and generally leads to rock avalanches. If an RSF is deposited onto a glacier surface, its emplacement geometry is affected by change in frictional forces, and glacier surface topography. In addition, the velocity of glacial movement may be altered along with mass disturbance such as less ablation in the area where the avalanche is deposited.

As outlined by Deline (2009), if the debris is redistributed by glacial movement, an open-work structure is left behind when the glacier melts. The description of this open-work structure (chapter 3.4.) seems to match the debris -landform system observed below the eastern cirque glacier in Fosdalen.

The solid vegetation cover on the westernmost ridge can be explained due to wet flows that followed the ice-margin (fig.5.30c-d). Additionally, boulders and finer sediments may be shed

from the ice. Reduced ablation caused by deposited rock avalanches also seem to close crevasses, and thus finer deposits may stay in a supraglacial position until glacial movement down slope and gravitational processes shed it over the ice margin (Hewitt, 2009). The front ridge (R2-YDM) may be facing similar conditions as the lateral ridge, if the deposits reached the terminal position of the glacier before it retracted or melted down.

Additionally, if rock falls occur repeatedly, the open-work structure may be greatly modified (Deline, 2009). The debris -landform system in Fosdalen seems to override a former DDA at its northwestern corner. This is due to observations of the northwestern corner which seems to consist of two outer ridges with solid vegetation cover (fig.5.26d). This indicates that a minimum of two rock avalanches or substantially large rock falls have been deposited onto the eastern cirque glacier at a time when the glacier was substantially larger than it is today.

A minimum of two DDAs favor the great height of the front, which is approximately 20 m high throughout most of its course. The northwestern part of the front however, is only about 7 m high. Hence indicating that where they coincide, a second DDA is deposited onto the former thus adding to the original front height. The debris cover is less thick behind the front. This is tentatively suggested explained due to a lot of debris reaching the front, while less remained at the glacier surface, and when the ice melted, the remaining supraglacial debris did not amount to the same height as the front. The meandering shape of the front (R2-YDM) is thus suggested a result of different velocities transecting the cirque glacier due to unevenly distributed debris accumulations from the rock avalanches.

Attempted reconstructions of a former arête in order to account for the volumes of the debris -landform system are rejected, due to the underlying topography making it highly unlikely for such an event to be visible at the eastern end of Fosdalen. However, as the lowest DDA is only observed in the northwestern corner, the possibility of a rock fall or rock avalanche as a result of RSF at the former arête cannot be ruled out, but is considered unlikely.

6.4.3 Estimated time of origin

Upslope, at the southeastern corner, a relict coalesced talus system can be observed. This thesis suggests that during a former stadial, the eastern toe of the eastern cirque glacier eroded into the talus system and modified it into the M3-LR as it is expressed today, and that later re-advances of the eastern toe continued to follow this slope. Due to morphostratigraphy i.e. the easternmost position of R2-YDM relative to the position of M3-LR, it is suggested that this

erosion occurred after the debris -landform was deposited, and furthermore that this erosion caused the formation of the lake in the M3-P area.

LIA_{max} moraines are deposited to far upslope to be considered as a significant contributor to the debris -landform system. Thus it cannot be of younger age than the Erdalen Event, which is the last event when a cirque glacier size could have been large enough to cause such erosion. Nevertheless, the debris -landform system can be older. Provided the interpretation during the Nor stadial in the previous chapter is correct, a possible scenario is that the DDAs that constitute the debris -landform system occurred due to paraglacial adjustment when the valley glaciers melted down after the Nor stadial. Tentatively it is suggested that a re-advance during the Vinsrygg stadial may have been time of origin. Next the talus system upslope developed after the Vinsrygg stadial. And finally, the erosion leading to the formation of M3-LR is believed to have happened no later than the Erdalen Event.

Due to the coalesced talus system upslope, frequent rock falls seem to have happened after the DDAs were deposited. Provided the discussion on possible permafrost conditions in chapter 6.3.2. is accurate, there is a possibility that some parts of the debris -landform system have been modified after its deposition due to later ice formation in cold periods that lead to creep of the ice/debris mixtures. This is suggested due to observations of longitudinal ridges that seem to have crept onto and/or over the front (R2-YDM).

6.5 Erdalen Event Cirque glacier

Former research by Nesje and Dahl (1992) used topographic observations in order to reconstruct a former western cirque glacier in Fosdalen during the Erdalen Event. From these observations, and consequently landform interpretations, the maximum elevation of lateral moraines were decided along with the former glacier front. In this thesis, the topography has been reinterpreted based on observations.

As suggested in previous chapters, former (and present) interpretations made in Fosdalen may be wrong. These errors may be the result of equifinality, which means that different processes may cause landforms of similar geomorphometry.

In this thesis it is suggested that the interpreted lateral moraine on R1-F2, is a longitudinal ridge on a relict rock glacier, hence not a lateral moraine. The interpreted lateral moraine further down slope on R1-F1 is suggested to be the surface of a relict rock glacier. The interpreted lateral moraine on the east side which constitute the westernmost part of the R2

site in this thesis, is suggested to be part of the debris -landform system described in the previous chapter.

Finally, the interpreted front of the former glacier is suggested to be a former river course for two reasons. First, R1-WCF consists of chaotic formations that involve complex and non-coherent shapes, rich in horizontally and vertically distinguishable creep systems that might indicate a complex story as pointed out by Frauenfelder and Kääb (2000). Second, the pile between the present river and R1-CR has the same altitude and inclination as the R1-WCF area next to the present river.

However, the creep systems in R1-WCF may derive from a former cirque glacier e.g. Berthling (2011), Whalley (1979), and Whalley and Azizi (2003). It is also possible that the glacier margin coincided with and partially influenced the longitudinal ridge on R1-F2 and the westernmost longitudinal ridge on R2-RG. This is however, difficult to prove.

The level area north of R2-YDM may be interpreted as a flood plain. The depth of the river bed increases from almost zero to > 10 m approximately where the reconstructed Erdalen Event cirque glacier supposedly crossed the valley floor. The latter observation combined with the suggestion of R1-CR being the former river course indicate a dammed lake in the north east part of the valley. Whether this was due to a cirque glacier extending across the valley during the Erdalen Event as suggested by Nesje and Dahl (1992), a cirque glacier during the Vinsrygg/Eide stadial, or a creep system consisting of ice/debris mixtures such as a rock glacier cannot be determined with certainty. Furthermore it is suggested that during a warmer period, the ice that was present at R1-WCF melted, causing a glacial lake outburst flood (GLOF), and a lowered topographic altitude. A further investigation of this hypothesis exceeds the limit of this thesis, and is thus suggested for prospective research.

7. Conclusions

The aim of this thesis has been to identify and investigate how several landforms have been developed in time and space in Fosdalen in Nordfjord, western Norway. The current topographic expression seems to be a result of both paraglacial and periglacial processes. The results and suggestions are summarized below:

- Based on volume calculations, and subglacial- and headwall retreat rates, the compound cirque in Fosdalen is believed to be very old. The excavated volume is calculated to >10x of current valley deposits, thus eliminating the possibility of the cirque being of Holocene age. A minimum age of 510.000 yr (Middle Pleistocene) assuming steady-state conditions is suggested.
- Based on the lichen type *Rhizocarpon geographicum*, the 5LL method and the Nordvestlandet curve, LIA_{max} for the western cirque glacier is estimated to 1769 AD ± 4 yr. LIA_{max} for the eastern cirque glacier is estimated to 1854 AD ± 4 yr. Based on comparison to a temperature reconstruction study from western Norway conducted on the Nigardsbreen outlet glacier, the Nordvestlandet curve apparently seems well suited for estimating lichen age in this area, and thus LIA_{max} estimates above are considered reliable.
- Based on morphostratigraphy, both cirque glaciers seem to have innermost ridges that are older than the moraine systems correlated to LIA, thus indicating that the glaciers flowed across the innermost ridges without deforming them.
- Based on former and recent research on permafrost, and talus and rock wall investigations, the permafrost lower limit is believed to be present at a higher altitude than present deposits. It is tentatively suggested that permafrost may have been present in the westernmost talus system during LIA, and hence activated or reactivated an early stage of rock glacier development at the step.
- Based on morphostratigraphy and topography, 2 relict rock glaciers have been identified below the westernmost talus system. Consequently lowering the limit of relict rock glaciers in southern Norway from 1000 m a.s.l. to 860 m a.s.l, hence contributing to the assumption that permafrost conditions may be present at higher MAAT than expected in marine areas. Time of origin is suggested to the Vinsrygg stadial during Younger Dryas.
- Based on reinterpretation of the Nor stadial and Vinsrygg stadial, it is suggested that the Strynedalen valley glacier flowed westward over the pass currently separating

Fosdalen from Strynedalen during the Nor stadial. As a result, the meandering ridge formerly mapped as a YD moraine from the Lodalen valley glacier, has been reinterpreted as part of the hitherto unmapped debris -landform system upslope. This system is proposed to be the remains of minimum two RSFs deposited onto the eastern cirque glacier during the Vinsrygg stadial.

- Based on observations and previous conclusions regarding the relict rock glaciers, it is tentatively suggested that the Lodalen valley glacier did enter Fosdalen, however during the Vinsrygg stadial, and with a maximum altitude of approximately 840 m a.s.l.
- Based on observations and previous conclusions in this thesis, it is suggested that the reconstruction of the Erdalen Event cirque glacier by Nesje and Dahl (1992) may be wrong due to equifinality, and that the present river course is due to a former GLOF penetrating a creep system at the western cirque glacier foreland when the ice within the creep system melted.

8. Prospective research

Throughout the course of the work applied in this thesis, several ideas have come to mind which could have been part of the thesis. They were however neglected due to the limited size of the thesis. Thus ideas and suggestions for prospective research are summarized below:

- In order to estimate a more accurate permafrost limit, input of solar radiation in different parts of Fosdalen could be measured (Frauenfelder and Kääb, 2000).
- A long-term study of rock falls could contribute to more accurate contemporary retreat rates.
- The FALL approach by McCarroll (1994) could be used on the deposits that are influenced by rock falls in order to estimate late Holocene rock fall rates.
- The angular boulders currently not colonized by lichens at the plain in M3-P could be reinvestigated in the upcoming years in order to verify the usefulness of the Nordvestlandet curve for the investigated area. Future research could also aim to figure out the exact year of deposition, either by the Be^{-10} method, or by acquiring photos that reveal time of deposition.
- As the present surface of the lake at M3-P lies > 5 m above the deposits north of R2-YDM, the permeability of the deposits nearby is interesting. InSAR or a borehole study could provide information on permeability as well as information regarding inner structure of the debris -landform system.
- In order to expand knowledge connected to glacier response to temperature fluctuations after LIA, a more thorough investigation of the moraines and comparison to other post LIA studies could be applied.
- The possibility of DDAs being relict rock glaciers or former rock avalanches deposited and repositioned by glacial activity could be further investigated throughout Norway.
- The possibility of a dammed lake north of R2-YDM and a subsequent GLOF could be investigated in order to strengthen or weaken the chronology suggested in this thesis.
- A more thorough investigation on the subglacial till terrace west in Fosdalen could contribute to strengthen or weaken the chronology suggested in this thesis.
- A more thorough investigation on the moraine below the south facing niche glaciers north of Fosdalen could contribute to strengthen or weaken the chronology suggested in this thesis.
- A more thorough investigation of the area between Skåla, Vesleskåla and

Rognjuvnibba could contribute to strengthen or weaken the possibility of the present cirque glacier south of Skåla being a former plateau glacier stretching westward.

References

ANDERSEN, B. G., MANGERUD, J., SØRENSEN, R., REITE, A., SVEIAN, H., THORESEN, M. & BERGSTRØM, B. 1995. Younger Dryas ice-marginal deposits in Norway. *Quaternary International,* 28**,** 147-169.

ANDERSEN, J. L. & SOLLID, J. L. 1971. Glacial Chronology and Glacial Geomorphology in the Marginal Zones of the Glaciers, Midtdalsbreen and Nigardsbreen, South Norway. *Norsk Geografisk Tidsskrift - Norwegian Journal of Geography,* 25**,** 1-38.

ANDRÉ, M.-F. 2003. Do periglacial landscapes evolve under periglacial conditions? *Geomorphology,* 52**,** 149-164.

BALLANTYNE, C. K. 2002. Paraglacial geomorphology. *Quaternary Science Reviews,* 21**,** 1935-2017.

BENN, D. & EVANS, D. 2010. Glaciers and glaciation.

BENN, D. I. & BALLANTYNE, C. K. 2005. Palaeoclimatic reconstruction from Loch Lomond Readvance glaciers in the West Drumochter Hills, Scotland. *Journal of Quaternary Science,* 20**,** 577-592.

BERTHLING, I. 2011. Beyond confusion: Rock glaciers as cryo-conditioned landforms. *Geomorphology,* 131**,** 98-106.

BERTHLING, I. & ETZELMÜLLER, B. 2007. Holocene rockwall retreat and the estimation of rock glacier age, Prins Karls Forland, Svalbard. *Geografiska Annaler: Series A, Physical Geography,* 89**,** 83-93.

BERTHLING, I. & ETZELMÜLLER, B. 2011. The concept of cryo-conditioning in landscape evolution. *Quaternary Research,* 75**,** 378-384.

BESCHEL, R. E. 1950. Flecten als altersmasstab Rezenter morainen. *Zeitschrift für Gletscherkunde und Glazialgeologie,* 1**,** 152-161.

BESCHEL, R. E. 1961. Dating rock surfaces by lichen growth and its application to glaciology and physiography (lichenometry). *Geology of the Arctic, University of Toronto Press, Toronto* 1044-1062.

BEYLICH, A. 8.10.2014 2014. *RE: Temperature decrease rate.*

BICKERTON, R. W. & MATTHEWS, J. A. 1992. On the accuracy of lichenometric dates: an assessment based on the'Little Ice Age'moraine sequence of Nigardsbreen, southern Norway. *The Holocene,* 2**,** 227-237.

BLIKRA & NEMEC 1998. Postglacial colluvium in western Norway: depositional processes, facies and palaeoclimatic record. *Sedimentology,* 45**,** 909-959.

BLIKRA, L., LONGVA, O., BRAATHEN, A., ANDA, E., DEHLS, J. & STALSBERG, K. 2006. Rock slope failures in Norwegian fjord areas: examples, spatial distribution and temporal pattern. *Landslides from massive rock slope failure.* Springer.

BOGEN, J. 1989. Glacial sediment production and development of hydro-electric power in glacierized areas. *Annals of Glaciology,* 13**,** 6-11.

BRADWELL, T. 2004. Lichenometric dating in southeast Iceland: the size–frequency approach. *Geografiska Annaler: Series A, Physical Geography,* 86**,** 31-41.

BRADWELL, T. 2009. LICHENOMETRIC DATING: A COMMENTARY, IN THE LIGHT OF SOME RECENT STATISTICAL STUDIES. *Geografiska Annaler: Series A, Physical Geography,* 91**,** 61-69.

BURKI, V., LARSEN, E., FREDIN, O. & MARGRETH, A. 2009. The formation of sawtooth moraine ridges in Bødalen, western Norway. *Geomorphology,* 105**,** 182-192.

COHEN, K., FINNEY, S., GIBBARD, P. & FAN, J. 2013. The ICS International Chronostratigraphic Chart. www.stratigraphy.org.

CURRY, A. M. & MORRIS, C. J. 2004. Lateglacial and Holocene talus slope development and rockwall retreat on Mynydd Du, UK. *Geomorphology,* 58**,** 85-106.

DAVIES, M., HAMZA, O. & HARRIS, C. 2001. The Effect of Rice in Mean Annual Temperature on the Stability of Rock Slopes Containing Ice-Filled Discontinuities. *Permafrost and Periglacial Processes,* 12**,** 137-144.

DELINE, P. 2009. Interactions between rock avalanches and glaciers in the Mont Blanc massif during the late Holocene. *Quaternary Science Reviews,* 28**,** 1070-1083.

DORREN, L. K. A. 2003. A review of rockfall mechanics and modelling approaches. *Progress in Physical Geography,* 27**,** 69-87.
DRĂGUŢ, L. & BLASCHKE, T. 2006. Automated classification of landform elements using object-based image analysis. *Geomorphology,* 81**,** 330-344.
ERIKSTAD, L. & SOLLID, J. L. 1986. Neoglaciation in South Norway using lichenometric methods. *Norsk Geografisk Tidsskrift - Norwegian Journal of Geography,* 40**,** 85-105.
ETZELMÜLLER, B., BERTHLING, I. & SOLLID, J. L. The distribution of permafrost in Southern Norway; a GIS approach. Seventh International Conference on Permafrost, Proceedings. Collection Nordicana. Centre d'Etudes Nordiques, Universite Laval, Quebec, PQ, Canada, 1998. 251-257.
ETZELMÜLLER, B., BERTHLING, I. & SOLLID, J. L. 2003. Aspects and concepts on the geomorphological significance of Holocene permafrost in southern Norway. *Geomorphology,* 52**,** 87-104.
EVANS, D. J. A., ARCHER, S. & WILSON, D. J. H. 1999. A comparison of the lichenometric and Schmidt hammer dating techniques based on data from the proglacial areas of some Icelandic glaciers. *Quaternary Science Reviews,* 18**,** 13-41.
EVANS, I. S. & COX, N. 1974. Geomorphometry and the Operational Definition of Cirques. *Area,* 6**,** 150-153.
EVANS, S. G. & HUNGR, O. 1993. The assessment of rockfall hazard at the base of talus slopes. *Canadian Geotechnical Journal,* 30**,** 620-636.
FARETH, O. W. 1987. *Glacial geology of middle and inner Nordfjord, western Norway*, Trondheim.
FRAUENFELDER, R. & KÄÄB, A. 2000. Towards a palaeoclimatic model of rock-glacier formation in the Swiss Alps. *Annals of Glaciology,* 31**,** 281-286.
GILES, P. T. & FRANKLIN, S. E. 1998. An automated approach to the classification of the slope units using digital data. *Geomorphology,* 21**,** 251-264.
GJØRVEN, A. 2014. *RE: The avalanche in 1868.* Type to GJØRVEN, A.
GORDON, J. E. 1977. Morphometry of Cirques in the Kintail-Affric-Cannich Area of Northwest Scotland. *Geografiska Annaler. Series A, Physical Geography,* 59**,** 177-194.
GRIMSTAD, E. 2005. The Loen rock slide - an analysis of the stability. *In:* SENNESET, K., FLAATE, K. & LARSEN, J. O. (eds.) *Landslides and Avalanches ICFL 2005 Norway.* London: Taylor & Francis Group.
GROVE, J. 1988. The Little Ice Age: London. *UK, Methuen*.
GROVE, J. M. 2004. Little ice ages: ancient and modern (2 volumes). Routledge, London.
GRUBER, S. & HAEBERLI, W. 2007. Permafrost in steep bedrock slopes and its temperature-related destabilization following climate change. *Journal of Geophysical Research: Earth Surface,* 112**,** F02S18.
HAEBERLI, W. 1985. Creep of mountain permafrost: internal structure and flow of alpine rock glaciers. *Mitteilungen der Versuchsanstalt fur Wasserbau, Hydrologie und Glaziologie an der ETH Zurich,* 77**,** 5-142.
HAEBERLI, W., HALLET, B., ARENSON, L., ELCONIN, R., HUMLUM, O., KÄÄB, A., KAUFMANN, V., LADANYI, B., MATSUOKA, N. & SPRINGMAN, S. 2006. Permafrost creep and rock glacier dynamics. *Permafrost and Periglacial Processes,* 17**,** 189-214.
HALL, K., THORN, C. E., MATSUOKA, N. & PRICK, A. 2002. Weathering in cold regions: some thoughts and perspectives. *Progress in Physical Geography,* 26**,** 577-603.
HALLET, B., HUNTER, L. & BOGEN, J. 1996. Rates of erosion and sediment evacuation by glaciers: A review of field data and their implications. *Global and Planetary Change,* 12**,** 213-235.
HAYNES, V. M. 1968. The Influence of Glacial Erosion and Rock Structure on Corries in Scotland. *Geografiska Annaler. Series A, Physical Geography,* 50**,** 221-234.
HEWITT, G. 2000. The genetic legacy of the Quaternary ice ages. *Nature,* 405**,** 907-913.
HEWITT, K. 2009. Rock avalanches that travel onto glaciers and related developments, Karakoram Himalaya, Inner Asia. *Geomorphology,* 103**,** 66-79.
HIPP, T., ETZELMÜLLER, B. & WESTERMANN, S. 2014. Permafrost in Alpine Rock Faces from Jotunheimen and Hurrungane, Southern Norway. *Permafrost and Periglacial Processes,* 25**,** 1-13.

HUMLUM, O. 1988. Rock glacier appearance level and rock glacier initiation line altitude: a methodological approach to the study of rock glaciers. *Arctic and Alpine research*, 160-178.
IKEDA, A. & MATSUOKA, N. 2006. Pebbly versus bouldery rock glaciers: Morphology, structure and processes. *Geomorphology,* 73, 279-296.
INNES, J. L. 1985. Lichenometry. *Progress in Physical Geography,* 9, 187-254.
ISAKSEN, K., BLIKRA, L. H. & EIKEN, T. The existence of warm permafrost in unstable rock slopes in western and northern Norway. Geophysical Research Abstracts, 2011.
JARMAN, D., WILSON, P. & HARRISON, S. 2013. Are there any relict rock glaciers in the British mountains? *Journal of Quaternary Science,* 28, 131-143.
JOHNSON, W. D. 1904. The Profile of Maturity in Alpine Glacial Erosion. *The Journal of Geology,* 12, 569-578.
JOMELLI, V., GRANCHER, D., NAVEAU, P., COOLEY, D. & BRUNSTEIN, D. 2007. Assessment study of lichenometric methods for dating surfaces. *Geomorphology,* 86, 131-143.
KING, L. 1986. Zonation and Ecology of High Mountain Permafrost in Scandinavia. *Geografiska Annaler. Series A, Physical Geography,* 68, 131-139.
KÄÄB, A., GUDMUNDSSON, G. H. & HOELZLE, M. Surface deformation of creeping mountain permafrost. Photogrammetric investigations on rock glacier Murtèl, Swiss Alps. 7th International Conference on Permafrost (Yellowknife, 23–27 June 1998), Collection Nordicana, 1998. 531-537.
LARSEN, E. & MANGERUD, J. 1981. Erosion Rate of a Younger Dryas Cirque a Glacier at Krakenes, Western Norway. *Annals of Glaciology,* 2, 153-158.
LIASET, K. E. 2006. *Skåla 1843 moh* [Online]. http://www.fjellside.com/skala.htm. [Accessed 2014-11-09.
LIEN, R. 1985. Kvartærgeologien i Bødalen, Loen, indre Nordfjord. *Unpublished ThesisUniversity of Bergen*.
LILLEØREN, K. S. & ETZELMÜLIER, B. 2011. A REGIONAL INVENTORY OF ROCK GLACIERS AND ICE-CORED MORAINES IN NORWAY. *Geografiska Annaler: Series A, Physical Geography,* 93, 175-191.
LILLEØREN, K. S., ETZELMÜLLER, B., SCHULER, T. V., GISNÅS, K. & HUMLUM, O. 2012. The relative age of mountain permafrost—estimation of Holocene permafrost limits in Norway. *Global and Planetary Change,* 92, 209-223.
LUCKMAN, B. & FISKE, C. 1995. Estimating long-term rockfall accretion rates by lichenometry. *Steepland geomorphology,* 3, 221-254.
MATSUOKA, N. & MURTON, J. 2008. Frost weathering: recent advances and future directions. *Permafrost and Periglacial Processes,* 19, 195-210.
MATSUOKA, N. & SAKAI, H. 1999. Rockfall activity from an alpine cliff during thawing periods. *Geomorphology,* 28, 309-328.
MATTHEWS, J. A. 1994. Lichenometric dating: a review with particular reference to 'Little Ice Age'moraines in southern Norway. *Dating in Exposed and Surface Contexts. University of New Mexico Press, Albuquerque*, 185-212.
MATTHEWS, J. A. 2005. 'Little Ice Age'glacier variations in Jotunheimen, southern Norwvay: a study in regionally controlled lichenometric dating of recessional moraines with implications for climate and lichen growth rates. *The Holocene,* 15, 1-19.
MATTHEWS, J. A., NESJE, A. & LINGE, H. 2013. Relict Talus-Foot Rock Glaciers at Øyberget, Upper Ottadalen, Southern Norway: Schmidt Hammer Exposure Ages and Palaeoenvironmental Implications. *Permafrost and Periglacial Processes,* 24, 336-346.
MAYR, E. & BOCK, W. J. 2002. Classifications and other ordering systems. *Journal of Zoological Systematics and Evolutionary Research,* 40, 169-194.
MCCARROL, D., SHAKESBY, R. A. & MATTHEWS, J. A. 1998. Spatial and Temporal Patterns of Late Holocene Rockfall Activity on a Norwegian Talus Slope: A Lichenometric and Simulation-Modeling Approach. *Arctic and Alpine Research,* Vol. 30, 51-60.

MCCARROLL, D. 1994. A new approach to lichenometry: dating single-age and diachronous surfaces. *The Holocene,* 4**,** 383-396.
MCCARROLL, D., SHAKESBY, R. A. & MATTHEWS, J. A. 2001. Enhanced rockfall activity during the Little Ice Age: further lichenometric evidence from a Norwegian talus. *Permafrost and Periglacial Processes,* 12**,** 157-164.
MERNILD, S. H. & LISTON, G. E. 2010. The influence of air temperature inversions on snowmelt and glacier mass balance simulations, Ammassalik Island, southeast Greenland. *Journal of Applied Meteorology and Climatology,* 49**,** 47-67.
METEOROLOGICAL INSTITUTE, N. 2014. Monthly Normal Values. www.eklima.met.no.
MILLAR, C. I. & WESTFALL, R. D. 2008. Rock glaciers and related periglacial landforms in the Sierra Nevada, CA, USA; inventory, distribution and climatic relationships. *Quaternary International,* 188**,** 90-104.
MINÁR, J. & EVANS, I. S. 2008. Elementary forms for land surface segmentation: The theoretical basis of terrain analysis and geomorphological mapping. *Geomorphology,* 95**,** 236-259.
MONNIER, S., CAMERLYNCK, C., REJIBA, F., KINNARD, C. & GALIBERT, P. Y. 2013. Evidencing a large body of ice in a rock glacier, Vanoise Massif, Northern French Alps. *Geografiska Annaler: Series A, Physical Geography,* 95**,** 109-123.
MONNIER, S., KINNARD, C., SURAZAKOV, A. & BOSSY, W. 2014. Geomorphology, internal structure, and successive development of a glacier foreland in the semiarid Chilean Andes (Cerro Tapado, upper Elqui Valley, 30° 08′ S., 69° 55′ W.). *Geomorphology,* 207**,** 126-140.
MOTTERSHEAD, D. N. & WHITE, I. D. 1972. The Lichenometric Dating of Glacier Recession, Tunsbergdal Southern Norway. *Geografiska Annaler. Series A, Physical Geography,* 54**,** 47-52.
MUSCHELER, R., KROMER, B., BJÖRCK, S., SVENSSON, A., FRIEDRICH, M., KAISER, K. & SOUTHON, J. 2008. Tree rings and ice cores reveal 14C calibration uncertainties during the Younger Dryas. *Nature Geoscience,* 1**,** 263-267.
NESJE, A. 1984. Kvartærgeologiske undersøkingar i Erdalen, Stryn, Sogn og Fjordane. *Unpublished Cand. Scient thesis, University of Bergen*.
NESJE, A. 1995. Indre Nordfjord-Geologi og landskap. Faghefte.
NESJE, A. 2005. Briksdalsbreen in western Norway: AD 1900-2004 frontal fluctuations as a combined effect of variations in winter precipitation and summer temperature. *The Holocene,* 15**,** 1245-1252.
NESJE, A., ANDA, E., RYE, N., LIEN, R., HOLE, P. & BLIKRA, L. H. 1987. The vertical extent of the Late Weichselian ice sheet in the Nordfjord-Møre area, western Norway. *Norsk geologisk tidsskrift,* 67**,** 125-141.
NESJE, A. & DAHL, S. O. 1992. Equilibrium-line altitude depressions of reconstructed Younger Dryas and Holocene glaciers in Fosdalen, inner Nordfjord, western Norway. *Norsk geologisk tidsskrift,* 72**,** 209-216.
NESJE, A. & DAHL, S. O. 1993. Lateglacial and Holocene glacier fluctuations and climate variations in western Norway: a review. *Quaternary Science Reviews,* 12**,** 255-261.
NESJE, A. & DAHL, S. O. 2003. Glaciers as indicators of Holocene climate change. *Global Change in the Holocene***,** 264-280.
NESJE, A. & KVAMME, M. 1991. Holocene glacier and climate variations in western Norway: Evidence for early Holocene glacier demise and multiple Neoglacial events. *Geology,* 19**,** 610-612.
NESJE, A., KVAMME, M., RYE, N. & LØVLIE, R. 1991. Holocene glacial and climate history of the Jostedalsbreen region, western Norway; evidence from lake sediments and terrestrial deposits. *Quaternary Science Reviews,* 10**,** 87-114.
NGU. 2011a. *Bergart 1:50.000*, 1:50.000. http://geo.ngu.no/kart/berggrunn/: NGU.
NGU. 2011b. *Berggrunn* [Online]. http://www.ngu.no/no/hm/Norges-geologi/Berggrunn/: NGU.
NGU & THORESEN, M. K. 1997. *Kvartærgeologisk kart over Norge: tema: Jordarter*, Norges geologiske undersøkelse.
NORDLI, P. Ø., LIE, Ø., NESJE, A. & DAHL, S. O. 2002. Spring/Summer Temperature Reconstruction Western Norway 1734-2002. *Oslo (Det norske meteorologiske institutt)*.

NORKART, A. 2001. Norge i 3D med Norkart Virtual Globe. *In:* AASGAARD, R. (ed.). www.norgei3d.no: Norkart AS.
NVE, METEOROLOGICAL INSTITUTE, N. & STATENS KARTVERK. 2014. *Normal middeltemperatur for året (1961-1990)*. www.senorge.no.
O'NEAL, M. A. & SCHOENENBERGER, K. R. 2003. A Rhizocarpon geographicum growth curve for the Cascade Range of Washington and northern Oregon, usa. *Quaternary Research,* 60**,** 233-241.
PÉREZ, F. L. 1989. Talus Fabric and Particle Morphology on Lassen Peak, California. *Geografiska Annaler. Series A, Physical Geography,* 71**,** 43-57.
POTTER, N. 1972. Ice-cored rock glacier, Galena Creek, northern Absaroka Mountains, Wyoming. *Geological Society of America Bulletin,* 83**,** 3025-3058.
RAUBER, R. M., WALSH, J. E., CHARLEVOIX, D. J. & RAUBER, R. M. 2008. Severe and hazardous weather.
RHOADS, B. L. 2005. Process/form. *Questioning geography***,** 131-50.
RHOADS, B. L. & THORN, C. E. 5 Toward a Philosophy of Geomorphology. The scientific nature of geomorphology: proceedings of the 27th Binghamton Symposium in Geomorphology, held 27-29 September, 1996, 1996. Bruce Rhoads, 115.
RYE, N., NESJE, A., LIEN, R. & ANDA, E. 1987. The Late Weichselian ice sheet in the Nordfjord–Sunnmøre area and deglaciation chronology for Nordfjord, western Norway.
SAMMUT, J. & ERSKINE, W. D. 2013. Age and hydrological significance of lichen limits on sandstone river channels near Sydney, Australia. *Geografiska Annaler: Series A, Physical Geography,* 95**,** 227-239.
SKARSTEN, S. 2007. *Variation in the frequency of rockfall activity in Erdalen, Western Norway.* Master thesis in Geography, Norwegian University of Science and Technology
STATENS KARTVERK 2005. Sogn 2005. *In:* KARTVERK, S. (ed.). www.norgeibilder.no.
STATENS KARTVERK 2010. Sogn 2010. *In:* AS, B. G. (ed.). www.norgeibilder.no.
STRYN KOMMUNE 2014. Topographic data. *In:* KOMMUNE, S. (ed.).
THORESEN, M. 1990. Kvartærgeologisk kart over Norge. *Tema: Jordarter. M,* 1.
TVEDE, A. & LIESTØL, O. 1977. Blomsterskardbreen, Folgefonni, mass balance and recent fluctuations. *Norsk Polarinstitutt Årbok,* 1976**,** 225-234.
WEBBER, P. J. & ANDREWS, J. T. 1973. Lichenometry: A commentary. *Arctic and Alpine Research,* 5**,** 295-302.
WHALLEY, W. B. 1979. The relationship of glacier ice and rock glacier at Grubengletscher, Kanton Wallis, Switzerland. *Geografiska Annaler. Series A. Physical Geography***,** 49-61.
WHALLEY, W. B. & AZIZI, F. 2003. Rock glaciers and protalus landforms: Analogous forms and ice sources on Earth and Mars. *Journal of Geophysical Research: Planets (1991–2012),* 108.
WHITE, W. A. 1970. Erosion of Cirques. *The Journal of Geology,* 78**,** 123-126.
WILSON, P. 2009. STORURDI: A LATE HOLOCENE ROCK-SLOPE FAILURE (STURZSTROM) IN THE JOTUNHEIMEN, SOUTHERN NORWAY. *Geografiska Annaler: Series A, Physical Geography,* 91**,** 47-58.
WINCHESTER, V. 1984. A proposal for a new approach to lichenometry. *British Geomorphological Research Group, Technical Bulletin,* 33**,** 3-20.
ØDEGÅRD, R. S., HOELZLE, M., VEDEL JOHANSEN, K. & L. SOLLID, J. 1996. Permafrost mapping and prospecting in southern Norway. *Norsk Geografisk Tidsskrift-Norwegian Journal of Geography,* 50**,** 41-53.
ØSTREM, G. 1964. Ice-cored moraines in Scandinavia. *Geografiska Annaler***,** 282-337.
ØSTREM, G. 1971. Rock glaciers and ice-cored moraines, a reply to D. Barsch. *Geografiska Annaler. Series A. Physical Geography***,** 207-213.
ØSTREM, G. 1975. Sediment transport in glacial meltwater streams.